Volume 7 No. 1, June 2023

SCIENCE & DEVELOPMENT

(Online)
ISSN 2821-9007

CBAS
College of Basic and Applied Sciences

A Journal of the College of Basic and Applied Sciences (CBAS), University of Ghana

Gene Action Controlling Seed Size in Cowpea (Vigna Unguiculata L. Walp)

Reuben Senyo Kudiabor, John Saviour Yaw Eleblu, Bright Hodasi, Eric Yirenkyi Danquah

Correspondence Author: John Saviour Yaw Eleblu, Email Address: jeleblu@wacci.ug.edu.gh

ABSTRACT

Cowpea with large seed sizes is one of Ghana's preferred traits for producers, consumers and other value chain actors. Limited information on gene action controlling the inheritance of large seed size confounds the choice of appropriate breeding methods. Generation mean analysis was conducted to identify the gene action controlling the inheritance of cowpea seed size. Data on the seed length, seed width, and seed thickness of five generations (P_1, P_2, F_1, F_2, and F_3) of a cross between Kansa (large seed-sized variety) and Hewale (small seed-sized variety) were analyzed. The scaling test analysis showed additive-additive epistasis, and the additive-dominance model was inadequate in explaining the gene action controlling cowpea seed size. Significant additive, dominance, additive-additive, and dominance-dominance gene actions were found to control seed size. Also, allelic and non-allelic gene action were found to control seed size, hence recurrent selection could be used to improve the trait. From this study we conclude that we cannot improve on Cowpea seed size by making between large-seeded lines and small-seeded lines and recommend that breeders should make crosses among large-seeded lines if larger seeds are the desired trait as is the case in Ghana.

Keywords: Gene action, Seed size, Cowpea, Generation mean

1.0 Introduction

Cowpea is a nutritious grain legume that is eaten in many parts of the world. It is widely cultivated in the tropical and subtropical areas of Africa, Asia, and the United State of America. Particularly in Africa, the crop is cultivated by rural farmers who have limited resources and low-quality seeds (Martey *et al.*, 2022). Cowpea provides for the protein needs of people who may not afford animal protein and those who prefer plant protein. There are reasons to direct research focus on the improvement of cowpea now that there is a call to improve and sustain access to nutritious food in derived countries. In Ghana a larger number of cowpea consumers purchase their cowpea from the open market. A consumer's choice for a particular variety is influenced by several factors including seed quality traits such as seed coat colour, seed size, and duration of cooking (Quaye *et al.*, 2011). Most consumers prefer varieties with a white seed coat, short cooking time, and large seed size (Egbadzor, 2013). The large seed size of cowpea, aside been a quality choice for consumers, influences many biological and physiological processes such as germination, and vigorous seedling growth (Kandasamy *et al.,* 2020). The large seed-size cowpea available on the Ghanaian local market attracts a 30% extra premium (Ira *et al.*, 2019). However, these high-priced varieties are imported from Niger and Burkina Faso and they cost the country a huge amount of foreign exchanges to import these varieties (USAID, 2016). Unfortunately, the introduced varieties are poorly adapted to the local cropping systems and environment in Ghana. Additionally, large seed size is correlated with high yield since large seeds weigh heavier than small seeds. The improved germination, enhanced seedling vigor and high market premium which are benefits derived from producing cowpea seeds with large seed sizes make it essential to develop local cowpea varieties

with large seed sizes. The choice of a breeding method depends on the amount of variability that exists in the breeding population, the number of genes controlling the trait, and the gene effect. Variations exist in seed size for cowpea and this variability can be harnessed in a breeding program that targets seed size. Several authors have reported that several genes control seed size (Lo *et al.,* 2019; Egbadzor, 2013) but information on the gene effect is limited and this makes the choice of a suitable breeding method for improving the seed size complicated. There is a need to determine the gene effect of the controlling genes to design an appropriate approach for developing cowpea varieties with large seed sizes. The present study seeks to determine the gene action controlling the seed size trait in cowpea.

2.0 Materials and Methods

Planting materials and Experimental design

The genetic materials comprise five generations of a cross between Kansa (large seed) and Hewale (small seed). The five generations are P_1, P_2, F_1, F_2, and F_3. The plants were raised in augmented design at the West Africa Centre for Crop Improvement (WACCI) research field at the University of Ghana.

Data Collection and Analysis

The seed length, seed thickness, and seed width of the five generations; P_1, P_2, F_1, F_2, and F_3 were recorded using a vernier caliper. A boxplot was constructed to visualize the distribution of traits across the five generations using R Software. The five-parameter model proposed by Hayman (1958) was used to perform the generation mean analysis. The scaling test C and D suggested by Mather (1949) was estimated to test the presence of epistasis. The scales C and D, and the five parameters which are mean effect (m), additive effect (d), dominance effect (h), additive-additive interaction (i) and dominance-dominance interaction (l) were estimated using the formula(e) below:

Scale test;

$$C = 4\overline{F_2} - \overline{2F_1} - \overline{P_1} - \overline{P_2}$$

$$D = 4(\overline{F_3} - 2\overline{F_2} - \overline{P_1} - \overline{P_2})$$

$$V_C = 16V\overline{F_2} + 4V\overline{F_1} + V\overline{P_1} + V\overline{P_2}$$

$$V_D = 16V\overline{F_3} + 4V\overline{F_2} + V\overline{P_1} + V\overline{P_2}$$

Genetic parameters;

m = mean of F_2

$$d = \frac{1}{2}\overline{P_1} - \frac{1}{2}\overline{P_2}\text{-}$$

$$h = \frac{1}{6}(4\overline{F_1} - 12\overline{F_2} - 16\overline{F_3})$$

$$I = \overline{P_1} - \overline{F_2} + \frac{1}{2}(\overline{P_1} - \overline{P_2}\text{+h})\text{-}\frac{1}{4}l$$

$$L = \frac{1}{3}(16\overline{F_3} - 24\overline{F_2} + 8\overline{F_1})$$

The variances of the gene effects were estimated as follows:

$$Vm = VF_2$$

$$Vd = \frac{1}{4}(V\overline{P_1} - V\overline{P_2})$$

$$Vh = \frac{1}{36}(16V\overline{F_1} + 144\overline{F_2} + 256\overline{F_3})$$

$$Vi = V\overline{P_1} + V\overline{P_2} + \frac{1}{4}(\overline{VP_1} + V\overline{P_2}\text{+Vh}) - \frac{1}{16}Vl$$

$$Vl = \frac{1}{9}(256V\overline{F_3} + 576V\overline{F_2} + 64V\overline{F_1})$$

The standard errors for the gene effects were obtained by taking the square root of their corresponding variances. The ratio of the genetic effects to their respective standard errors was used to calculate a "t" to test for the significance of the genetic effects and their variances.

3.0 Results

3.1. Scaling test for seed length, seed width and seed thickness

The results of the scaling tests indicated that the scaling test C was not significant for all traits. However, scaling test D deviated significantly from zero for all traits (Table 1). The significant values of D suggest that the additive-dominance model was not adequate due to the presence of additive-additive epistasis.

Table 1: Scaling test for the adequacy of additive-dominance model for seed size in cowpea

	Scaling test		Variance		Calculated t value	
Traits	C	D	C	D	C	D
Seed length	**-0.66ns**	**-102.97****	5.9137±2.43	8.5497±2.92	-0.27	-35.21
Seed Width	**1.16ns**	**-73.66****	8.328±2.89	5.184±2.28	0.40	-32.35
Seed thickness	**0.76ns**	**-60.26****	3.4204±1.84	10.06±3.17	0.41	-18.99

ns= non-significant, **significant at 0.01.

3.2. Generation mean analysis for seed length, seed width, and seed thickness in five cowpea generation (P_1, P_2, F_1, F_2 and F_3)

The generation means, means of genetic parameters and the type of epistasis are presented in Table 2. The values of genetic components, m (mean effect), d(additive), and h(dominance) were significant for seed length, seed width and seed thickness. The i (additive*additive) interaction effect was significant for seed length, but it was not significant for seed width and seed thickness. The dominance-dominance (l) interaction was not significant for all three traits. The h and l gene effect were both negative for seed length indicating a complementary type of epistasis. The h and l gene effects had opposite signs for seed width and seed thickness. This indicates a duplicate type of epistasis for the two traits.

3.3. Distribution seed length, width, and thickness in five cowpea generation (P1, P2, F1, F2 and F3).

The five generations exhibited different levels of seed length (Figure 1A). The lower extreme, first quartile, median, third quartile, and upper extreme values of F_1 (7.75, 7.77, 8.03, 8.17, and 8.75), F_2 (7.57, 7.79, 8.15, 8.40, and 9.21), and F_3 (6.59,7.75, 8.16, 8.59, and 9. 82) was higher than their corresponding values in the P_2 (10.07, 10.81, 11.23, 11.68, and 12.65) and lower than their corresponding values in the P_1 (5.17, 5.91, 6.29, 6.62, and 7.39). The upper extreme value of the F_3 (9.82) was lower than the lower extreme of the P_1 but higher than the upper extreme of the P_2 (7.39). The outlier observed for seed length for the F_3 generation (9.878) was lower than the minimum value (10.07) for the higher parent (P_1) and greater than the maximum value (7.39) for the lower parent (P_2). The F_1 generation had an outlier (6.05) which was lower than the minimum seed length value (7.75).

For seed width, the lower extreme, first quartile, median, third quartile, and upper extreme values of the F_1 (5.83, 6.18, 6.39, 6.59, and 6.99), F_2 (5.68, 6.13, 6.38, 6.52, 6.81, and 6.81), and F_3 (5.21, 6.02, 6.42, 6.69, and 7.39) were lower than the corresponding values for P_1 (6.17, 6.57, 6.91, 7.26, and 7.78) and higher than their corresponding values for P_2 (4.32, 4.78, 5.04, 5.13, and 5.35) (Figure 1B). The value of the upper quartile for the

F_3 (7.39) was greater than the third quartile value (7.26) of the P_1. The value of the outlier for seed width in the F_2 generation (9.42) was greater than the maximum value (7.78) for the higher parent (P_1). The value of the outlier in the F_3 generation (4.98) was lower than the minimum value (6.17) in the higher parent and greater than the first quarter value of the lower parent (4.78). The outlier value observed in the F_1 (4.07) was lower than the minimum value (4.32) of the lower parent. The value of outliers (6.86, 6.04, and 6.1) observed for the F_2 population was below the median value of the higher parent (6.91).

The median value of the seed thickness in F_2 (5.18) was below the lower quartile (5.22) of the P_1 (Figure1C). The third quartile value for the seed thickness of the F_2 (5.69) was equal to the first quartile value of the P_1 and greater than the third quartile value of the P_2 (4.14). The median value of the seed thickness for the F_3 (5.063) was found to be lower than the minimum value of the P_1 (5.22) and higher than the third quartile value of the P_2 (4.14). The third quartile value of the F_3 (6.098) was greater than the median value of the P_1 (5.92) and lower than the third quartile value of the P_1 (6.42). The outlier observed within the F_1 population (3.28) was below the minimum value of the lower parent (3.30). Transgressive segregants for seed thickness were identified within the F_2 and F_3 generations. The outliers for the F_2 generation (4.38 and 4.50) were below the minimum value (4.82) of the F_2 population. The outliers for the F_2 population (4.38, 4.50) had higher seed thickness values compared to the maximum seed thickness value of the lower parent (P_2) but these outliers were below the minimum value (5.22) of the higher parent (P_1). The value for the outlier in the F_3 population was below the first quartile value of the lower parent (3.56)

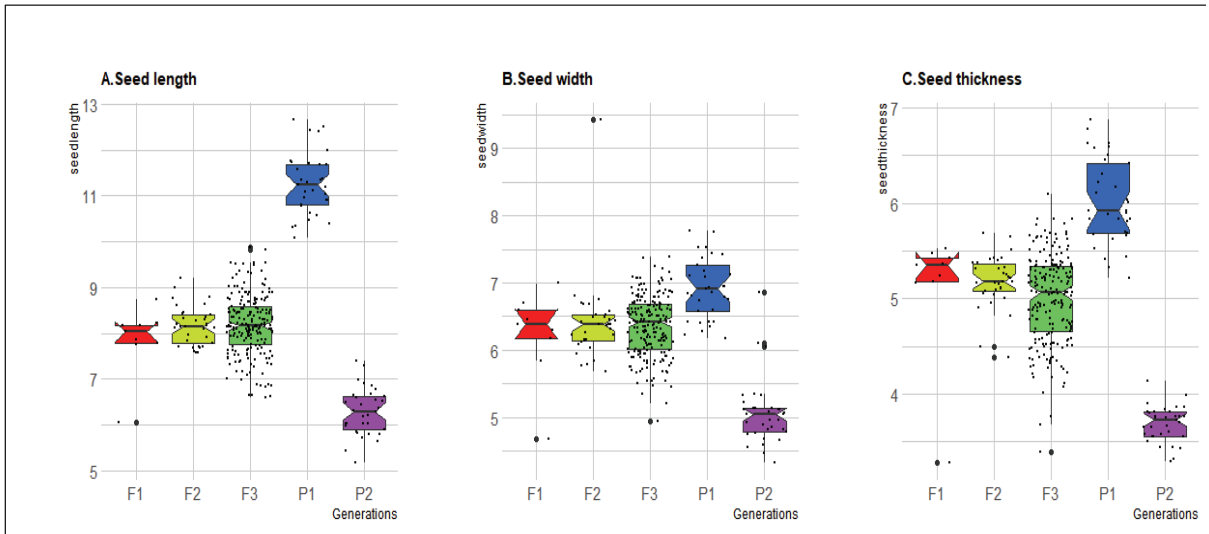

Figure1: The seed length, seed thickness, and seed width distribution in five generations of cowpea.
P_1=Paternal parent (large seed); P_2,= maternal parent(small seed); F_1=first filial generation; F_2=second filial generation; F_3=third filial generation; black dots are outliers; points are data points

4.0 Discussions

The types and magnitude of gene action influencing the inheritance of a trait are important in determining the breeding methodology for crop improvement. The scales C and D were used to test the adequacy of additive-dominance interaction of genes. The results from this study indicated that scale C was insignificant for seed length, width, and thickness. However, scale D was significant for seed length, seed width, and seed thickness. This could be a result of non-allelic interaction Panigrahi et al., (2020) obtained similar results in blackgram cowpea.

The results from the generation mean analysis estimated using five generations (P_1, P_2, F_1, F_2 and F_3), we deduce that the mean effect *(m),* additive effect *(d),* dominance effect *(h)* and additive-additive effect *(i)* were significant for seed length. Therefore, the additive, dominance and the epistatic component of additive-additive gene actions control seed length. This result is consistent with reports by Vadive *et al.,* (2019).

However, the dominance-dominance effect (*l*) was not significant for seed length. Also, the gene effects, m, d and h were significant for seed width and seed thickness but the gene effects *(i)* and *(l)* were not significant for seed width and seed thickness. This shows that additive and dominance gene action controls seed width and seed thickness, and that epistatic effect did not play major role in the control of the traits. This result agrees with reports from Thamdhara *et al.,* (2017). The value of the dominance (h) gene effect was relatively greater than that of the value of the additive gene effect signifying the prevalence of dominance allelic gene action on the inheritance of the traits. Consequently, the overall observation on the generation mean analysis confirms earlier reports by Egbadzor, (2013) that seed size was controlled by both additive and non-additive gene action.

Recurrent selection should be used for improvement on the trait. The seed width, seed thickness, and seed length distribution indicated that the progeny generations showed higher values over the lower parent (P_2) but lower values relative to the higher parent (P_1) and this shows that there is progress in the improvement of small seed size in cowpea however slow. Among the progeny generations, the F_3 generation had the highest values over the lower parent (P_2) indicating that selection for large seed size can begin from the F_3 generation. Also, the seed length, seed width, and seed thickness observed in the F_1, F_2, and F_3 generations were lower than the higher parent (P_1). This implies repeated backcrossing to the higher parent will be required to enhance selection for large seed size.

5.0 Conclusions

Seed size trait in cowpea is heritable and regulated by dominance, additive-additive, and dominance-dominance gene actions. Breeding programmes can make progress by using recurrent selections and backcrosses to make quick genetic gains when breeding for larger seeds. From this study we conclude that we cannot improve on Cowpea seed size by making between large-seeded lines and small-seeded lines and recommend that breeders should make crosses among large-seeded lines if larger seeds are the desired trait as is the case in Ghana.

Competing Interest: The authors declare none.

References

Egbadzor K F. (2013). Genetic Control and Breeding for Seed Size and Colour in Cowpea [Vigna Unguiculata (L.) Walp]. http://ugspace.ug.edu.gh/handle/123456789/7625.

Hayman BI. (1958). The separation of epistatic from additive and dominance variation in generation means. Heredity 12, 371–390.

Ira AH Zhenyu, J and Francis K. (2019). Market preferences for cowpea (Vigna Unguiculata [L.] Walp) dry grain in Ghana. African Journal of Agricultural Research, 14(22), 928–934.

Kandasamy S, Weerasuriya N, Gritsiouk D, Patterson G, Saldias S, Ali S and Lazarovits G. (2020) Size

Variability in Seed Lot Impact Seed Nutritional Balance, Seedling Vigor, Microbial Composition and Plant Performance of Common Corn Hybrids. Agronomy. 10(2):157. https://doi.org/10.3390/agronomy10020157

Lo S, Muñoz-Amatriaín M, Hokin SA, Cisse N, Roberts PA, Farmer AD, Xu S and Close TJ (2019). A genome-wide association and meta-analysis reveal regions associated with seed size in cowpea [Vigna unguiculata (L.) Walp]. Theor Appl Genet. 2019 Nov;132(11):3079-3087. doi: 10.1007/s00122-019-03407-z. Epub 2019 Jul 31. PMID: 31367839; PMCID: PMC6791911.

Martey E, Etwire PM., Adogoba DS, and Tengey TK. (2022). Farmers' preferences for climate-smart cowpea varieties: implications for crop breeding programmes, Climate and Development, 14:2, 105-120, DOI: 10.1080/17565529.2021.1889949

Mather K. (1949). Biometrical Genetics. Methuen and Co. Ltd., London

Panigrahi KK., Mohanty A, Panigrahi P, Mandal P, Pradhan R, and Baisakh B. (2020).

Generation mean analysis using five parameters genetic model for quantitative traits in black gram (Vigna mungo L. Hepper). The Pharma Inno-vation Journal, 9(7), 368–371.

Quaye W, Adofo K, Buckman E, Frempong G, Jongerden JP and Ruivenkamp G (2011). A socio-economic assessment of cowpea diversity on the Ghanaian market: implications for breeding. International Journal of Consumer Studies - Int J Consum Stud. 35. 679-687. 10.1111/j.1470-6431.2010.00980.x.

Thamdhara G, Ramalingam A and Geetha S (2017). Estimation of genetic parameters and combining ability analysis in blackgram [Vigna mungo (L.) Hepper]. Legume Research (40):401-408.

USAID (2016). Resilience and Economic Growth in the Sahel –Accelerated Growth (REGIS-AG) Value Chain and End Market Assessment: Cowpea. https://www.usaid.gov/sites/default/files/documents/1860/USAID_REGIS-AG_Cowpea_Value_Chain_and_End_Market_Assessment.pdf

Vadive K, Manivannan N, Mahalingam A, Satya VK, Vanniarajan C and Saminathan, VR. (2019). Generation Mean Analysis for Yield, Yield Components and MYMV Disease Scores in Blackgram [Vigna mungo (L). Hepper]. International Journal of Current Microbiology and Applied Sciences, 8(05), 1989–1995.https://doi.org/10.20546/ijcmas.2019.805.23.

Determination of Local Reference Renal Volumetric Ellipsoid Coefficient For Clinical Application In Ghana

Issahaku Shirazu [1], Y. B Mensah[2], Cyril Schandorf [3], S. Y. Mensah[4], T. A. Sackey[5], E. K. Tiburu[6*].

[1] University of Cape Coast, School of Agriculture and Physical Sciences Faculty of Physical Sciences, Department of Physics, Cape coast, Ghana

[2] University of Ghana Medical School, Department of Radiology, Korle-Bu Teaching Hospital, Accra Ghana

[3] Graduate School of Nuclear and Allied Sciences, University of Ghana, Legon, Ghana

[4] Ghana Atomic Energy Commission, Radiological and Medical Sciences Research Institute, Medical Radiation Physics Centre, Accra, Ghana

***Corresponding Author:** etiburu@ug.edu.gh

ABSTRACT

Mathematically modelled kidneys are described as variably ellipsoid representing a type of quadric surface of a 3D analogue. Hence this mathematical descriptive of the volume of a kidney can be represented by mathematical relationship using the three dimensions of its quadrant surface **and** an ellipsoid constant. Therefore, with a known renal volumetric ellipsoid constant, a measured renal length, renal width and renal thickness, the volume of an ellipsoid kidney can be estimated. In clinical practice this ellipsoid model is used to estimate kidney volume in other to determine a possible kidney condition using varied ellipsoid constants. The objective of this study was to determined renal volumetric ellipsoid constant, that will provide a simplified approach in estimating renal volume. This would aid Clinicians in estimating renal volume for various diagnostic interpretation. The methodology involved the voxel count method used to determine the renal volume on clinical real acquired images and the result divided by the product of the linear measurements of the renal length, renal width and renal thickness of the kidney. The results showed that the renal volumetric ellipsoid coefficient determined was approximately 0.53±0.01 for both age and gender variations. Generally, the volumetric ellipsoid coefficient was not affected by either age or gender variation. In conclusion, GUI has been designed for a comfortable working process in clinical application of renal volume calculation by clinicians and researchers in Ghana.

Key words: Renal volume, volumetric ellipsoid constant, renal length, renal width and renal thickness

Introduction

Generally, kidneys are described as rotational ellipsoid which can be ued to describe the volume and associated various dimensions of the kidney. Mathematically, the volume of an ellipsoid is calculated by estimating the product of the length, width, thickness and the ellipsoid constant. This is expressed mathematically as:

$$V = \frac{4\pi}{3} abc, \qquad (1)$$

where 'a' is the longitudinal (length), 'b' is the transverse (width), 'c' is the A-P (thickness) diameter of the ellipsoid and $\frac{4\pi}{3}$ is the ellipsoid constant. From Equation (1), unknown ellipsoid coefficient, K^* (ellipsoid like shape, e.g. kidney) can be estimated as:

$$V \times K = \frac{4\pi}{3} abc \times K$$

$$\text{If } V \times K = V^* \text{ and } \frac{4\pi}{3} K = K^*$$

Then,

$$K^* = \frac{V^*}{abc}, \quad (2)$$

where K^*, a, b and c are the renal volumetric ellipsoid coefficients, renal length (longitudinal diameter), renal width (transverse diameter) and renal thickness (A-P diameter) respectively. Thus, renal volume (V^*) can be estimated with known longitudinal diameter, transverse diameter, renal thickness and renal volumetric ellipsoid coefficient K^*. However, in regular clinical practice the K^* is determined as a reference standard value and usually multiplied by the three estimated linear dimensions (length, width and thickness) to determine the renal volume (Equation (3)).

With known K^*, the RV (where is RV defiend?) is determined from the expression:

$$RV = K^* * \text{renal length (a)} * \text{renal width (b)} * \text{renal thickness (c)} \quad (3)$$

It is of interest to note that the application of the rule of estimating renal volume among radiologist in Ghana varied hence there is the need for unification based on data from Ghanaian population.

Objectives

The aim of this study is to determine a unified local based standard reference renal volumetric ellipsoid coefficient to be used in Ghana for clinical application.

Methodology

The data collection involved the use of blinded images in two processes: the measurements of renal linear parameters and renal voxel measurements on MeVisLab (MVL) application software. The measured parameters include measurements of longitudinal diameter, transverse and A-P diameters. The renal volume on the MVL application platform using voxel count method to determine the total voxel in the image.

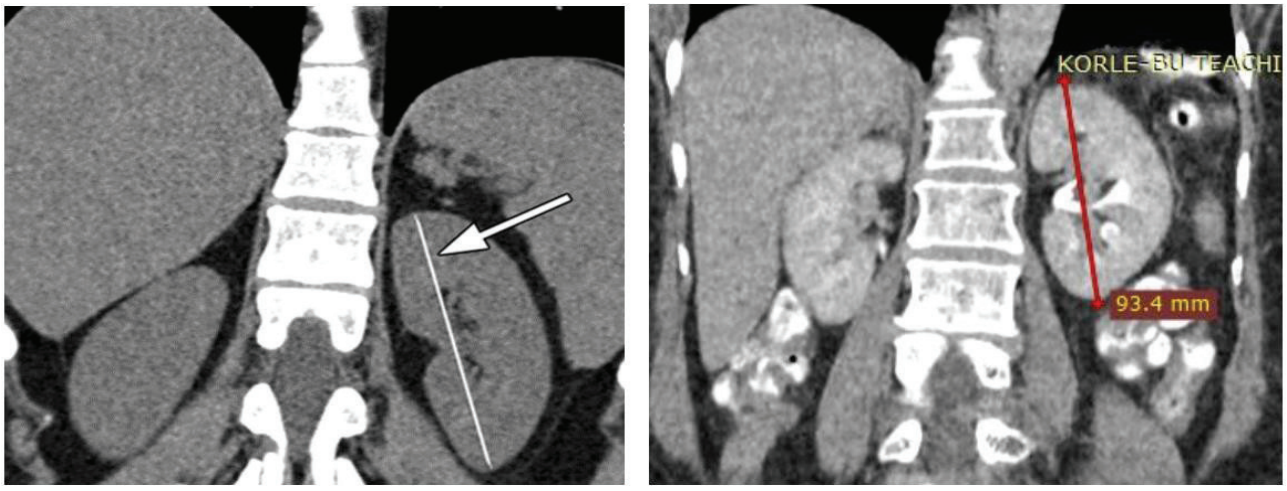

Figure. 1: Measurements of renal length using what methodology? using what methodology and how do you choose the section to measure

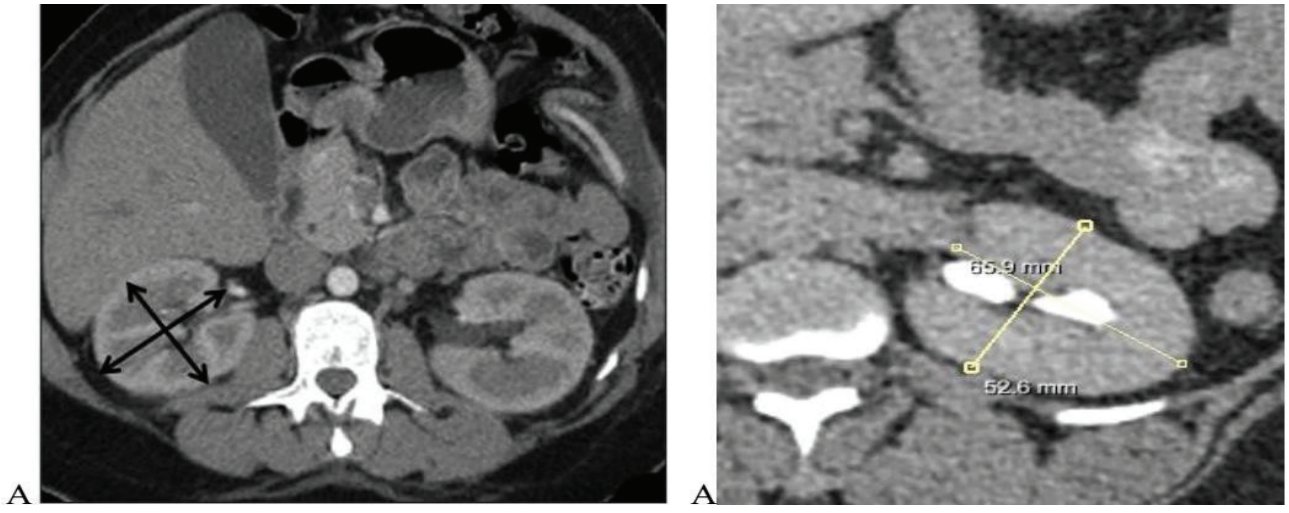

Figure 2: Measurements of lateral and A-P diameters using what methodology and how do you section the place to measure

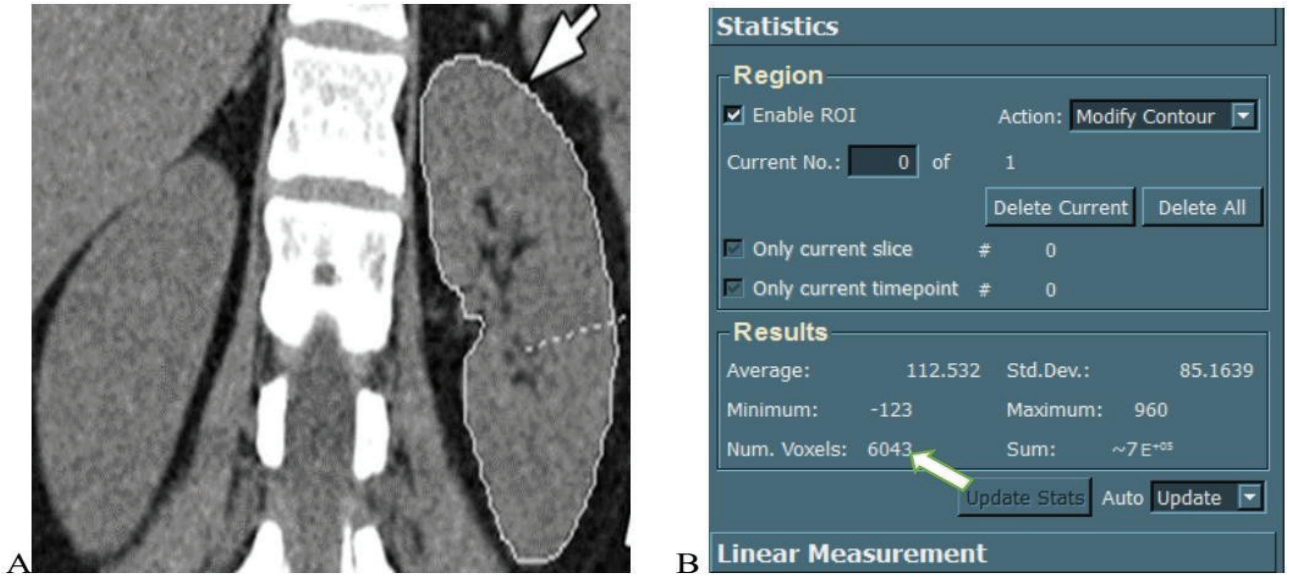

Figure 3: Measurements of RSA using what methods?

Renal Linear and Volume Measurements

Measurements of Linear Renal Dimensions

The first measured parameters include three linear dimensions, renal length, renal width and renal thickness. All these dimensions were measured at maximum values of strictly longitudinal, transverse and Anterior-Posterior sections through the center of the kidney respectively. The renal lengths were evaluated using the coronary images while the axial images were applied to measure Anterior-Posterior and lateral diameters. The width and thickness were evaluated in the transverse plane perpendicular to the longitudinal axis of the kidney. The level of this transverse section was placed at the level of the hilum.

Renal length was measured on the coronary images by drawing a single straight line from one edge of the renal parenchyma to another end with the linear measuring tool on the MVL platform as shown in Figure 1. Renal with was measured from the lateral extent of the kidney to the renal sinus and renal thickness measured perpendicular to the lateral diameter as shown in Figure 2.

The second component of this study was the measurements of renal volume from contiguous CT slices with voxel measuring tool on the MVL application software as shown in Figure 4B. These measurements were done using 3D volume-rendered image of the kidney shown in Figure 4A. The maximum length of the kidney was measured in the longitudinal plane and was visually estimated to represent the largest longitudinal section. Two different methods were also applied to estimate renal volumes. The first method was the calculation of the total renal volume by using the voxel-count method of the MVL application software (block white arrow in Figure 3A), with a region of interest (ROI) drawn for both right and left kidneys on each slice to indicate the renal boundaries. The total voxel was generated on each slice (block white arrow in figure 3B) by considering the amount of the voxel lying within the boundaries, including the central sinus fat but excluding perinephric fat.

Furthermore, with a known pixel size, slice thickness and the total number of voxels (black arrow in Figure 4B), in addition to computing for each average count and standard deviation of the voxels (yellow and blue arrows in Figure 4 respectively) equation 3 was used to estimate renal volume:

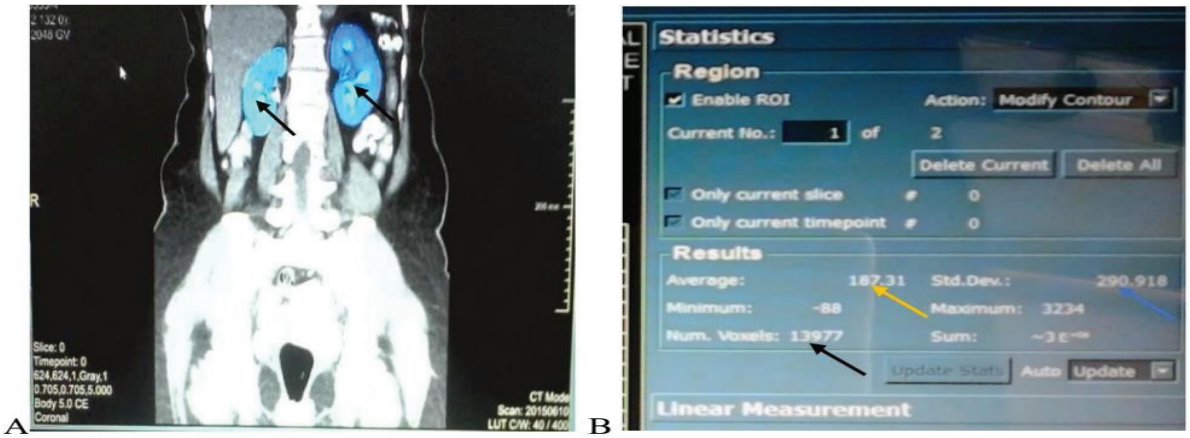

Figure 4: Measurements of renal volume by voxel count method using what instrument and parameter set.

Estimate of Renal Volumetric Ellipsoid Coefficient

The renal volumetric ellipsoid coefficient K^*, was calculated by dividing the measured renal volume by the product of the linear renal length, renal width and renal thickness. It is the constant of proportion in the ellipsoid equation as shown in equation 2. The K^*-values were determined by using the ellipsoid equation for estimating renal volume define as:

RV = K^* * renal length (RL) * renal thickness (RT) * renal width (RW),

This means that,

$$K^* = \frac{RV}{RL*RT*RW}. \quad (4)$$

Therefore, with a known renal volume by the voxel count method, renal length, renal width and renal thickness by linear measurements using MVL, then K^* was estimated and the standard reference ellipsoid equation with known K^* defined as:

$$RV = K^* * RL * RT * RW. \quad (5)$$

Results

Table 1 is presented as left and right renal thickness (Anterior-Posterior), renal width (Lateral) and renal length (Longitudinal) diameters, in terms of the mean, maximum and minimum values based on age and gender variation. Whilst Table 2 is a presentation of three measured renal parameters, including left and right RV and K parameters. These measurements of the renal volume and the ellipsoid constant are presented in terms of their mean, maximum and minimum values based on age and gender variation which are summarized in Table 3 and Table 4 for male and female respectively (not clear). This represent a reference chat of renal volumetric ellipsoid coefficient which has been made available to clinicians for clinical application. The summary of renal volume are presented in Table 5, for various age and gender variations. Whilst the overall summary are presented in Table 6 independent of age, but depends on gender variations.

Table 1: Estimated renal linear parameters with volume for male The letters have shadows. Create a table for the results

Table 1A: Measured A-P, LT and LNG diameters and renal volume

Sex/Age	STATS	AGE Yrs	$A\text{-}P_R$ mm	$A\text{-}P_L$ mm	LT_R mm	RV_R mL^3	LT_L mm	LNG_R mm	LNG_L mm	RV_L mL^3
MALE	MEAN	32	45.39	45.3	62.3	147.4	61.7	104.9	107.9	153.6
20-40	MAX	40	63.9	62.7	75.5	183.4	73	124.8	126.6	195.7
	MIN	20	39.3	39.1	51.5	97.52	48.1	85.9	88.5	116.1
41-60	MEAN	54	44.59	45.6	61.8	146.0	61.1	105.2	106.9	153.8
	MAX	60	58.3	59.5	71.3	229.8	76.8	118.3	121.6	254.4
	MIN	41	37.6	38.5	50.4	100.3	47.8	89	75.3	96.27
61-80	MEAN	73	42.0	43.6	57.7	124.5	57.9	98.9	99.6	132.3
	MAX	80	53.7	59.1	66.3	211.5	68.8	119.3	119.2	297.1
	MIN	61	31.9	26.7	49.3	74.41	47.9	84.2	83.6	66.89
20-80	MEAN	52	44.1	45.0	60.8	146.7	60.4	103.4	105.1	151.8
	MAX	80	63.9	62.7	75.5	312.0	76.8	124.8	126.6	272.9
	MIN	20	31.9	26.7	49.3	75.54	47.8	84.2	75.3	77.85

Table 2: Estimated renal linear parameters with volume for female The letters have shadows. Create a table for the results

Table 1B: Measured A-P, LT and LGN diameters and renal volume

Sex/Age	STATS	AGE Yrs	$A\text{-}P_R$ mm	$A\text{-}P_L$ mm	LT_R mm	RV_R mL^3	LT_L mm	LNG_R mm	LNG_L mm	RV_L mL^3
FEMALE	MEAN	34	43.46	45.2	60.2	155.5	59.2	105.4	107.6	159.5
20-40	MAX	40	52.6	54.8	68.4	311.9	66.0	124.1	126.6	272.9
	MIN	20	38.8	37.9	53.5	103.7	47.1	83.8	90.9	104.8
41-60	MEAN	51	44.0	45.3	60.1	152.6	60.5	103.9	105.3	158.0
	MAX	60	56.2	65.6	69.5	224.9	68.7	121.7	120.3	218.0
	MIN	41	38.8	39.1	47.4	108.5	47.1	86.4	87.4	108.8
61-80	MEAN	72	42.0	44.2	57.8	128.3	57.5	97.0	98.3	133.9
	MAX	80	56	59.8	68.8	205.7	71.7	124.3	134.8	190.3
	MIN	61	32.9	34.7	41.6	75.53	43.6	75.6	74.8	77.85
20-80	MEAN	56	43.1	44.8	59.2	142.0	59.0	101.4	103.0	148.3
	MAX	80	56.2	65.6	69.5	311.9	71.7	124.3	134.8	297.1
	MIN	20	32.9	34.7	41.6	74.41	43.6	75.6	74.8	66.89

Table 3: Estimated renal ellipsoid constant for male---The letters have shadows. Create a table for the results

Table 2A: *Estimated Renal K and RSI Parameters*

Sex/Age	STATS	Age (yrs.)	K_R	K_L	RSI_R	RSI_L
MALE	MEAN	34	0.526	0.532	1.0	1.0
20-40	MAX	40	0.596	0.578	1.2	1.3
	MIN	20	0.493	0.500	0.8	0.9
41-60	MEAN	52	0.528	0.532	1.0	1.0
	MAX	60	0.606	0.620	1.3	1.2
	MIN	43	0.495	0.490	0.9	0.9
61-80	MEAN	72	0.529	0.530	1.0	1.0
	MAX	80	0.606	0.588	1.2	1.3
	MIN	61	0.491	0.495	0.8	0.7
20-80	MEAN	52	0.528	0.530	1.0	1.0
	MAX	80	0.595	0.595	1.3	1.3
	MIN	20	0.485	0.491	0.8	0.7

Table 4: Estimated renal ellipsoid constant for female The letters have shadows. Create a table for the results

Table 2B|: *Estimated Renal K and RSI Parameters*

Sex/Age	STATS	Age (yrs.)	K_R	K_L	RSI_R	RSI_L
FEMALE	MEAN	32	0.529	0.529	1.0	1.0
20-40	MAX	40	0.586	0.595	1.2	1.2
	MIN	20	0.489	0.491	0.8	0.8
41-60	MEAN	53	0.528	0.530	1.0	1.0
	MAX	60	0.568	0.593	1.2	1.2
	MIN	41	0.485	0.491	0.9	0.7
61-80	MEAN	73	0.529	0.530	1.0	1.0
	MAX	80	0.595	0.588	1.3	1.3
	MIN	61	0.491	0.498	0.9	0.8
20-80	MEAN	54	0.528	0.530	1.0	1.0
	MAX	80	0.606	0.620	1.3	1.3
	MIN	20	0.485	0.490	0.8	0.7

Table 5: Summary of Renal ellipsoid constant with age and gender variation The letters have shadows. Create a table for the results

Table 3: Summary of Estimated K and RSI Parameters

Age	Age (yrs)	Sample	K_R	K_L	RSI_R	RSI_L
Male	Mean		±0.008	±0.009	±0.02	±0.01
	33	107	0.529	0.5289	1.02	1.02
	53	122	0.528	0.5303	1.00	1.01
	70	59	0.529	0.5301	0.99	1.01
	49	288	0.528	0.5297	1.00	1.01
Female	Mean		±0.020	±0.019	±0.01	±0.02
	34	68	0.526	0.532	1.02	1.03
	53	135	0.528	0.532	1.02	1.02
	70	122	0.529	0.530	0.97	0.98
	55	325	0.528	0.530	1.00	1.01

Table 6: Over all summary of Renal ellipsoid constant for both gender

Table 4: *Ghanaian Reference Renal K and RSI Parameters*

PARAMETER	M/R	M/L	MEAN	F/R	F/L	MEAN
K	0.5283	0.5297	0.5290	0.5280	0.5304	0.5292
RSI	1.00	1.01	1.01	1.00	1.01	1.00

Discussions

The K is an important renal parameter that represents the constant of proportionality for a renal ellipsoid equation and for the estimate of a unique Ghanaian renal volume. This has been made available to be used by clinicians in a comfortable working process in the form of GUI for clinical application. The statistical detailed age and gender representation of these renal parameters are shown in Table 1 and 2 as reference chat for clinicians and researchers.

The renal volumetric ellipsoid coefficient (K) was determined as summarized in Table 6??? The highlight of the summarized measurements are presented in Table 4?? and 5?? (this must come first before 6) with an average maximum and minimum values. The average K was approximately the same for both gender and age variations with the value of 0.53±0.01 for right and left, male and female and with all age variations.

Conclusion

In conclusion, an accepted unified local based standard reference renal volumetric ellipsoid coefficient was determined and led to the establishment of renal volume model for clinical application in Ghana. The results shows that the renal volumetric ellipsoid coefficient was approximately 0.53±0.01 for both age and gender variations. Generally, the mean volumetric ellipsoid coefficient were not affected by either age or gender variation. In conclusion, GUI has been designed to be used to estimate renal volume by clinicians.

Recommendation

The radiologist should use the results obtained by this method in relation to the renal volumetric ellipsoid coefficient for clinical application in Ghana. It is recommended that the established reference values be used as clinical guidelines values for estimation of renal volume for clinical application.

Reference

Breau, R. H., Clark, E., Bruner, B., Cervini, P., Atwell, T., Knoll, G., & Leibovich, B. C. (2013). A simple method to estimate renal volume from computed tomography. Canadian Urol Assoc Journal, 7(5), 189–192.

Bakker, J. (1999). Renal volume measurement: Accuracy and repeatability of US compared with that of MR imaging. Rad Num., 211(3), 623-628.

Brandt, T. D., Neiman, H. L., Dragowski, M. J., Bulawa, W., & Claykamp, G. (1982). Ultrasound assessment of normal renal dimensions. Journal of Ultrasound Medicine, 7(15), 49-52.

Emamian, S. A., Nielsen, M. B., & Pedersen, J. F. (1995). Intraobserver and interobserver variations in sonographic measurements of kidney size in adult volunteers. A comparison of linear measurements and volumetric estimates. Acta Radiol. 36(4), 399-401.

Emamian, S. A., Nielsen, M. B., Pedersen, J. F., & Ytte, L. (1993). Kidney dimensions at sonography: Correlation with age, sex, and habitus in 665 adult volunteers. AJR, 160, 83-86.

Feeman, T. G. (2010). The mathematics of medical imaging: A beginner's guide. Berlin: Springer Undergraduate Texts in Mathematics and Technology.

Ferrer, F. A., McKenna, P. H., Bauer, M. B., & Miller, S. F. (1997). Accuracy of renal ultrasound measurements for predicting actual kidney size. Journal of Urol., 157(6), 78-81.

Geraghty, E. M., Boone, J. M., McGahan, J. P., & Jain, K. (2004). Normal organ volume assessment from abdominal CT. EPUB Abdom Imaging, 29(4). 482-490.

Optimized Bids Evaluation Model for Improved Performance and Quality Delivery in Public Procurement Sector and Construction Projects

F.O. Aranuwa[1] and TOPE-GABRIELS Bunmi Sade[2]

[1]Department of Computer Science, Adekunle Ajasin Uiversity, Akungba – Akoko, Ondo State, Nigeria
[2]Physical Planning Uniit, Adekunle Ajasin University, Akungba – Akoko, Ondo State, Nigeria
***Corresponding Author:** felix.aranuwa@aaua.edu.ng

ABSTRACT

Traditionally, public sector procurement and construction project contract awards are largely based on the lowest bid award system. However, this practice has been characterized with problems of inferior quality of construction facilities, high incidence of litigations and frequent cost overruns. Therefore, this study is focused at designing an optimized bids evaluation model to overcome the challenges of the traditional methodologies. A multi-parameter bids responsiveness evaluation model that integrates both the mandatory and weighted sub-factors criteria was designed to achieve this purpose. A cross-sectional quantitative and qualitative research technique was employed to formulate the instruments used for the research data collection. Purposive and random sampling techniques were deployed in drawing data samples from respondents to identify cases, make inferences about population, save time and reduce cost of the study. Two hundred and six datasets was collected, 66% of the datasets was devoted to training while the remaining 34% was used for testing during the data modeling. Relative importance index (RII) and ranker's search method was used to measures the strength of relationship between the observed data and ranking of the relative importance indices of the attributes used respectively. Four different classification algorithms, namely: Pruned Decision Tree (PDT), Logistics Model Tree (LMT), Justified Repeated Incremental Pruning (JRIP) and PART were considered in the modeling. The algorithms were tested to determine the model with the best predictive accuracy. From the experiment, the PDT and JRIP outclassed the other two algorithms in the layer. They both have the same correctly classified instances of 99.4%, mean absolute error of 0.062, true positive rate and false positive rate of 0.994 and 0.001 respectively, the ROC Area of 0.994 and recall weighted average of 0.994 respectively. This proves that both algorithms are suitable for the model. However, the pruned decision tree was preferred the best algorithm as a result of the time taken to build the model. The algorithm took 0.01 seconds compared to JRIP with 0.1 seconds. With this performance, the new model will suitably improve the efficiency of the existing methodologies, guaranteed quality delivery and maximum value in any construction projects. Therefore, the model is highly recommended for efficient bid evaluation in the procurement and construction sectors. Meanwhile, the research still paves the way for future research using additional more inputs, larger database and other background factors.

Keywords: Bids responsiveness, Evaluation model, Classification algorithms, Multi-parameter, Quality delivery

Introduction

Bid evaluation system is an integral component of performance in public procurement sector and construction projects. The choice of selecting a contractor or supplier for a project depends on the bid award approach in place, which has a significant influence on the success or failure of such project or services. [1]. Customarily, public procurement and construction projects are largely based on the competitive lowest bid award system. This practice is universally accepted since it ensure the lowest cost of completing a project. However, clients and construction industries have realized that accepting the least bid price does not guarantee maximum value and quality delivery [2]. Hence, the quest for an alternative method to overcome the challenges of the customary practices motivated this research work. The study is focused at developing an optimized model based on bids responsiveness strategy in procurement and construction projects to improve on the conventional approaches. By definition, bid responsiveness is an alternative method that incorporates both the mandatory and weighted sub-factors criteria other than just lowest price system into the selection process [3]. According to [4], a bid is said to be responsive when it substantially complies with the procedures and requirements laid out in the bidding documents.

2.0 Literature Review

2.1 Overview of Bidding and Bid Evaluation System

Bidding is the most common means by which contractors or suppliers submit proposal to obtain contracts and services [5]. Meanwhile, the choice of selecting a contractor or supplier for a contract or service depends on the bid evaluation strategy, which has a significant contribution to the success or failure of the project, particularly in the procurement and construction sectors [6]. According to [7], bid evaluation is defined as the organized process of examining and comparing bids to select the best offer in an effort to acquire goods and services necessary to achieve the goals of an organization. The main purpose of bid evaluation is to determine the most economically advantageous tender.

2.2 Bid Evaluation Approach

The three main bid evaluation strategies presented by [8] are discussed as follows:

2.2.1 Lowest bidding

Lowest bidder approach is a common method applied for selection of contractors in many procurement and construction projects [9]. It is a bidding methods in which the party that bids at the lowest price is determined as the successful bidder. This type of bidding compels contractors to lower their costs to ensure that they win a bid. However, a project awarded based on the least price has its own inherent flaws. The practice has been characterized with continuous problems of inferior quality of construction facilities, high incidence of claims and litigation, frequent cost overruns and use of poor quality of materials. According to [10], the abolition of the lowest bidding system is under discussion as it is pointed out to be one of the major causes for deteriorating construction companies' profitability and poor-quality delivery.

2.2.2 Responsive Bid

A responsive bid is referred to a bid or proposal that substantially complies with the invitation to bid or request for proposals with all prescribed bid conditions [3]. According to [11], a responsive bid or tender is one that conforms to all the terms, conditions, and specifications of the tender documents without material or qualification deviation.

A responsive bid is expected to meet all the criteria laid out in the bidding documents. The components of the criteria include product specifications, deliverable, prescribed bid conditions and submittal deadlines [8]. According to [1], the substantially lowest evaluated responsive bid

may or may not necessarily be the lowest priced bid. But, to determine a fully responsive bid, a logical systematic evaluation procedure designed must cover all aspects of bid criteria (Frayda, 2002). A responsive bid could fall in to one of these categories:

- Fully Responsive/Fully Compliant: A bid is said to be fully responsive, if the bid submitted by a bidder is entirely in accordance with the requirements and criteria given in the bid document.
- Substantially Responsive/Substantially Compliant: A bid is substantially responsive when the bid is 'to a large extent' in accordance with the requirements/criteria given in the bid document. Such bid must be without material deviation, reservation, or omission.
- Non-Responsive/Non-Compliant: A bid is said to be non-responsive or non-complaint, if there is any deviation from the required solicitation, or a failure to supply required information or fill in line items on the bid schedule. Any deviation from the requirements of the bid documents is considered non-responsive and should be rejected.

2.2.3 Responsible Bidder

A responsible bidder is a business entity or individual who has the financial and technical capacity to perform the requirements of the solicitation and subsequent contract. He is a bidder that has the experience, integrity, personnel, and equipment to perform the requirements for a contract. The requirements to be a "responsible" bidder vary from owner to owner. However, common issues related to a bid responsiveness include bid submission prior to the bid submittal deadline [3].

2.3 Bids Evaluation Criteria

Evaluation criteria are the standards against which bids are evaluated. Generally, evaluation criteria are categorized into three categories, these include (i) mandatory criteria, (ii) weighted criteria and (iii) weighted criteria with mandatory elements.

(i). Mandatory criteria are used in straight forward bid evaluation methods where they are rated as pass or fail, responsive or non-responsive or comply or non-comply. They are usually used in evaluation for goods procurement and infrastructure projects. The mandatory criteria are the first criteria against which bids are evaluated in order to eliminate bids that do not conform to requirements, especially the product specifications and submittal deadlines [8].

(ii). Weighted criteria are criteria which can be measured in terms of degree of responsiveness. The scale used to measure the degree of responsiveness depends on the procurement method and category of procurement. In accordance with the Procurement Act (section 5) of Nigeria, the following describes the weighted criteria principles in establishing the qualifications of suppliers and contractors. Those that are considered appropriate include:

(a) Technical competence, financial resources, facilities, reliability, experience and reputation of product and personnel to perform the contract
(b) Legal capacity
(c) Solvency
(e) Fulfillment of tax and social security obligations
(d) Absence of criminal record
(f) Satisfactory past performance

(iii). Weighted criteria with mandatory elements are criteria that combined both mandatory minimum requirements defined and weighted criteria. Bid evaluation approach may require different methods and parameters (e.g., using merit point or scoring systems). An effective bid management and tender process is expected

to provide a positive evaluation approach that leads not only to the appointment of appropriate suppliers, but also ensures maximum value and quality [13]. A wholly balanced and highly efficient bid and tender management process is expected to improve the quality of supplies, minimize costs and manage project risks. .

This present study assesses the bids criteria and their index factors. The research also considered existing works on lowest bidding system [2]; [9]; [10]. Most of the study focused only on investigating the effects of lowest bid award system on contractor's efficiency and performance. The work that was used as a benchmark developed a support decision-making system for contractor selection in construction projects based on individual indicators and collaborative indicators [14]. These indicators were used to formulate the problem as a binary optimization problem. The work indeed added value to the body of knowledge, but did not address the challenges of the conventional methodologies. Hence, the need for this optimized model.

3. Research Methods and Material

3.1 Research Design and Approach

This study employed quantitative and qualitative research techniques to formulate the instruments used for the research data collection. Purposive and simple random sampling technique was adopted to draw samples from respondents who have good knowledge and experience about the subject in question, more importantly looking at the nature of building construction industry, the study seeks to solicit information from a section of the population of contractors, consultants, clients and other related professionals who have experience in building construction. The first section of the research instrument present demographic information with respect to gender, age, academic background, professional background of respondents, years of experience in building construction, rank and positions. This aspect was deemed necessary in order to ascertain the reliability and credibility that the information gathered are from experts and professionals in the domain. The second section of the instrument presents research questions using five-point likert scale to collate responses from experts and professionals indicating their level of support to the factors affecting the responsiveness of bids in construction projects. Respondents were requested to answer the research questions in section B measuring the level of support on a five-point likert scale. The third section of the instrument was specifically designed to acquire and assess the compliance of some past projects executed by bidders as per the various criteria listed in the bidding documents based on the logical Yes/No. This section was purposefully administered to selected professionals including Directors of Works and Physical Planning who directly supervised such projects. The study was conducted in selected tertiary institutions and related parastatals in the Western region of Nigeria.

3.2 Data Collection

The main part of the research study is the collection of required data, which were obtained through questionnaire survey developed for the study and personal interviews from the targeted population. The researcher collected a total sample data of 206 as the actual number of respondents. The total number of two hundred and fifty (250) copies of research questionnaire was distributed, 224 were completed and returned, representing 89.6% response rate. The returned copies were scrutinized for errors, omissions, completeness and inconsistencies, and two hundred and six (206) questionnaires were found to be adequately completed representing 82.4%.

3.3 Data Presentation and Analysis

Tables 1 presents the assessed factors that affects the responsiveness of bids in construction projects. All respondents (contractors, clients and consultants) were asked to indicate their agreement regarding these factors in Section B of the research questionnaire on the likert scale of 1 to 5. The mean and standard deviation of the

aggregated agree and disagree variables from the responses were calculated and corresponding relative importance index (RII) computed using equation 1.

$$\text{Relative importance index (RII)} = \frac{\sum w}{AN} = \frac{5n_5 + 4n_4 + 3n_3 + 2n_2 + 1n_1}{5N} \quad \text{.....Equation (1)}$$

W is the weight given to each factor by the respondent, ranging from 1 to 5;
n_1 = number of respondents for strongly disagree;
n_2 = number of respondents for disagree;
n_3 = number of respondents for fairly disagree;
n_4 = number of respondents for agree;
n_5 = number of respondents for strongly agree;
A is the highest weight (i.e. 5 in the study);
N is the total population; and
The RII ranges from 0 to 1.

Table 1: Assessing Factors affecting responsiveness of bids in construction projects

Research Question	SA	A	FD	D	SD	Aggregated Agree	Aggregated Disagree	RII	Rank
RQ1	154	49	0	3	0	203	3	0.943689	1
RQ2	146	56	0	4	0	201	4	0.933981	4
RQ3	152	46	3	5	0	198	5	0.934951	3
RQ4	148	49	2	7	0	202	4	0.928155	8
RQ5	147	50	3	6	0	199	4	0.928155	9
RQ6	135	62	2	6	1	200	4	0.914563	14
RQ7	146	50	5	5	0	200	5	0.927184	10
RQ8	145	55	1	5	0	197	7	0.930097	7
RQ9	146	54	2	3	1	197	6	0.931068	6
RQ10	144	55	2	3	2	196	5	0.926214	11
RQ11	151	50	1	4	0	199	5	0.937864	2
RQ12	147	48	1	10	0	200	4	0.92233	13
RQ13	139	61	2	4	0	195	10	0.925243	12
RQ14	128	51	2	23	2	197	7	0.871845	15
RQ15	150	49	3	2	2	179	25	0.93301	5
Mean value						***197.8***	***6.4***		
Standard Deviation						***5.75***	***5.75***		

3.3.1 The Multi-Parameters Criteria Variables for the Model Building

The multi-parameters criteria evaluation variables are of two levels: the mandatory criteria and the weighted sub-factors criteria as presented in Table 2: Table 3 presented the multi-parameters model format.

Table 2: The Multi-Parameters Criteria Evaluation Variables

S/N	CRITERIA	
A	**MANDATORY CRITERIA**	**LABEL**
1	Meets Submittal Deadline & Project Specification Determination	MSD
2	Is the Lowest bid responsiveness (Bids conforms " Substantially" to the bid specification)	LBR
B	**WEIGHTED AND SUB FACTORS CRITERIA**	
3	Has a history of satisfactory performance	HSP
4	Has good reputation regarding integrity (No petitions for bankruptcy by contractor or principals of contractor)	GR
5	Evidence of financial capability to execute the project by submission of reference letter from a reputable commercial bank in Nigeria indicating willingness to provide credit facility for the execution of the project when needed.	FC
6	Has adequate equipment and facilities for the contract?	AEF
7	Able to deliver according to the contract schedule/bids documents?	ATD
8	Evidence of Certificate of Incorporation issued by Corporate Affairs Commission (CAC) including forms CAC2 and CAC7 or (CAC1.1).	CAC
9	Evidence of company income tax clearance for the last 3 years valid till December 31st of the year award or year in question.	TAX
10	Evidence of current pension compliance certificate valid till December 31st of the year in question.	PEN
11	Evidence of current Industrial Training Fund (ITF) compliance certificate valid till 31st of the year in question.	ITF
12	Evidence of current Nigeria Social Insurance Trust Fund (NSITF) compliance certificate valid till December 31st of the year in question.	NSITF
13	Evidence of registration on the National Database of Federal Contractors, Consultants and Service providers, and submission of Interim Registration Report (IRR) with valid certificate issued by BPP till 31st of the year in question.	NDF
14	Sworn Affidavit disclosing whether or not any officer of the relevant committees of the Tertiary Institution or the Bureau of Public Procurement is a former or present directors, shareholders or has any pecuniary interest in the bidder and to confirm that all information presented in its bid are true and correct in all particulars.	BPP
15	Letter of Authorization as representatives of the original equipment manufacturers (OEMs).	OEM
16	Company Audited Accounts for the last 3 consecutive years	CAA
17	Company's profile with the curriculum vitae of the key staff to be deployed for the project including copies of their academic/ professional qualifications.	CPV
18	Verifiable documentary evidence of at least three (3) similar jobs executed in the last five (5) years including letters of award, evaluation certificates, job completion certificates and photocopies of the project.	JEC

Table 3: Multi-Parameters Model Format

Bidder	MSD	LBR	HSP	GR	FC	AEF	ATD	CAC	TAX	PEN	ITF	NSITF	NDF	BPP	OEM	CAA	CPV	JEC	PREDICTION
B1	Y	Y	Y	Y	Y	Y	Y	Y	Y	Y	Y	Y	Y	Y	Y	Y	Y	Y	QUALIFIED
B2	Y	N	Y	Y	Y	Y	Y	Y	Y	Y	Y	Y	Y	Y	Y	Y	Y	Y	QUALIFIED
B3	Y	Y	N	N	N	Y	Y	Y	Y	Y	Y	Y	Y	Y	Y	Y	Y	Y	NQ
B4	Y	Y	Y	Y	Y	Y	Y	Y	Y	Y	Y	Y	Y	Y	Y	Y	Y	N	PQ
B5	N	Y	Y	Y	Y	Y	Y	Y	Y	Y	Y	Y	Y	Y	Y	Y	Y	Y	REJECTION
B6	N	Y	Y	Y	Y	Y	Y	Y	Y	Y	Y	Y	Y	Y	Y	Y	Y	Y	REJECTION
B7	Y	Y	Y	Y	N	Y	Y	Y	N	Y	Y	Y	N	Y	Y	Y	Y	Y	NQ
B8	Y	Y	Y	N	Y	Y	Y	Y	N	Y	Y	Y	N	Y	Y	Y	Y	Y	NQ
B9	Y	N	Y	Y	Y	Y	Y	Y	Y	Y	Y	Y	Y	Y	Y	Y	Y	N	PQ
B10	Y	N	Y	Y	Y	Y	Y	Y	N	Y	Y	Y	N	Y	Y	Y	Y	Y	NQ

3.4. Model Building Experiment

In the experiment, attribute importance analysis was carried out to rank the attributes used in the study. Information Gain and Gain Ratio attribute evaluators were used on the Waikato Environment Knowledge Analysis (WEKA) platform to rank the relative importance indices of the attributes. The Ranker's Search method was used to achieve this. Out of the eighteen (18) criteria identified, it is observed that the attribute with label MSD (deadline submission and determination of the lowest bid responsiveness) was ranked the first with 0.7692 value in the information gain ratio ranking on the WEKA experiment, followed by the other attributes as presented in Table 4. Figure 1 and Figure 2 depicts the Information Gain and Gain Ratio ranking from the WEKA platform respectively. Figure 3 depicts the graphical comparison of the ranking.

Table 4: Attributes Ranking using Information Gain and Gain Ratio

Information Gain Ranking			Gain Ratio		
Ranked Attributes	**Value**	**Rank**	**Ranked Attributes**	**Value**	**Rank**
MSD	0.7692	1	MSD	1	1
JEC	0.6691	2	JEC	0.943	2
TAX	0.6252	3	TAX	0.678	3
NDF	0.6252	4	NDF	0.678	4
FC	0.2922	5	FC	0.412	5
GR	0.2922	6	GR	0.412	6
LBR	0.1834	7	HSP	0.269	7
HSP	0.1093	8	LBR	0.206	8
NSITF	0.010	9	NSITF	0.010	9
ATD	0.010	10	ATD	0.010	10
AEF	0.010	11	AEF	0.010	11
CAA	0.010	12	CAA	0.010	12
OEM	0.010	13	OEM	0.010	13
CPV	0.019	14	CPV	0.196	14
BPP	0.019	15	BPP	0.196	15
ITF	0.019	16	ITF	0.196	16
PEN	0.019	17	PEN	0.196	17
CAC	0.019	18	CAC	0.196	18

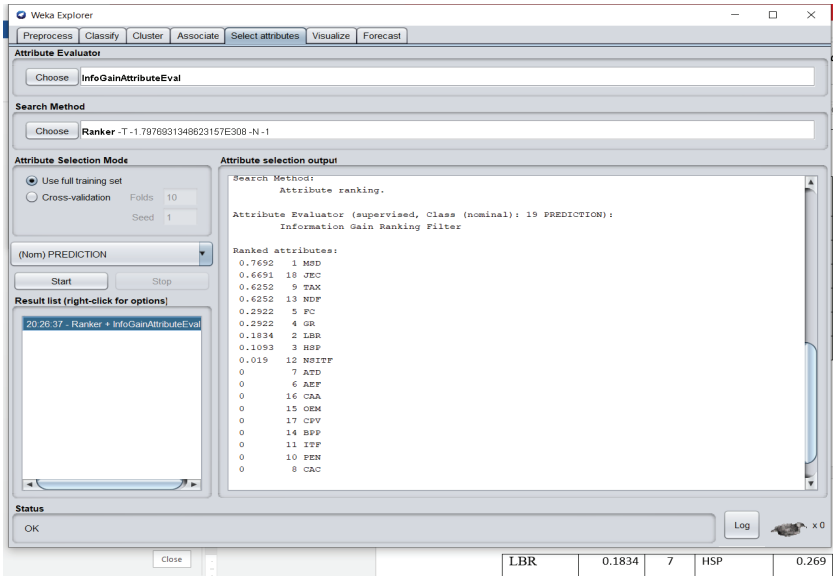

Figure 1: Information Gain Ranking Information

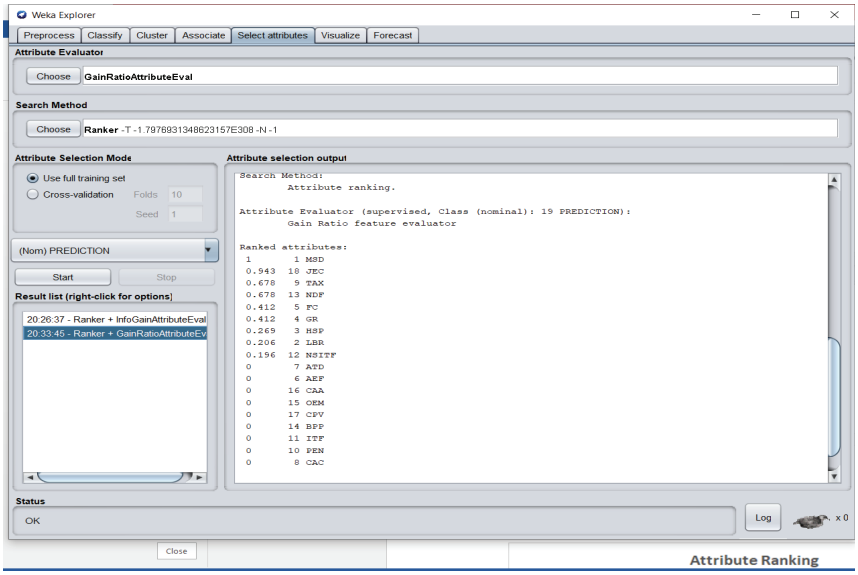

Figure 2: Gain Ratio Ranking Information

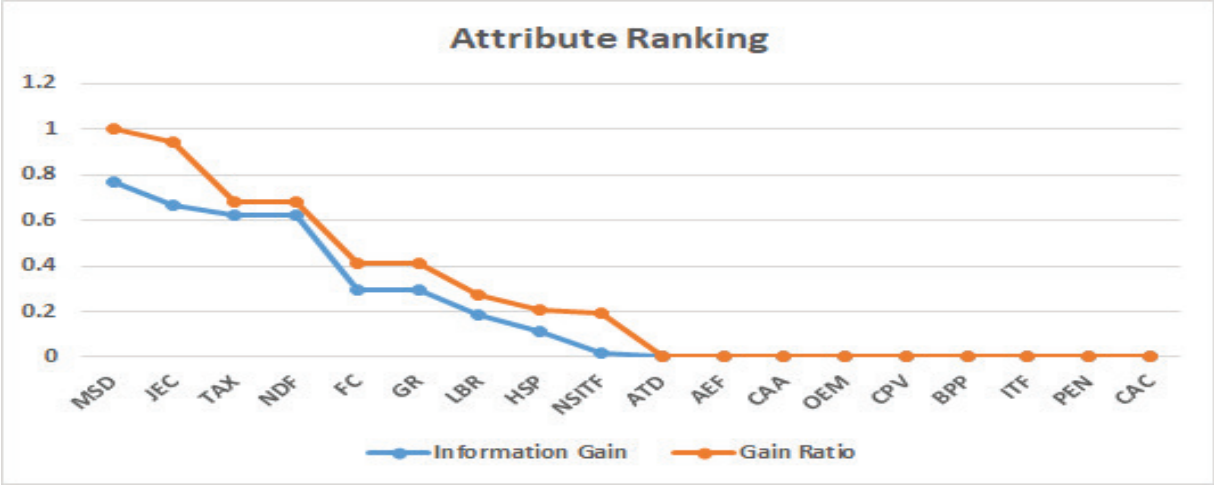

Figure 3: Information Gain and Gain Ratio Ranking Chart

During the model building, the datasets for the experiment was divided into two. By default 66% of the datasets was devoted to training while the remaining 34% was used for testing of randomly selected new data. Ten (10)-fold cross validation test mode also was used to validate the modeling. The 10-fold cross-validation test mode was considered the best since it produced the best model. The 10-fold cross validation mode have been widely used, and it is described a better option to determine the performance of a classifier [15]. Four (4) different classification algorithms from two classifier family of Decision Tree and Rule Inductions were used for the modeling. The Pruned Decision tree and Logistics Model Tree (LMT) belong to the Decision Trees family, while Justified Repeated Incremental Pruning (JRip) and PART belongs to Rule Inductions. The classifiers were tested on the datasets to determine the classifier that best models the data with best predictive accuracy. The performance of the algorithms based on the two modes was carried out using standard metrics of accuracy, precision, recall and f-measure for classification as shown in Table 5.

Table 5: Performance Metric for all the classifiers considered in the modeling

Classifiers	Pruned Decision Tree		LMT Logistics Model Tree		JRIP Justified Repeated Incremental Pruning		PART	
Measure Evaluation	10 fold - Cross-Validation	Percentage Split (66/34)%	10 fold - Cross-Validation	Percentage Split (66/34)%	10 fold - Cross-Validation	Percentage Split (66/34)%	10 fold - Cross-Validation	Percentage Split (66/34)%
Total Number of Instances	160	54	160	54	160	54	160	54
Time taken to build model:	0.01 sec	0.1 sec	0.05 sec	0.25 sec	0.1 sec	0.1 sec	0.1 sec	0.1 sec
Correctly Classified Instances	99.4%	100 %	99.3%	100%	99.4%	100%	99.3%	100%
Incorrectly Classified Instances	0.6 %	0 %	0.7%	0%	0.6%	0	0.6%	0
Kappa statistic	0.9912	1	0.9912	1	0.9912	1	0.9912	1
Mean absolute error	0.0062	0.0041	0.0682	0.0641	0.0062	0.0034	0.0062	0.0034
Root mean squared error	0.0571	0.0151	0.1067	0.09	0.0571	0.0134	0.0571	0.0134
Relative absolute error	1.7452%	1.1588%	19.193%	17.8575%	1.7452%	0.9502%	1.7452%	0.9502%
Root relative squared error	13.5421	3.5982%	25.3095	21.0288%	1.5421%	3.13%	1.5421%	3.13%
TP Rate (Weight Average)	0.994	1	0.994	1	0.994	1	0.994	1
FP rate (Weight Average)	0.001	0	0.001	0	0.001	0	0.001	0
Precision	0.994	1	0.994	1	0.994	1	0.994	1
Recall (Weight Average)	0.994	1	0.994	1	0.994	1	0.994	1
F-Measure (Weight Average)	0.994	1	0.994	1	0.994	1	0.994	1
ROC Area (Weight Average)	0.995	1	0.998	1	0.995	1	0.995	1

From the performance metrics, the Pruned Decision Tree and the JRip rules performed better than the other two algorithms in the layers. The duo have the same correctly classified instances of 99.4%, mean absolute error of 0.062, True positive (TP) rate and False positive (FP) rate of 0.994 and 0.001 respectively, ROC Area of 0.994 and recall weighted average of 0.994 respectively. This ascertains that both algorithms are suitable for the model. However, the pruned decision tree was chosen as the best algorithm in this study because it has a lesser time of 0.01 seconds to build the model compared to JRip with 0.1 seconds. Additionally, pruned decision tree algorithms generally has this ability to produce a simple tree structure with high accuracy in term of classification rate [16]. Pruning methods have been introduced to reduce the complexity of tree structure without any decrease in classification accuracy. The standard metric details of the decision tree, its tree structure and rules classification as generated by WEKA are presented in Figure 4 and Figure 5 respectively.

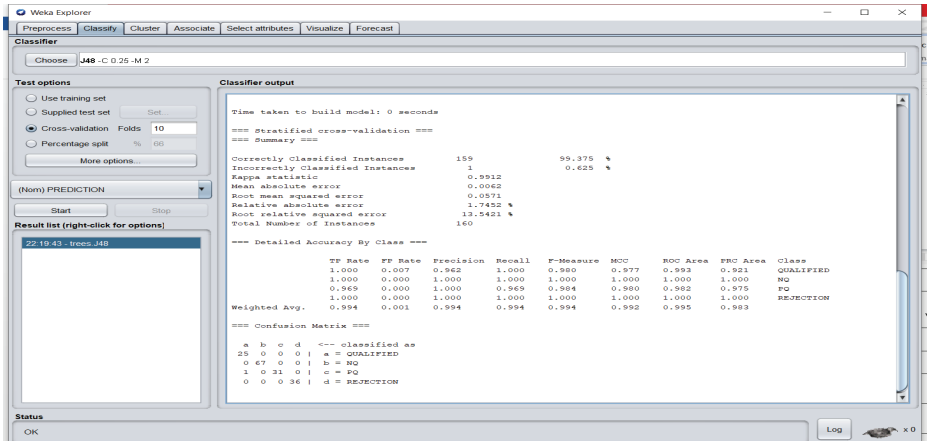

Figure 4: Standard Performance Metrics of Pruned Decision Tree

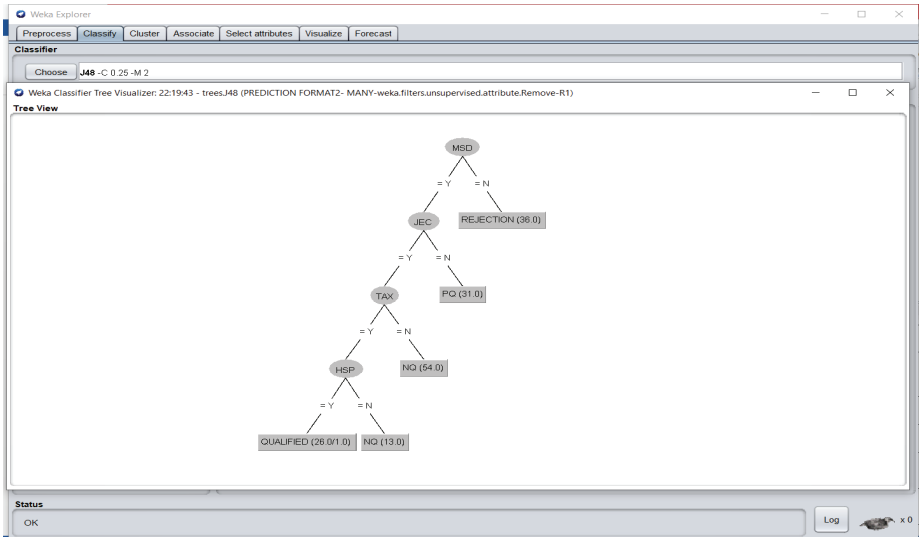

Figure 5: Pruned Decision Tree Structure

3.5 Rules Generation and Mathematical Model

Few of the rules generated from the best algorithm (pruned decision tree) are stated as follows:

Rule 1: IF MSD = Y and JEC = Y and TAX = Y and HSP = Y THEN Recommendation = QUALIFIED

Rule 2: IF MSD = N and JEC = Y and HSP = N and TAX = N THEN Recommendation = REJECTION

Rule 3: IF MSD = Y and JEC = Y and TAX = Y and HSP = Y THEN Recommendation = PQ (MAY BE CONSIDERED)

Rule 4: IF MSD = Y and JEC = N and TAX = N and HSP = Y THEN Recommendation = NOT QUALIFIED

Rule 5: IF MSD = Y and JEC = N and TAX = Y and HSP = N THEN Recommendation = NOT QUALIFIED

Rule 6: IF MSD = N and JEC = Y and TAX = Y and HSP = Y THEN Recommendation = NOT QUALIFIED

The whole rules cannot be exhausted here, a back-end for updating the rules as the situation arises will be incorporated into the system to match other conditions.

3.6 Architecture of the Bid Responsive Evaluation Model (BREM)

Architecture of the Bid Responsiveness Evaluation Model (BREM): The architecture as shown in figure 6 is composed of six (6) major components: namely the bids criteria databank, consisting of the (mandatory criteria and weighted sub-factors criteria) components, the mandatory criteria measure whether the bid is responsive, while the weighted sub-factors measure whether the bidder is responsible. The second component is the data preprocessing, which involves data filtering and cleaning to remove noisy data and make it formatable for modeling. The third component is the data modeling, built using WEKA platform, the fourth component is the model output, which is the pattern that is generated from the experiment, and will be subjected to the fifth component which is the evaluation and selection mechanism component for final recommendations output.

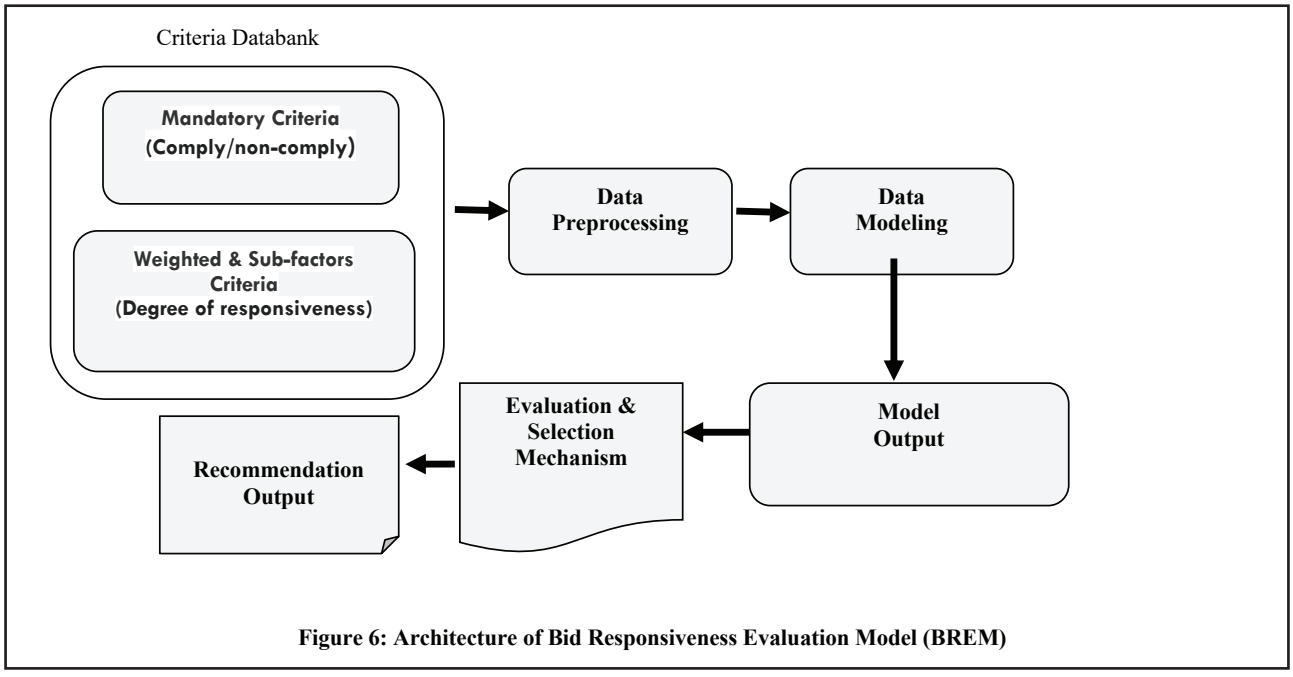

Figure 6: Architecture of Bid Responsiveness Evaluation Model (BREM)

Process flow of the model: Firstly, the mandatory criteria determines the bids that meet with the submittal deadline, coupled with the determination of the bids that meets the bid specification. Secondly, the conditions above are tested to determine whether the lowest bid cost is also responsive. If considered substantially conformed to the bids specifications, it goes for the next stage, and if not, such bid is rejected and the next lowest proposed cost bids are tested. The next stage then determine whether the lowest bidder is responsible or not considering the quality, past performance and time specified for performance in the bidder's proposal. Bidder's skill, financial capability, ability and integrity are determined. The final stage determine if the lowest bid is responsive and lowest bidder is responsible. If the two conditions are met, the contract is awarded to the contractor that qualifies

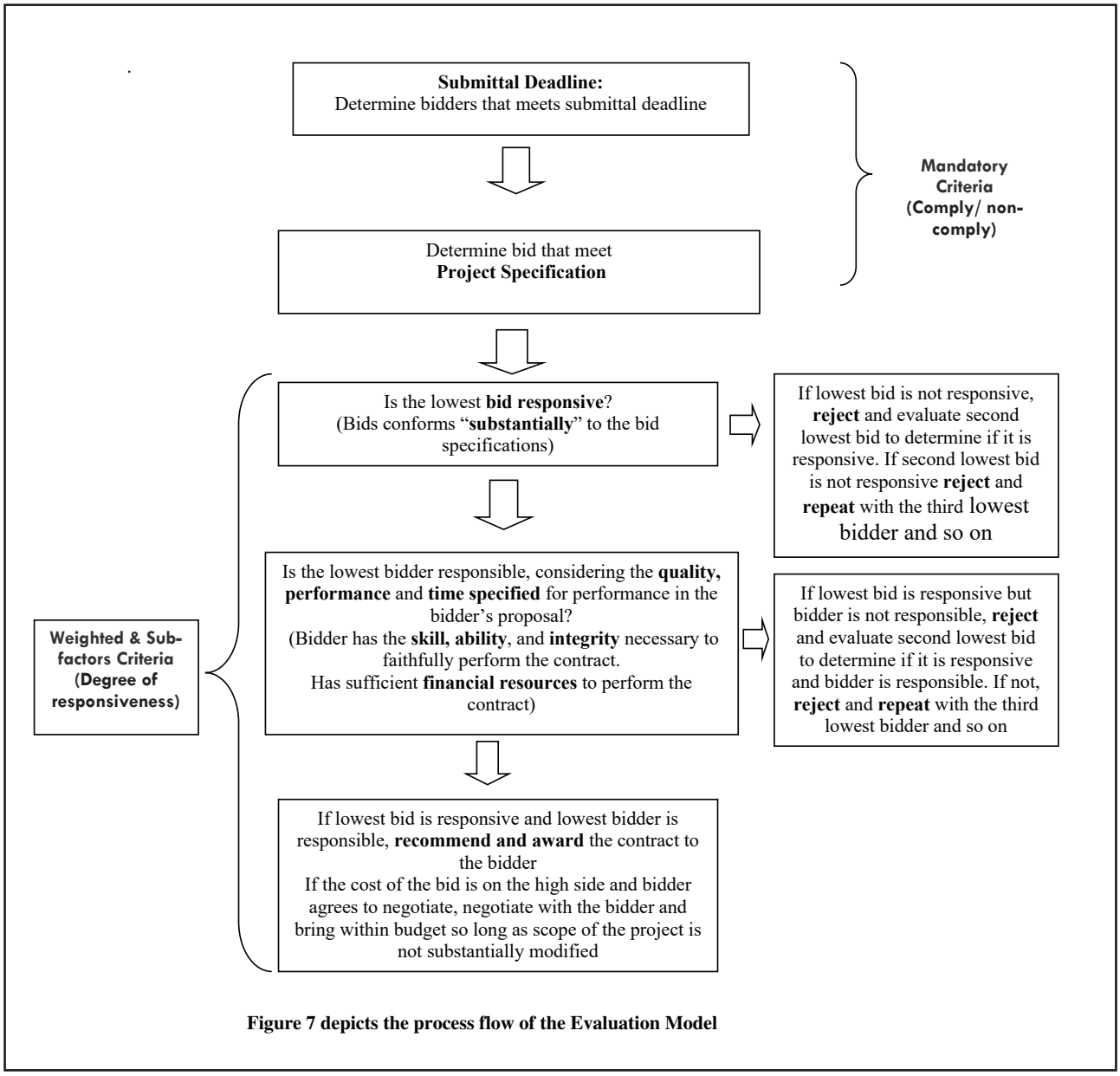

Figure 7 depicts the process flow of the Evaluation Model

Conclusion

The quest for an optimized evaluation method to overcome the challenges of the customary practice of bid evaluation in the public procurement and construction projects motivated this research. The research was focused at developing an optimized model for evaluation based on bids responsiveness strategy. To achieve the objectives of the research work, the researcher established a theoretical foundation for the research work through a considerable review of literature and consultations to find out what was already done in the field. A research instrument was developed using quantitative and qualitative techniques to collect respondents perceptive and evaluate the responses as regards their markup choice between bid responsiveness and lowest bid system. The study adopted purposive sampling technique and the targeted population comprises of contractors, consultants, clients and other civil engineer professionals. Various criteria outlined in bidding documents of construction projects and factors affecting the success of bids in construction projects were identified and assessed. Fourteen (14) identified factors affecting bid responsiveness in construction project were presented and ranked. Ability to comply with the bids specification criteria, financial capabilities, good history of satisfactory past performance as well as overall good reputation, are considered the key factors affecting bid responsiveness in construction projects. The model presented was tested and met its objectives. The model showed to be an improvement over the classical methodologies. When fully implemented, it will suitably improve the efficiency in the bid system and quality delivery in general construction projects. Therefore, the model is highly recommended for efficient bid evaluation in general procurement and construction projects.

6. References

Letarge, B, Quezon, E T & Macarubbo, Y. C (2016). Evaluation on the Performance of Lowest Responsive Bid Contract and the Quality of Materials Used on Governmental Building Projects in Jimma Town. *International Journal of Scientific & Engineering Research,* 7(12), 60-73.

Tariq, H. K & Abdul Q. K (2015). Effects of Lowest Bidding Bid Awarding System in Tertiary Institutions Construction Projects In Pakistan. *Developing Country Studies* www.iiste.org ISSN 2224-607X (Paper) ISSN 2225-0565 (Online) 5(3), 132-146.

Satya, V (2017). Evaluation of Bids to Determine 'Substantial Responsiveness'. October.

Oregon (2020). Definitions for Public Contracting Code. 2020 ORS Vol. 7 Chapter 279, A Section 279A.010. Oregon laws.org

Corporate Finance Institute (CFI) (2016). Competitive Bidding. Retrieved online from https://corporatefinanceinstitute.com/resources/knowledge/other/competitive-bidding/ on 09/02/2021.

Oyeyipo, O. O., Odusami, K. T., Ojelabi, R.A., & Afolabi, A.O.(2016). Factors affecting contractors' bidding decision for construction projects in Nigeria. *Journal of Construction in Developing Countries,* 2016. 1(1) 1-21

Aaron, K.D (2020). The Bid Evaluation Process. The Procurement Classroom. Retrieved on 24/09/2020 from https://procurementclassroom.com/the-bid-evaluation-process/

Schreyer, P (2020). What is a "Responsive, Responsible" Bidder? *JOC Operations for the Northeast Region. Retrieved 24/09/2020 from* https://www.gordian.com/resources/what-is-a-responsive-responsible-bidder/

Shumank , D., Mohd, B. K., Sabih, A & Adeeba, S (2017). A study of Various Factors Affecting Contractor's Performance in Lowest Bid Award Construction Projects. *International Journal of Civil Engineering and Technology*, 8(2), 28–33. http://www.iaeme.com/IJCIET/issues.asp?JType=IJCIET&VType=8&IType=2.

Woo, S. Lee, S, Cho, C.S & Kim, S.B (2017). Study on the issues of the lowest bidding through the analysis of working budget ratio of Korean construction companies. *KSCE Journal of Civil Engineering* volume 21, 1587–1594. [10]. Frayda, S. B (2002). Understanding the Responsiveness Requirement in Competitive Bidding. *Local Government Law Bulletin* No. 102 (May 2002), available at http://www.sog.unc.edu/pubs/electronicversions/pdfs/lglb102.pdf.

CIDB (2008). Construction Industry Development Board. Best Practice Guideline #A3 Evaluating tenders offers. Fifth edition of CIDB document 1003. Available at (www.cidb.org.za).

Frayda, S. B (2002). Understanding the Responsiveness Requirement in Competitive Bidding. Local Government Law Bulletin No. 102 (May 2002), available at http://www.sog.unc.edu/pubs/electronicversions/pdfs/lglb102.pdf.

Opus Kinetic (2019). Bid Management and tender Evaluation. http://www.opuskinetic.com/training

Liang, R, Sheng, Z, Xu, F & Wu, C (2016). Bidding Strategy to Support Decision-

Making Based on Comprehensive Information in Construction Projects. *Discrete Dynamics in Nature and Society*. Hindawi Publishing Corporation. 2016(1)1-15. https://doi.org/10.1155/2016/4643630.

WEKA,(2011): WEKA Tutorial. The University of Waikato (2011). *Available at*: http://www.cs.waikato.ac.nz/ml/weka/, (Accessed 20 July, 2013).

Mohamed, W. Nor Haizan W, Mohd N. S, & Abdul H. O (2012). A Comparative Study of Reduced Error Pruning Method in Decision Tree Algorithms. *IEEE International Conference on Control System, Computing and Engineering*, 23 - 25 Nov. 2012, Penang, Malaysia.

Determination of the Lumbar Lordotic and Lumbosacral Angles in Normal Adults Ghanaian Population Using Radiologic Imaging Technique

***Issahaku Shirazu[1,2], Eric Sackey[2], Elvis K. Tiburu[2], Theophilus A. Sackey[1].**

[1]Radiological and Medical Sciences Research Institute, Ghana Atomic Energy Commission, Accra-Ghana.
[2]Department of Biomedical Engineering, University of Ghana, Legon-Accra, Ghana
***Corresponding Author:** *shirazu.issahaku@gaec.gov.gh, or sissahaku@ug.edu.gh or sissahak@ictp.it

Abstract

Changes in posture is among the risk factors of low back pain. The shape of the lumbar spine is influenced in a way by a strain on tendons and muscles because of abnormal posture. Little is known about what the nominal value of key radiologic angles for the Ghanaian populace is and accordingly, what comprises hypo-/ hyper-lordosis. The Lumbar Lordotic Angle (LSA) and Lumbosacral Angle (LSA) are potential angles, for the examination of low back issues, in addition to treatment and diagnosis. The study was intended to measure LLA and LSA of this populace using the local data. A retrospective methodology was adopted to gather typical laterally prostrate lumbosacral radiographs of 140 subjects (15 years or more) in a recumbent position.

Results:

The normal LLA values varied between 20.9^0 to 68.0^0 with the mean (standard deviation) of 35.9 (9.82)° and there exist a significant difference with sex but insignificant variations among the age categories comparable to a number of the literature values. The normal LSA values varied between 15.0^0 and 51.0^0 with the mean (standard deviation) of 34.3 (7.45) ° and there was no significant variation with sex and among the age categories.

Conclusion:

Furthermore, it has been established that the measured values at which to consider hypolordosis (below LLA=17.9°; LSA=12.0^0), and hyper-lordosis (above LLA=72.0°; LSA=55.0^0) in the Ghana population. This study have also established that in all the various age groups between 15 and 80 years, there exist no significant difference in the mean LLA and LSA among the groups, and this affirms that the development of lumbar lordosis reaches a plateau when spine is fully developed. Furthermore, female LSA and LLA shows higher measured values compared to their male counterpart in the Ghanaian population which confirmed other study values in literature. Finally, a reference chart of LSA and LLA has also been developed for clinical application in Ghana.

Key words: Lumbar Lordosis, Lumbosacral, radiographs, retrospective, lateral, diagnosis

Background

Estimations of the angles of curvature of human body are applicable of describing a low back pain, which are significant medical problems because of the diagnosis and therapy challenges. Ongoing research recommends that notwithstanding the morphology of the bend of lumbar spine which is a helpful measure for the conclusion of low back (waist) torment, there might be a hereditary component. Numerous examinations have assessed the connection between varieties in the angle of the lumbar spine and back pain (1). In the light of these recommendations, there has been various methodologies and strategies to gauge and measure Lumbar lordosis

that prompts lower back pain. These methodologies are comprehensively sorted into conventional radiographic and non-radiographic techniques. Examples of Non radiographic strategies include the following, adaptable rulers, spinal mouse, inclinometer spinal pantograph, and magnetic resonance imaging etc (2). The spinal mouse and adaptable ruler approaches are tedious and can hence not be effortlessly utilized where there is the requirement for snappy feedback response. Then again, the disadvantages of the radiographic strategy incorporate irradiation, generally significant expense of assessment, restricted equipment space and time to acquire and peruse the image. Despite these downsides of the radiographic method, it remains the highest quality level which allows precise measurement of the Lordotic angle in a lateral spine radiograph (3). The radiographic technique is one such modality and a prostrate lateral lumbosacral spine radiograph precisely measures Lumbar lordosis that agitates lower back pain. Among the clinically significant radiographic angles for the assessment of Lumbar lordosis, research uncovers that the Lumbar

Lordotic Angle (L.L.A) and Lumbosacral Angle (L.S.A) are critical in the physical life of the individual's life (4, 5, 6, 7). Lumbar Lordotic Angle (L.L.A) is for the most part and generally determined by the Cobbs Method or procedure where lines are drawn along the superior end plates of the lumbar vertebrae to reach out past the vertebral body. Perpendiculars are then added on the side of convergence of the two lines, and the point of the convergence of these perpendiculars is estimated, forming Cobb's angle, which subsequently has given a worldwide assessment of lumbar lordosis (8, 9). Lumbosacral Angle (L.S.A) is measured using the Ferguson's technique.

Lamentably, there is next to zero data about what the typical estimations of these radiologic angles for the Ghanaian populace is. This study is consequently pointed toward quantifying the normal values of the Lumbar Lordotic Angle (L.L.A) and Lumbosacral Angle (L.S.A) of the Ghanaian populace using five referral health facilities Government Hospital as contextual analysis.

Aim

The aim of this study is to quantify the Lumbar Lordotic Angle (LLA) and Lumbosacral Angle (LSA) and to classify the quantified values as constitutes hypo/hyper lordosis, for Ghanaian population.

Scope

This is a retrospective study to measure both Lumbar Lordotic and Lumbosacral angles in intact lateral supine radiographs of 140 Adults (above 15 years) collected across the country. This study was also facilitated by an extensive literature review related to his study, data collection and analysis using readily available software, testing of hypothesis, evaluating relationships and finally interpretation of the results. Conclusion was drawn and deductions were made from the accumulated results which was an agreement or rejection of the hypothesis specifically null hypothesis.

Literature on the Methods of Measurement

Numerous techniques are utilized to assess the curvature of the lumbar spine. Notwithstanding, there are two normal techniques for assessment; this includes; physical clinical examination and diagnostic image assessment (10). Clinical examinations assess the extent of lordosis directly on the person's body. Diagnostic image assessment utilizes tomography, radiographs, and magnetic resonance imaging. Every strategy for assessment has its advantages and detriments, yet the serious issue is that it is hard to look at the estimations when performed by various approaches. Clinical techniques for assessing lordotic angles incorporate different posture examination systems and surface geography systems (11). A large portion of these strategies utilize the spinous processes of the lumbar vertebrae to assess the extent of lordosis. The fundamental bit of these estimations is the utilization of non-radiological techniques, this permit incessant assessment of the spinal bends or the lordosis angle. Even though clinical strategies have a good reproducibility,

radiologic techniques are better with an interobserver accuracy of 87% (12, 13 14 15).

A couple of articles have proposed the utilization of laser and electronic technologies to estimate the lordotic angle. Using an adaptable plastic ruler and an AutoCAD for lordotic angle estimations, Letafatkar et al. demonstrated that these techniques are reliable technique, and suggested the use of these techniques as alternative to the radiography method in assessing lumbar lordosis. Celan et al (16). estimated the lordotic and kyphotic angles utilizing a laser triangulation strategy with accurate precision. Additionally, in spite of the fact that there are advanced 3D posture examination frameworks for displaying and measuring LLA, for example, Optotrak, Vicon Motion Systems, Motion Analysis and surface geography systems. Unfortunately, these systems are not open for most clinicians even though despite its numerous advantages in assess the lordotic angle in various stances and settings 916). Hence it is conclusive to suggest that using clinical strategies using radiologic method for assessing lordosis angles is still a better option to the many proposed techniques due to the unreliable results from most of these techniques.

Radiologic Measurement of Lumbar Lordosis (LL)

Different efforts have been made to quantify the Lumbar Lordosis measuring technique; nonetheless, as researchers have significantly shown that radiography is still a better technique, with a prostrate lateral lumbosacral spine radiograph to precisely measures LLA (17, 18, 19). Clinically there are a number of radiographic angular measuring technique that are available to be use to measure Lumbar Lordosis include lumbosacral angle (LSA), Lumbar Lordotic Angle (LLA)/Cobb point, Sacrohorizontal point and Sacral Inclination angle (SIA). However, the widely used and most accepted method and technique in measuring radiographic Lumbar Lordosis is the Cobb method and the Ferguson's angle technique (18, 19). These two accepted methods are used to estimate scoliosis using the LSA and LL angle among others, hence has been adopted in this study.

Materials

Materials used include the digital X-ray equipment and the MeVisLab DICOM application software for image analysis. The X-ray was used to acquire the images of the lumbar spine while the MeVisLab DICOM application software was used to view and measure the various angles.

X-ray Machine

Digital image data was retrieved from the PACS which were acquired by the x-ray machine with the following detailed specifications and features shown in figure 1 and Table 1.

Figure 1: X-Ray Machine (YSX200G)

Table 1: Specification of X-ray Equipment

CONTENTS	**YSX200G**
Intermittent mode	100kV, 200mA, 20kW
Tube current	16mA~200mA
Output voltage	40-125KV step by 1kV
Exposure time	0.0025s~6.4s adjustable
Anode rotating speed	2800r/min
Anode heat capacity	140KHU
Focus	Small focus:1.0mm & Big focus:2.0mm
Focus distance	100cm

Normal and Abnormal Images

Normal radiographs as shown in Figure 2A, of the lumbar spine were used for the study. Radiographs that were judged by experience radiologist to be abnormal as shown in Figure 2B were excluded in the study. Below is the representation of normal and abnormal curvature of lumbar spine radiograph in a recumbent position for Female (Figure 2A and 2B) and Male (Figure 3A and 3B).

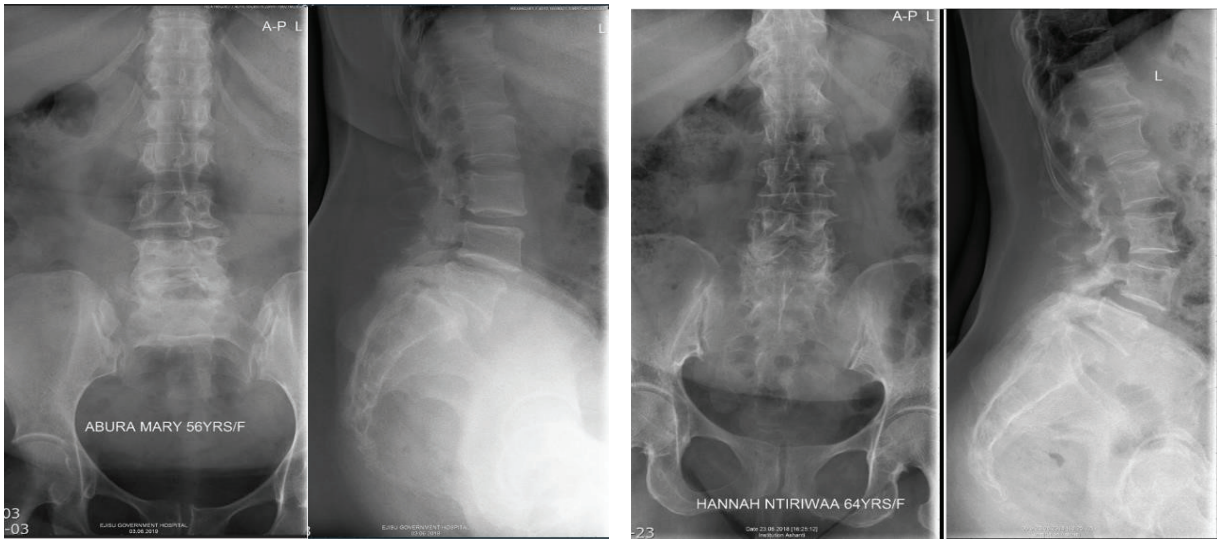

A **B**

Fig 2: Female normal curvature of spine (A) and abnormal curvature (B) of the lumbar spine

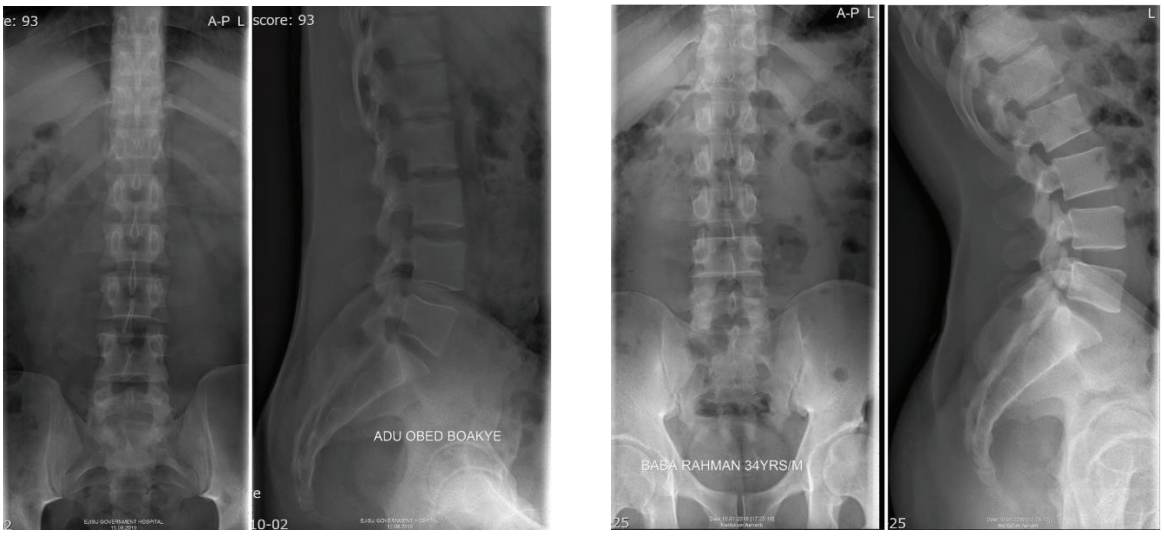

A **B**

Fig 3: Male normal curvature of spine (A) and abnormal curvature (B) of the lumbar spine

MeVisLab DICOM Application Software

MeVisLab is an application framework for medical image processing and scientific visualization. It includes advanced algorithms for image registration, segmentation and quantitative morphological and functional image analysis. There is also an integrated development environment (IDE) for graphical programming. MeVisLab is an integrated platform for medical image processing and visualization. It features a high quality volume renderer known as Giga voxel renderer that is based on OpenGL. The software supports rendering of large volume datasets based on an Octree algorithm, which takes the region of interest (ROI) into consideration. The software incorporates active contour model (Snake technique), which is a framework in computer vision for delineating outline of objects in a 2D image space. This advance application software was used in viewing and measuring LSA and LLA with 99.9% accuracy and precision.

Methodology

A retrospective study design approach was used for this study where the Lumbar Lordotic Angle (L.L.A) and Lumbosacral Angle (L.S.A) of healthy lumbar spine radiographs were measured. This was done, using radiograph which were taken in the recumbent position among 140 sampled patients' images with age and gender variation of adult patients.

The largely accepted Cobb's method, was used in this study which was done as follows:

A tangent line was drawn along the superior end of L1 and another one at the superior end of S1 vertebra.

Perpendiculars lines to each of the tangential lines were also drawn to form Lumbar Lordotic Angle (L.L.A) as shown in Figure 4A.

The Lumbosacral Angle (LSA) was obtained by drawing two lines, the first line across the upper border of the sacrum and the lower border of the L5 vertebra using the Ferguson's technique as shown in Figure 4B.

Figure 4: A) LLA Measurements B) LSA Measurement

Selection Criterion

The selection criterion includes normal radiographs of adults age 15 and above that include the following:

It must be declared as accepted radiography (2A and 3C) on a scale of 4 out of 5 by radiologist.

All the five lumbar sacral vertebras must be present in the radiograph

The age and gender variation must be clearly visible on the radiograph

There must be no expansion in vertebral range from L1 to L5.

Patients under 15 years old, or whose age as well as sex were not recorded were excluded

Low quality radiographs and radiographs indicating uncertainty or inherent anomaly were exempted.

Data Collection

Measurements of Lumbar Lordotic Angle (LLA) and Lumbosacral angle (LSA) were recorded from radiographs of normal patients. However, 25% of the data included radiographs of abnormal in nature who were diagnose of suffering from low back pain. This was to enable the difference between normal LLA and LSA to be established. The Lumbar Lordotic Angle was measured using Cobbs Method while the Lumbosacral Angle was measured using the Ferguson's technique.

Data Analysis

Data was analyzed using Minitab statistical tool. The analyzed data was represented in tables, charts and graphs. Both descriptive and inferential statistical analysis was performed on the data to quantify the normal value of the Lumbar Lordotic Angle (L.L.A) and Lumbosacral Angle (L.S.A) of the Ghanaian population and distinguished the normal measured values from the abnormal values. Statistical models tool were also used to establish how LSA, LLA and age variation were interrelated with reference to gender.

Ethical Consideration

Approval was obtained from the Ethical and Protocol Review Committee of the College of Basic and Applied Science, University of Ghana and the participating facility and the Department for the radiographs to be use for this study.

Declarations:Ethics approval

Approval was given for the research by the ethical and Protocol Review Committee of the College of Basic and Applied Science, University of Ghana, and the Participating Health Facilities. Additionally, the protocol and the application of same for this study was granted ethical clearance by the Committee. All participants were assured of confidentiality and anonymity throughout the study. The approval of the study was done in accordance with relevant guidelines and regulations of the Ethical and Protocol Review Committee of the College of Basic and Applied Science.

Consent to participate.

All the participants were adults of age 18 years or more. Each participant gave informed consent at study entry and offered the choice to exit from the study at any point during data collection without providing a reason for doing so.

Consent for publication

Not Applicable

Availability of data and materials

The data raw and comprehensive research materials to be use for the publication are all available upon request at any time.

Competing interests

Not Applicable

Funding

Not applicable

Authors' contributions

All the Authors were involved in Data collection and analysis during the study.

The following specific activities were done by the Authors.

Concept Note: Issahaku Shirazu and Eric Sackey

Pre-data collection activities including application for ethical clearance: Issahaku Shirazu, Elvis K Tiburu and Eric Sackey

Data collection and analysis: All Authors (Issahaku Shirazu, Eric Sackey, Elvis K. Tiburu, Ken Dapaa, Theophilus A. Sackey)

Drafting of Text: Issahaku Shirazu, Eric Sackey and Elvis K. Tiburu

Review of Text: Issahaku Shirazu, Eric Sackey, Elvis K. Tiburu, Theophilus A. Sackey

Statistical analysis: Issahaku Shirazu, and Isaac Dapaah

Acknowledgements

I knowledge Korle-Bu Teaching Hospital, Accra and Komfo Anokye Teaching Hospital, Kumasi for their support during the data collection and proving ethical clearance for the study.

Results and Discussion

Demographics

The figure 5 show a representation of the gender distribution of 140 radiographs that was analysed. Out of the sample population of 140, 71 patients were females representing 50.7% and 69 were males which represents 49.3 % of the total studied radiographs.

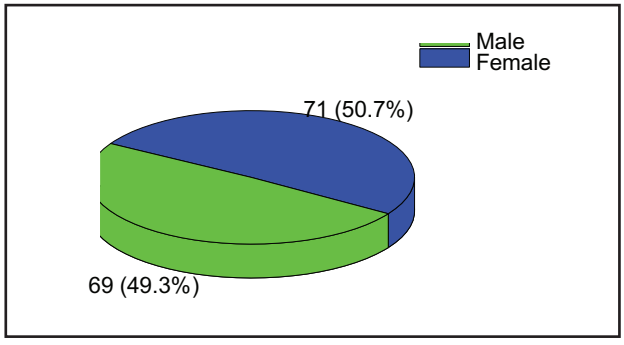

Figure 5: Gender Distributions from Radiographs

This study is a retrospective study where Lumbar Lordotic Angle (L.L.A) and Lumbosacral Angle (L.S.A) measured using the radiograph of the lumbar spine. Descriptive statistic analysis was use to compute the mean, range and standard deviation of the various parameters, in terms of sex, age, and the radiologic angles.

One Sample T-Test was conducted to ascertain the significant difference between the measured mean and other published data. The null hypothesis of this test was that there is no difference between the mean measured values and the published data. For a computed P-value greater than α- level (**0.05**) at **95%** confident interval, it implies that the null hypothesis was accepted that there is no significant difference in the mean values. For a computed P-value lesser than or equal to α- level (**0.05**) at **95%** confident interval, it also implies that the null hypothesis is rejected and the alternate hypothesis is accepted that, there is a significant difference between the mean values of interests.

Independent Sample T-Test was used to establish whether or not there is any significant difference in the mean value of a common variable among the male and female population of this study. The null hypothesis of this test is that there is no difference between the mean values of the two groups. For a computed P-value greater than α-level (**0.05**) at **95%** confident interval, it implies that we accept the null hypothesis that there is no significant difference in the mean values. For a computed P-value lesser than or equal to α-level (**0.05**) at **95%** confident interval, it also implies that we reject the null hypothesis and accept the alternate hypothesis that, there is a significant difference between the mean values.

Table 2: Descriptive Statistics

Variable	Mean	Minimum	Maximum	Std. Deviation
Age (years)	41.19	80	18	13.92
Lumbar Lordotic Angle (degrees)	35.9	20.9	68.0	9.82
Lumbosacral Angle (degrees)	34.3	15.0	51.0	7.45

Table 2 shows a summary of the descriptive statistics of the 140 radiographs. This were presented as the mean, the minimum, maximum values and the standard deviation. The average age was **(Mean=41)** with a standard deviation of **(SD=14).** The high SD means a broad range of the sample population with a minimum and maximum ages between 18 years and 80 years respectively and a mean age of 41±14 (27-55) years. Considering the measured values of the Lumbar Lordotic Angle (LLA), the computed average value was **(Mean= 35.9^0)** with a standard deviation of **(SD= 9.82).** The measured minimum and maximum angles were 20.9^0 and 93.0^0 respectively. Furthermore, the measured values of the Lumbosacral Angle, the computed average value was **(Mean= 34.3^0)** with a standard deviation of **(SD= 7.45).** The associated minimum and maximum angles were 15.0^0 and 68.0^0 respectively. This implied that the mean values of the LLA and LSA was **$35.9^0 \pm 9.82$ (26.08-45.72)** and **$34.3^0 \pm 7.45$ (26.85 – 41.75)** respectively.

Table 3: **Analysis of gender variation**

Radiologic Angle	Gender	sample	Mean	Std. Deviation
Lumbar Lordotic Angle	Female	71	37.5^0	11.32
	Male	69	34.3^0	7.73
Lumbosacral Angle	Female	71	35.1^0	8.31
	Male	69	33.4^0	6.40

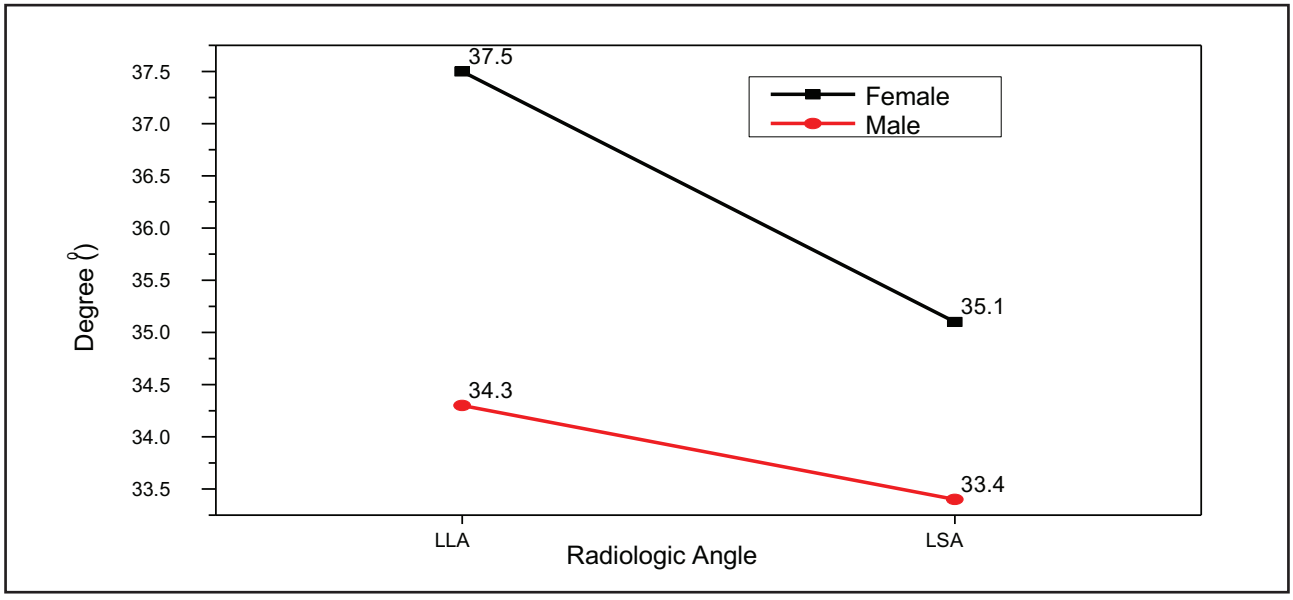

Figure 6: mean values of radiologic angles for Females and Males

The table 3 shows a summary of the group statistics of the radiologic angles with reference to the gender distribution. The general observation from figure 6 shows the average, LLA value **(37.5^0)** for females is comparatively higher than that of the males **(34.3^0).** Similarly, LSA values shows that females **(35.1^0)** is higher than the corresponding average value for males **(33.4^0).** These observations are similar to reported literature from other studies. In the Caucasians study, Bryan reported LSA changes in the range of 15° and 25° and that males have lower values than females. Okpala in his 2016 study using 279 subjects reported LSA values of 45.5^0 and 43.4^0 for females and males respectively. This trend was repeated in his study in 2018 using 200 subjects, where he reported LSA values of 45.2^0 and 43.1^0 for females and males respectively. In this study, the measured LLA values were 52.4^0 and 47.4^0 for females and males respectively. Following these observations in the difference in radiologic angles between females and males, an Independent Sample T-Test was conducted to validate whether the observed difference is statistically significant. The results of the analysis are shown in Table 4.

Table 4: T-Test for similarity of average values

Radiological Angle	t Value	Difference in mean values	Std. Error Difference	P-Value
Lumbar Lordotic Angle	1.95	3.21	1.64	**0.05**
Lumbosacral Angle	1.32	1.66	1.26	0.19

The outcome of the analysis as shown in Table 4 shows that there is a statistically significant difference between the female and male LLA measurements. This implies that the average LLA value measured for females in this study is significantly higher than that of males. This is based on the P-value which was equal to significance level of 0.05. This measured value is similar to the study conducted by Okpala which compared four radiologic angle. He mentioned that the gender difference was significant for the Cobb Angle which in this study is the Lumbar Lordotic Angle (LLA). This is contrary to the observation made for LLA measurements, where there is statistically insignificant difference between the female and male LSA measurements. As shown in the P-value which is greater than the significance level of 0.05.

Table 5: Comparative analysis of the current study with similar studies

Author, Year	Study Type (Posture)	Reported LSA	P-Value
Splithoff, 1953	Prospective	42.0^0	0.000
Hellems &Keats, 1971	Retrospective	41.1^0	0.000
Troyanovich et al. 1997	Retrospective	39.0^0	0.000
Maduforo et al., 2012	Retrospective	36.0^0	0.007
Okpala, 2014	Retrospective	44.5^0	0.000
Lin RM,1992	Prospective	33.2^0	0.001
Ella Been et al., 2007	Prospective	51.0^0	0.000
Okpala, 2016	Retrospective	35.6^0	0.711
Okpala, 2018	Retrospective	49.9^0	0.000

The normal value reported by a number of authors in Table 5 show great variation. Lin Rm recorded mean of LLA to be $33.2^0 \pm 12.1^0$ in a prospective study of 149 subjects. Ella Been *et al.* who also adopted a prospective approach in the assessment of lateral radiographs of the lumbar spine of 379 subjects, the reported mean LLA was $51.0^0 \pm 11.0$. According to Okpala who conducted a retrospective measurement of lumbar lordosis in normal supine lateral lumbosacral spine radiographs of 27 children aged 0.04-14.00 years, he reported an average LLA of 35.6^0. In 2018, another retrospective study conducted by Okpala using 200 normal adult subjects, (100 males, 100 females) in recumbent position revealed that the mean (SD) LLA recorded as 49.9^0. In this

current study, irrespective of gender, the measured mean LLA was 35.9^0 ±9.82. A One Sample T-test was further conducted to observe whether the measured value of LLA was distinct from similar studies as shown in Table 4, it was observed that there was a statistically significant difference between the measured mean LLA and most of the reported values in the other studies (thus, P-value < 0.05) with the exception of the outcome reported by Okpala in 2016 which showed no significant difference.

Multiple Comparison between groups (Age categories) of sample

Table 6 and Figure 7 gives a tabular and graphical distribution of the mean value of LLA with regards to the various categories. A total number of 70 subjects between 21-40 years, had the highest mean LLA of approximately 36.7^0 ±11. This was followed by 51 subjects between 41-60 years with mean LLA of approximately 35.7^0 ±9.12. Then 4 subjects who are less than 20 years had mean LLA of 34.5^0 ±8.35. Finally, 15 subjects who were older than 60 years had the least mean LLA of approximately 33.3^0 ±5.86.

Table **6**: **Lumbar Lordotic Angle**

Age	Mean	N	Std. Deviation
<20	34.5000	4	8.34666
21-40	36.6614	70	10.99757
41-60	35.7392	51	9.17946
> 60	33.3467	15	5.86404
Total	**35.9086**	**140**	**9.81717**

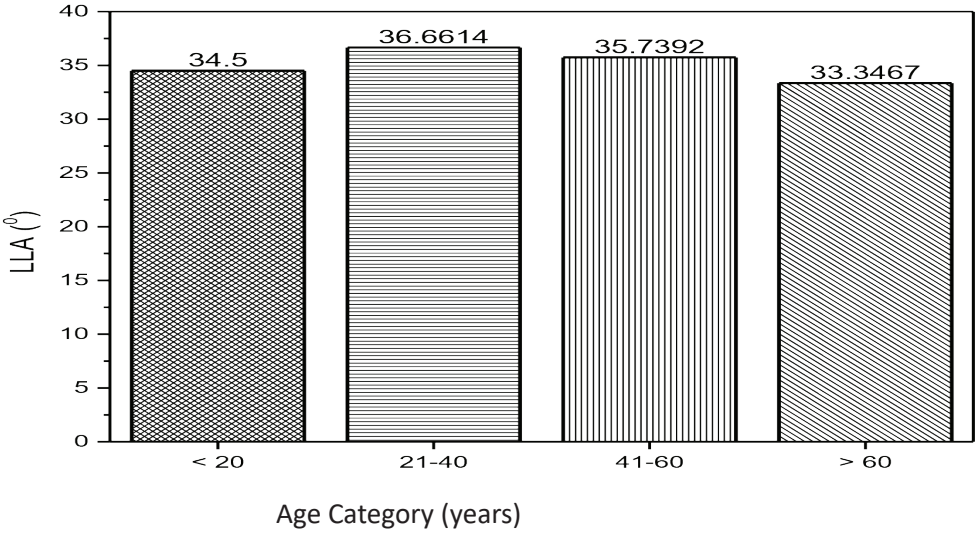

Figure 7: Lumbar Lordotic angle across various age categories

Table **7**: **Lumbosacral Angle**

Age category of patient	Mean	N	Std. Deviation
Below 20	37.0000	4	5.88784
21-40	34.4000	70	8.13716
41-60	34.1353	51	7.14663
Above 60	33.4067	15	5.67683
Total	34.2714	140	7.45283

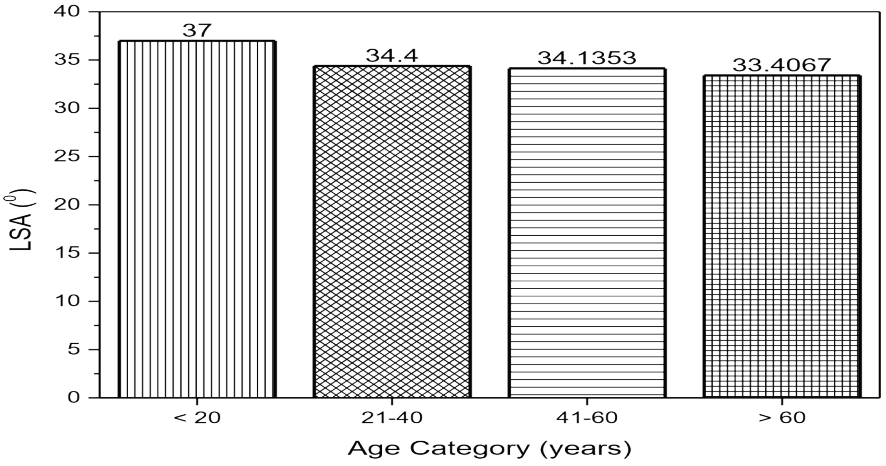

Figure 8: Lumbosacral angle across various age categories

Table 7 and Figure 8 represent a tabular and graphical distribution of the mean value of LSA with regards to the various age categories. A total number of 4 patients who are less than 20 years, had the highest mean LSA of $37.0^0 \pm 5.89$. This was followed by 70 patients between 21-40 years with mean LSA of $34.4^0 \pm 8.14$. Additionally, between 41-60 years had mean LSA of $34.1^0 \pm 7.15$. Finally, 15 subjects who were older than 60 years had the least mean LSA of approximately $33.4^0 \pm 5.68$.

Conclusion

The study concluded that, the normal range of LLA value is $20.9\text{-}68.0^0$ and LSA is 15-51° irrespective of gender or age variation. This mean value, obtained in a retrospective study was distinct as compared to a number of the literature values that were either obtained using retrospective or prospective approach. Furthermore, it has been established that the measured values at which to consider hypolordosis (below LLA=17.9°; LSA=12.0^0), and hyper-lordosis (above LLA=72.0°; LSA=55.0^0) in the Ghana population. This study have also established that in all the various age groups between 15 and 80 years, there exist no significant difference in the mean LLA and LSA among the groups, and this affirms that the development of lumbar lordosis reaches a plateau when spine is fully developed. Furthermore, female LSA and LLA shows higher measured values compared to their male counterpart in the Ghanaian population which confirmed other study values in literature. Finally, a reference chart of LSA and LLA has also been developed for clinical application in Ghana.

References

Chernukha. (1998). *Lumbar lordosis measurement. A method versus Cobb technique*. 74–79.

Rajabi, R., & Mohamsdi, F. (2008). Which Method is Accurate When Using the Flexible Ruler to Measure the Lumbar Curvature Angle? Deep Pint or mid Pint of Arch? World Applied Sciences Journal, 6, 849–852.

Been, E., Pessah, H., Been, L., Tawil, A., & Peleg, S. (2007). New method for predicting the lumbar lordosis angle in skeletal material. *Anatomical Record*, *290*(12), 1568–1573. https://doi.org/10.1002/ar.20607

Been, E., Barash, A., Marom, A., & Aizenberg, I. (2010). *A New Model for Calculating the Lumbar Lordosis Angle in Early Hominids and in the Spine of the Neanderthal From Kebara*. *1145*(March), 1140–1145. https://doi.org/10.1002/ar.21145

Been, E., & Kalichman, L. (2014). Lumbar lordosis. *Spine Journal*, *14*(1), 87–97. https://doi.org/10.1016/j.spinee.2013.07.464

Been, E., Pessah, H., Been, L., Tawil, A., Peleg, S., & Aviv, T. (2007). *New Method for Predicting the Lumbar Lordosis Angle in Skeletal Material*. *1573*(April), 1568–1573. https://doi.org/10.1002/ar.20607

Allegri, M., Montella, S., Salici, F., Valente, A., Marchesini, M., Compagnone, C., Baciarello, M., Manferdini, M. E., & Fanelli, G. (2016). *Mechanisms of low back pain : a guide for diagnosis and therapy Mechanisms of low back pain : a guide for diagnosis and therapy [version 1 ; referees : 3 approved]*. *June*. https://doi.org/10.12688/f1000research.8105.1

Evcik, D., & Yu, A. (2003). *Lumbar lordosis in acute and chronic low back pain patients*. 163–165. https://doi.org/10.1007/s00296-002-0268-x

Evcik, D., & Yücel, A. (2003). Lumbar lordosis in acute and chronic low back pain patients.

Rheumatology International. https://doi.org/10.1007/s00296-002-0268-x

Bordes, S. J., & Tubbs, R. S. (2020). Lumbar Vertebrae. In *Surgical Anatomy of the Lateral*

Transpsoas Approach to the Lumbar Spine. https://doi.org/10.1016/b978-0-323-67376-1.00007-0

Castillo, E. R., & Lieberman, D. E. (2015). Lower back pain. *Evolution, Medicine and Public Health*. https://doi.org/10.1093/emph/eou034

Cholewicki, J., & McGill, S. M. (1996). Mechanical stability of the in vivo lumbar spine: Implications for injury and chronic low back pain. *Clinical Biomechanics*. https://doi.org/10.1016/0268-0033(95)00035-6

Czervionke, L. F. (2011). Lumbar Spine Anatomy. In *Imaging Painful Spine Disorders - Expert Consult*. https://doi.org/10.1016/b978-1-4160-2904-5.00003-3

Damasceno, L., Silvio, C., Campos, A., & Defino, H. (2006). O Riginal a Rticle Lumbar Lordosis : a Study of Angle Values and of Vertebral Bodies and Intervertebral Discs Role. *ACTA ORTOP BRAS*, *14*(4), 193–198.

Dephilip, R. M., & McGraw, J. K. (2004). Spinal Anatomy. In *Interventional Radiology of the Spine*. https://doi.org/10.1007/978-1-59259-418-4_1

Ebraheim, N. A., Hassan, A., Lee, M., & Xu, R. (2004). Functional anatomy of the lumbar spine. In *Seminars in Pain Medicine*. https://doi.org/10.1016/j.spmd.2004.08.004

Ehrlich, G. E. (2003). Low back pain. *Bulletin of the World Health Organization*, *81*(9), 671–676. https://doi.org/10.1590/S0042-96862003000900010

Feden, J. P. (2016). Lumbar spine. In *Sports Medicine for the Emergency Physician: A Practical Handbook*. https://doi.org/10.1017/CBO9781316084328.011

Hansen, L., De Zee, M., Rasmussen, J., Andersen, T. B., Wong, C., & Simonsen, E. B. (2006). Anatomy and biomechanics of the back muscles in the lumbar spine with reference to biomechanical modeling. *Spine*.

Evaluation of Rice Landraces for Nitrogen Use Efficiency on Soil of Toje Series

Nana Muhammed Opuni, Patrick Bonney, Beatrice Elohor Ifie and John Saviour Yaw Eleblu

[1]Department of Crop Science, University of Ghana, Legon, Ghana

***Corresponding Author:** John Saviour Yaw Eleblu, jeleblu@wacci.ug.edu.gh

ABSTRACT

Background: To ameliorate challenges of environmental pollution due to over-use of nitrogen fertilizer, juxtaposed with soil-nitrogen depletion as a limitation to subsistent farming, utilizing varieties responsive to minimal application of fertilizer is of priority.

Aim: The goals of the study were to: identify genotypes that are nitrogen use efficient, assess genotypic variations including relationship and heritability of yield related traits and nitrogen use efficiency components.

Methods: Twenty rice landraces with two nitrogen levels (0 and 50 kg/ha) replicated thrice in pot and field experiments were conducted. The experimental design for pot experiment was completely randomized design in a factorial arrangement while split plot design was used for field experiment.

Results: Landraces such as GH1550, GH1801, GH1822, GH1535, GH1590, GH1515 and GH2145 were efficient and responsive to both nitrogen levels. Analysis of variance showed significant differences for filled spikelets, panicle number, panicle length, 1000-grain weight, spikelet per panicle and harvest index. Nitrogen Use Efficiency, Nitrogen Uptake Efficiency, Nitrogen Utilization Efficiency, Grain Nitrogen Concentration and Straw Nitrogen Concentration showed significant increase under 0kg/ha of N compared to 50kg/ha in both pot and field experiments. Nitrogen use efficiency correlated significantly with filled spikelet, grain yield, panicle length, 1000-grain weight and nitrogen uptake efficiency. Broad-sense heritability estimates were high for traits such as filled spikelet, grain yield, panicle number, panicle length, 1000-grain weight, spikelet per panicle and harvest index as well as nitrogen use efficiency and its components.

Conclusion: The identified Nitrogen Use Efficient landraces have the genetic potential needed to accelerate rice improvement for increased productivity in the characteristic smallholder low input cultivation systems in Ghana.

Keywords: Heritability, Nitrogen Uptake Efficiency, Nitrogen Utilization Efficiency, Traditional cultivars

Introduction

Rice occupies a leading position among cereal crops along with wheat and maize, thus, considered a food security crop (*Maclean* et al. 2002). Aside from the provision of food and forage, it aids in alleviating poverty via the provision of raw materials for industries, and the generation of income for small holder farmers (*Olembo* et al. 2010). Despite its numerous benefits, its production is faced with lots of challenges especially in sub-Saharan Africa (SSA). Its cultivation in SSA is mostly carried out via subsistent farming with high dependence on soil nitrogen availability (*Saito* and *Futakuchi,* 2009). In situations where access to industrial fertilizer is available, its application is in high doses to replenish the already

depleted nitrogen for increased yield. Though adoption of industrial nitrogen fertilizers aids in improving crop yield, it has caused havoc to the environment due to its over-use. Analysis on application of synthetic fertilizer globally for the past 4 decades, indicates the amount of fertilizer agricultural crops utilized is 7.4-fold as against the yield of 2.4-fold. This suggests that the application of fertilizers in high doses does not necessarily guarantee high yield, but rather has considerable negative effect on biodiversity and the environment (*Samonte* et al., 2006even though it has economic and ecological implications. This study examined the significance and magnitude of variation in N content, NUE, N translocation ratio (NTR; *Hirel* et al., 2011). To curb the environmental and ecological challenges faced with nitrogen fertilizer, an optimum fertilization level in paddy fields where Nitrogen Use Efficiency (NUE) is of utmost priority is the need of the hour.

Nitrogen use efficiency (NUE) can be described as the total biomass or grain yield produced per unit available N fertilizer. It may be due to the interplay between the environment and genetic factors (*Xu* et al., 2012; *Haung* et al., 2004). It is divided into two main mechanisms: the absorption of N; nitrogen uptake efficiency (NUpE) and the assimilation of the absorbed N necessary for grain production; nitrogen utilization efficiency (NUtE) (*Han* et al. 2015). The decline in NUE among rice genotypes may be due to deficiency in either/both NUpE and NUtE. Thus, screening for genotypic variability and heritability of traits related to NUE and its components (NUpE and NUtE) in breeders' germplasm, coupled with genotype x Nitrogen (N) interactions as well as the precision in selection under varied levels of N is essential (*Garnett* et al. 2015). More so, to allow understanding of phenotypes associated with high NUE from simplistic to complex growth conditions, relating data from both pot and field experiments is imperative (*Beatty* et al. 2010). Several studies show that variability in the genotypes used as well as heritability of traits related to NUE and its components have been investigated in irrigated or rainfed low land rice in Asia (*Inthapaya* et al., 2000; *Koutroubas* and *Ntanos*, 2003; *Haefele* et al., 2008; *Wu* et al., 2016). In addition, a negative relationship has been recorded among NUtE, grain and straw N concentrations (*Inthapanya* et al., 2000; *Koutroubas* and *Ntanos*, 2003; *Samonte* et al., 2006), while another study indicated a strong association between grain yields of rice and NUE (*Haefele* et al. 2008). *Kumar* et al. (2016) recorded high heritability for plant height, number of productive tillers, panicle length, number of spikelets per panicle, grain yield per plant and NUE at low N levels. *Rao* et al. (2018) studied NUE on rice landraces in Asia and they identified donors for high N uptake and N translocation in grain resulting in higher yields under low N.

Landraces are better adapted to environmental stress under low input conditions and constitute a unique germplasm for ascertaining NUE lines (*Ali* et al. 2018). Though NUE lines have been identified in various rice genotypes in Asia and some parts of Africa (*Fageria* et al., 2010; *Segda* et al., 2014; *Rao* et al., 2014; *Lakew*, 2015; *Rao* et al., 2018), there is a dearth of information on the identification of NUE lines in rice germplasm collections in several countries in West Africa which includes Ghana (*Segda* et al. 2014). Hence, the objectives of this study were to: identify landraces that are nitrogen use efficient; assess genotypic variations including relationships and heritability of yield related traits and nitrogen use efficiency components.

3 Materials and methods

3.1 Experimental Site

Field and Pot experiments were conducted at the research farm of the Department of Crop Science, University of Ghana, Legon from February 2019 to June 2019. The farm experiences a bi-modal seasonal rainfall pattern with an annual average precipitation of 700-1000 mm. It lies within latitude 5° 39′ N and longitude 0° 539′ W and has a gentle topography of 0.30. The major and minor rainfall seasons start from April - July and September - December, respectively. Average annual temperature recorded at the site during the period is about 26.9 °C and relative humidity ranges from 60 to 90 % at night and 20 - 55 % throughout the year. The soil

type is savanna ochrosol locally called Toje series classified by *Eze*, (2008) as a Rhodustalf and Rhodic Lixisol according to *USDA* (1999, 2003). Toje series is among the most widely cultivated soils of the Accra Plains. Toje is developed on Quartzite schist (*Fiagbedzi*, 1989). The soil contained 0.13% of nitrogen, 30.1% of phosphorus, 0.79 cmol/kg of potassium, 2.99 mg/kg of carbon and particle size constituting; 56% sand, 25% clay and 19% silt in the top 15cm of the soil profile.

3.2 Plant material:

Twenty (20) rice landraces were used for the study out of which nineteen were from the Plant Genetic Resource Research Institute, Bonsu (PGRRI), and one was from the Crop Research Institute, Kumasi (Table 1).

Table 1: The twenty accessions used in the study and the respective institutions from which they were collected.

Accessions	Institutions
GH1514, GH1515, GH1516, GH1519, GH1531, GH1535, GH1538, GH1549, GH1550, GH1552, GH1574, GH1583, GH1587, GH1590, GH1599, GH1597, GH1801, GH1822, GH2145	Plant Genetic Resource Research Institute, Bonsu
Aunty Jane	Council for Scientific and Industrial Research - Crops Research Institute, Kumasi

3.3 Experimental design and nitrogen application

A total of 120 polythene bags serving as pots with width 23 cm and length 20 cm were used. Five kilograms (5 kg) of the experimental soil was weighed into each pot. A completely randomized design arranged in a factorial manner was employed with three replicates. Forty combinations of treatments were compared (20 varieties × 2 levels of fertilization) with three seeds sown in each pot. The field experiment was conducted using a split plot design with three replicates. Plot size was 2 m by 1.7 m. Beds were raised and the spacing between each bed and row was 70 cm with an alley of 1 m between blocks. Two treatment levels of nitrogen (N) were used thus, available N (no N) and low N (50 kg/ha). Nitrogen fertilizer was applied in two split doses: 50% at tillering (25 kg/ha) and 50 % at panicle initiation (25 kg/ha). Other major nutrients such as phosphorus (P) and potassium (K), were applied to all pots at 90 kg/ha. Phosphorus (P) in the form of triple superphosphate and potassium (K) in the form of potassium chloride were applied in two split applications; tillering (45 kg/ha) and panicle initiation (45 kg/ha). Plants were watered on a daily basis to maintain moisture in the soil. The trial was conducted in an upland condition during the rainy season. Weeds on beds were controlled by hand.

3.4 Phenotypic data

Data collection was conducted during harvest as prescribed by *Getachew* and *Nabiyu* (2018) for both pot and field experiments. For each sampling, three representative plants (in pot experiments) or hills (in field trials) for each landrace were garnered. At maturity, plants were reaped and disjointed into straw and panicle. Filled grains (spikelets) were separated from unfilled spikelets, oven dried at 60˚C for 72 h and weighed. Filled grains were used to evaluate grain yield (GY) and grain N concentration (GNC). 250 filled grains and 250 empty grains were weighed for the estimation of the total number of filled and empty grains. Straw samples were oven dried at 60 °C for 72 h and weighed to measure straw yield (SY). Fifteen trait were calculated as suggested by *Rakotoson* et al. (2017) (Table 1). Based on the grain yield data, landraces were grouped into efficient (E), responsive (R), and efficient and responsive (ER) as per *Fageria* and *Baliger* (1993).

Table 2: Description of the 15 measured and calculated yield and NUE related traits

Code	Trait	Method	Unit
FG	Filled grain	100 × FG / total number of spikelets	%
GNC	Grain N concentration	Grain N concentration of 3 hills at maturity	%
GY	Grain yield	PN × SPIPAN × FG × TGW	kg/ha
HI	Harvest Index	GY/(GY + SY)	-
NUE	Nitrogen use efficiency	GY/N supply	kg grain kg/N
NUpE	Nitrogen uptake efficiency	TNUP/N supply	kg N kg/N
NUtE	Nitrogen utilization efficiency	GY/TNUP	kg grain kg/N
PN	Number of panicles	Mean of panicle number of 3 hills	-
SNC	Straw N concentration	SNC of 3 hills at maturity	-
SPIPAN	Number of spikelets per panicle	Mean of number of spikelets of 3 hills	%
SY	Straw Yield	Biomass of 9 hill	-
TGW	1000-grain weight	Weight of 250 filled spikelets × 4	kg/ha
TNUP	Total plant N uptake	GNC × GY + SNC × SY	g

3.5 Tissue nitrogen concentration

N concentration in the straw and grain were analyzed by Kjeldahl procedure using the standard protocol (*Piper*, 1966). The samples were oven dried at 65°C for 72 hours and pulverized separately into fine powder. 0.1g of the samples was used for the analysis. The percent N was calculated using the formula below:

$$\% \text{ Total Nitrogen} = \frac{(\text{Titre value} - \text{Blank}) * 1400}{\text{weight} * 5 * 1000} \quad \text{.... Equation (1)}$$

3.6 Statistical Analysis

3.6.1 Growth parameters, yield and NUE components

Analysis of variance was computed using GENSTAT statistical package (version 12) sources of variation such as genotype, N level, replication and the interaction of genotype × N level were used in the statistical model. These were considered as fixed effects (genotype, N level, replication, genotype × N). A significant level of $p \leq 0.05$ was computed and a Post Hoc test for values with $p \leq 0.05$ using Turkey's test was carried out.

Pearson *phenotypic correlation* coefficients based on means of varieties over replicates were calculated for all traits using Minitab® 19 statistical analysis package

3.6.2 Estimates of variance components

The population's variability was estimated using mean, phenotypic, genotypic and coefficient of variation based on *Rosmania et al.* (2016) as follows:

$$\sigma^2 G = [(MSG) - (MSE)] / r \quad \text{..... Equation (2)}$$

$$\sigma^2 P = [\sigma^2 G + (\sigma^2 E/r)], \quad \text{..... Equation (3)}$$

Where: σ^2 G = Genotypic variance; σ^2 P = Phenotypic variance; σ^2 E = Environmental variance (error mean square from the analysis of variance); MSG = mean square of genotypes; MSE = error mean square; r = number of replications. Genotypic coefficient of variation (GCV) = $(\sigma^2 G)^{1/2}/x) \times 100$; Phenotypic coefficient of variation (PCV) = $(\sigma^2 P)^{1/2}/X) \times 100$, where: σ^2 G = Genotypic variance; σ^2 P = Phenotypic variance; X is grand mean of a character. Broad-sense *heritability* (H^2) for all traits at each level of N was calculated from variance components using the formula:

$H = \sigma^2_G/\sigma^2_P$ ..... Equation (4)

4 Results

4.1 Grain yield at two levels of N application in both pot and field experiments

The grain yield recorded at N0 and N50 aided grouping of the landraces into four; efficient (E), responsive (R), efficient and responsive (ER), and non-efficient and non-responsive (NE, NR) as prescribed by *Fageria* and *Baliger* (1993). Similar landraces were observed to fall into the four categories under pot and field experiments respectively, indicating that the yield was consistent in spite of environmental variability (Table 2). GH1587 was efficient (E) due to its yield being higher than the mean yield of the 20 landraces at N0 level but its response to N application at N50 was lower than average yield ($p < 0.001$). GH1549 belonged to the responsive (R) group, because its yield was less than the mean yield of the 20 landraces at N0 level but had more yield than the average at N 50. The third group is considered as efficient and responsive (ER) and had yields that were above the average yield of 20 landraces both at N0 and N50 levels ($p < 0.001$). GH1822, GH1550, GH1515, GH1535, GH2145, GH1801 and GH 1590 fell into this category.

Table 2: Mean Grain yield (kg/ha) under two levels of N treatment

	Grain yield (kg/ha) pot			Grain yield (kg/ha) field		
Land race	N0	N50		N0	N50	
GH1549	357.00	2970.00		403.33	3002.00	
GH1587	1117.10	1459.00		1131.00	1481.00	
GH1574	597.10	1449.00		621.00	1551.00	
GH1822	1676.10	2841.00		1702.00	2941.00	
GH1514	957.50	1173.00		1009.00	1251.00	
GH1550	1099.00	4703.00		1201.00	4804.00	
GH1515	1024.00	3564.00		1051.00	3701.00	
GH1552	699.10	2448.00		711.00	2551.00	
GH1535	1160.10	2995.00		1201.00	3002.00	
GH1538	703.00	1921.00		721.00	2001.00	
GH1531	679.00	1792.00		691.00	1801.00	
GH2145	2092.10	8035.00		2121.00	8107.67	
GH1801	1970.00	2800.00		2003.00	2851.00	
GH1519	599.20	1652.00		611.00	1701.00	
GH1599	450.00	627.00		497.00	636.00	
GH1590	1785.00	3420.00		1801.00	3501.00	
GH1583	579.20	1741.00		601.00	1761.00	
GH1591	576.00	1359.00		651.00	1381.00	
GH1516	779.10	1539.00		806.00	701.00	
Aunty Jane	699.10	3002.00		1591.00	3051.00	
Mean	**979.94**	**2574.08**		**1011.72**	**2633.33**	
G			**			**
N			**			**
G × N			**			**
CV (%)			0.4			0.1

4.2 *,**,ns are significant at the 5 and 1% probability level and non-significant respectively

Yield related traits of rice landraces under no and low nitrogen levels in pot and field experiments

Genetic variations were observed among the landraces due to significant differences and interactions indicated by analysis of variance (Table 3). A wide range with a general trend of reduction for eight yield related traits was observed in the twenty landraces under N0 compared to N50 across both pot and field evaluation (Table 3). However, unfilled spikelets (UFS) was higher as nitrogen level increased which ranged from 70 – 750 and 86 – 781 in pot and field experiments respectively. Low UFS was recorded at N0 level ranging from 10 – 90 and 31 – 71 in pot and field experiments, respectively. Genotypes showed significant differences for harvest index (HI) with mean ranging from 38.36 – 50.06 % in pot experiment and 33.19 % - 46.78 % in field experiment under N0 and N50 respectively.

4.3 Nitrogen use efficiency and its component traits in pot and field experiments

Analysis of variance indicated that genotypic effects were significantly different for N use efficiency and its component traits ($p< 0.05$) (Table 4). In this study, varied ranges of means were recorded with a common trend in increase for NUE, NUpE, and NUtE under N0 as compared to N50 in pot and field experiments.

Table 3: Summary of ANOVA for yield related traits under no and low nitrogen levels of twenty rice landraces in pot and field experiment

Trait	Range				Mean						
	Pot		Field		Pot		Field				
	No N	Low N	No N	Low N	No N	Low N	No N	Low N	N	G	G × N
FS	300.00-1400.00	522.00 – 3360.00	311.00 – 1461.00	580.00 – 3407.00	683.40	1419.20	730.83	1482.25	**	**	**
GY	357.00-2092.00	627.13 – 8035.00	403.00 – 2121.00	636.00 – 8107.00	979.94	2574.08	1011.72	2633.33	**	**	**
PN	7.00 – 14.00	11.00 – 30.00	10.00 – 19.00	15.00 – 34.00	10.40	19.83	14.18	23.35	**	**	*
PL	16.00 – 26.50	20.00 – 30.00	18.00 – 29.00	22.00 – 33.00	20.80	25.31	22.27	26.83	**	**	**
TGW	10.00 – 20.00	10.00 – 25.00	9.00 – 24.00	17.00 – 32.00	14.45	17.75	16.41	20.77	**	**	**
UFS	10.00 – 90.00	70.00 – 750.00	31.00 – 71.00	86.00 – 781.00	32.72	381.91	50.65	415.70	**	**	**
SPN	50.00 -100.00	70.00 – 150.00	55.00 – 121.33	76.00 – 161.00	65.45	91.15	77.55	101.15	**	**	**
HI	21.36 – 61.65	29.43 – 65.25	21.23 – 50.31	26.14 – 69.25	38.36	50.06	33.19	46.78	**	**	**

*, **, ns are significant at the 5 and 1% probability level and non- significant, respectively

FS: Filled spikelet
UFS: Unfilled spikelet
TGW: 1000-grain weight
GY: Grain yield
SPN: Spikelet per panicle
PL: Panicle Length
PN: Panicle number
HI: Harvest Index

4.4 Genotypic and phenotypic coefficient of variations and heritability estimates for yield related traits and NUE components in pot and field experiments

Genotypic coefficient of variation (GCV) was less than its corresponding estimates of phenotypic coefficient of variation (PCV) for all yield related traits (Table 5). GCV was lower than its equivalent evaluations of PCV for all yield related traits and NUE components signifying the vital role of the environment in the expression of these traits. The GCV for NUtE, GNC and SNC are same as their PCV resulting in zero environmental variance. This makes the heritability of such characters 100%. Broad-sense heritability estimates for the yield related traits ranged from 97.83% to 100% under pot and field conditions (Table 6). NUE components observed for both pot and field experiments had heritability estimates of 95.37% to 100.00% (Table 6).

Trait	Range				Mean				N	G	G × N
	Pot		Field		Pot		Field				
	No N	Low N	No N	Low N	No N	Low N	No N	Low N			
NUE	27.46 – 160.88	27.17 – 160.71	30.94 – 163.11	12.72 – 163.11	75.38	51.47	76.11	71.75	**	**	**
NUpE	79.77 – 609.20	34.15 – 567.85	102.80 – 566.71	41.89 – 546.57	255.98	159.10	262.19	159.44	**	**	**
NUtE	0.13 – 0.93	0.22 – 0.69	0.19 – 0.75	0.23 – 0.59	0.33	0.35	0.32	0.35	**	**	*
GNC	0.65 – 2.37	0.78 – 2.88	0.68 – 2.33	0.79 – 2.82	1.53	1.79	1.53	1.77	**	**	**
SNC	0.71 – 1.77	0.82 – 1.87	0.53 – 1.72	0.65 – 1.97	1.07	1.21	0.88	1.05	**	**	**

Table 4: Summary of ANOVA for Nitrogen use efficiency parameters under no and low nitrogen levels in pot and field experiments of twenty rice landraces.

**, * Significant at 1% and 5% probability level respectively

NUE: Nitrogen Use Efficiency NUtE: Nitrogen Utilization Efficiency NUpE: Nitrogen Uptake Efficiency GNC: Grain nitrogen concentration

SNC: Straw nitrogen concentration

Table 5: Estimation of genetic variability parameters for yield related traits in rice landraces under pot and field conditions.

Trait	Mean		σ^2G		σ^2P		GCV (%)		PCV (%)		H (%)	
	Pot	Field	Pot	Field	Pot	Field	Pot	Field	Pot	Field	Pot	Field
FG	1051.3	1106.54	11200.89	12246.05	11201.97	12246.05	10.00	9.74	10.00	9.75	99.00	100.00
GY	1777.01	1822.53	74874.29	80090.67	74874.99	80092.08	15.39	15.53	15.40	15.53	99.99	99.99
PN	15.11	18.76	0.69	0.90	0.70	0.91	5.50	5.05	5.54	5.08	98.57	98.90
PL	23.05	24.55	0.45	0.68	0.46	0.69	2.91	3.35	2.94	3.38	97.83	98.55
TGW	16.10	18.59	0.93	1.01	0.94	1.02	5.98	5.40	6.02	5.43	98.94	99.02
UFS	211.32	233.18	755.60	782.37	756.87	782.38	13.01	11.99	13.02	11.99	99.83	99.99
SPIPAN	78.30	89.35	23.75	26.59	23.76	26.59	6.22	5.77	6.23	5.77	99.96	100.00
HI	44.26	39.98	7.61	6.24	7.64	6.26	6.23	6.25	6.24	6.26	99.61	99.68

FG: Filled spikelet
GY: Grain yield
HI: Harvest Index
PN: Panicle number
PL: Panicle length
TGW: 1000- grain weight
SPIPAN: Spikelet per panicle
UFS: Unfilled spikelet

Table 6: Estimation of genetic variability parameters for nitrogen use efficiency in rice landraces under pot and field under conditions.

Trait	Mean		σ^2G		σ^2P		GCV (%)		PCV (%)		H (%)	
	Pot	Field	Pot	Field	Pot	Field	Pot	Field	Pot	Field	Pot	Field
NUE	63.43	73.93	76.98	170.44	80.72	171.54	13.83	17.65	14.16	17.72	95.37	99.34
NUpE	207.54	210.81	1220.39	1187.08	1221.31	1187.38	16.83	16.34	16.84	16.35	99.92	99.97
NUtE	0.34	0.33	0.01	0.01	0.01	0.01	29.41	30.30	29.41	30.30	100.00	100.00
GNC	1.65	1.65	0.01	0.01	0.01	0.01	6.06	6.06	6.06	6.06	100.00	100.00
SNC	1.14	0.96	0.01	0.01	0.01	0.01	8.68	9.43	8.73	9.43	100.00	100.00

NUE: Nitrogen Use Efficiency
NUpE: Nitrogen Uptake Efficiency
NUtE: Nitrogen Utilization Efficiency
GNC: Grain nitrogen concentration

4.5 Correlations among yield related traits and NUE components in pot and field experiments

Significant correlations were observed for 21% of trait combinations (Fig.1, 2). GY correlated positively with FS and PL. SPIPAN showed positive correlation with FS and UFS. NUE had strong correlation with FS, GY, PL, 1000-grain weight. NUpE had strong correlation with FS and GY. HI also correlated with GY, PL, 1000 - grain weight, NUE. On the other hand, 59% of the trait combinations had weak correlations. GNC and SNC correlated with FS, GY, NUE and NUpE.

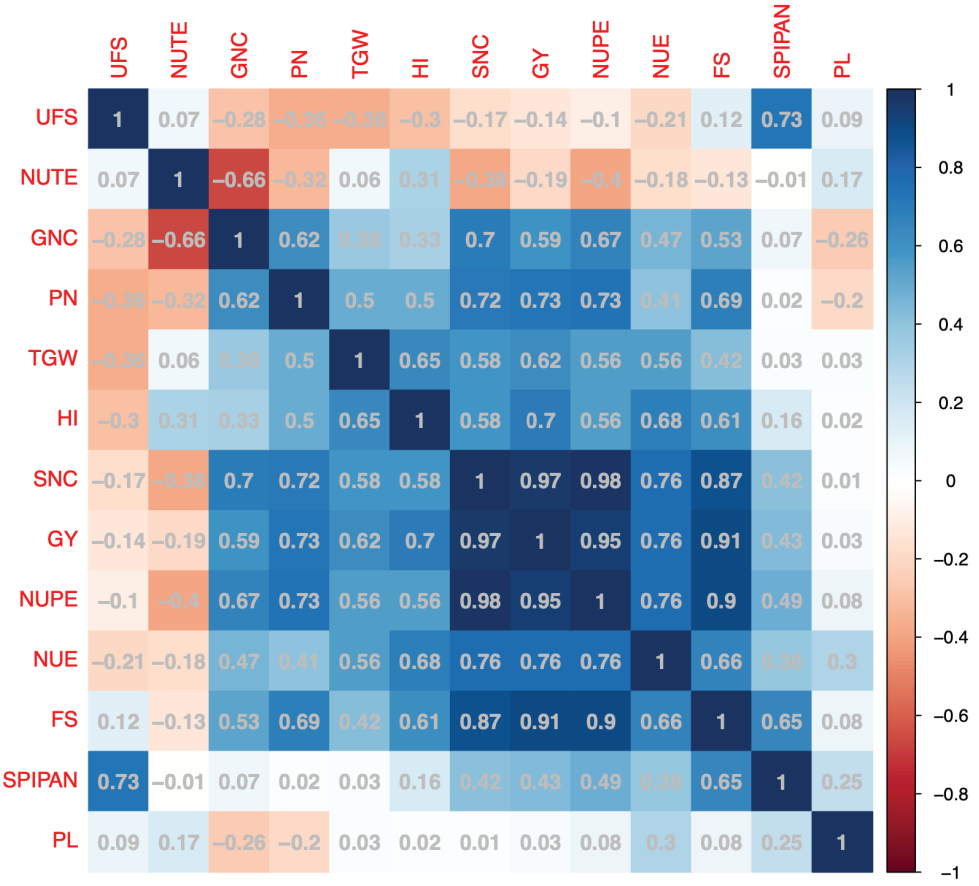

Fig 1: Correlation for yield related traits and nitrogen use efficiency in field experiment

*, **, ^{ns} are significant at the 5 and 1% probability level and non- significant, respectively

FG: Filled spikelet	UFS: Unfilled spikelet	NUpE: Nitrogen uptake efficiency
GY: Grain yield	SPN: Spikelet per panicle	GNC: Grain N concentration
PN: Panicle number	HI: Harvest Index	SNC: Straw N concentration
TGW: 1000-grain weight	NUE: Nitrogen use efficiency	NUtE: Nitrogen utilization efficiency

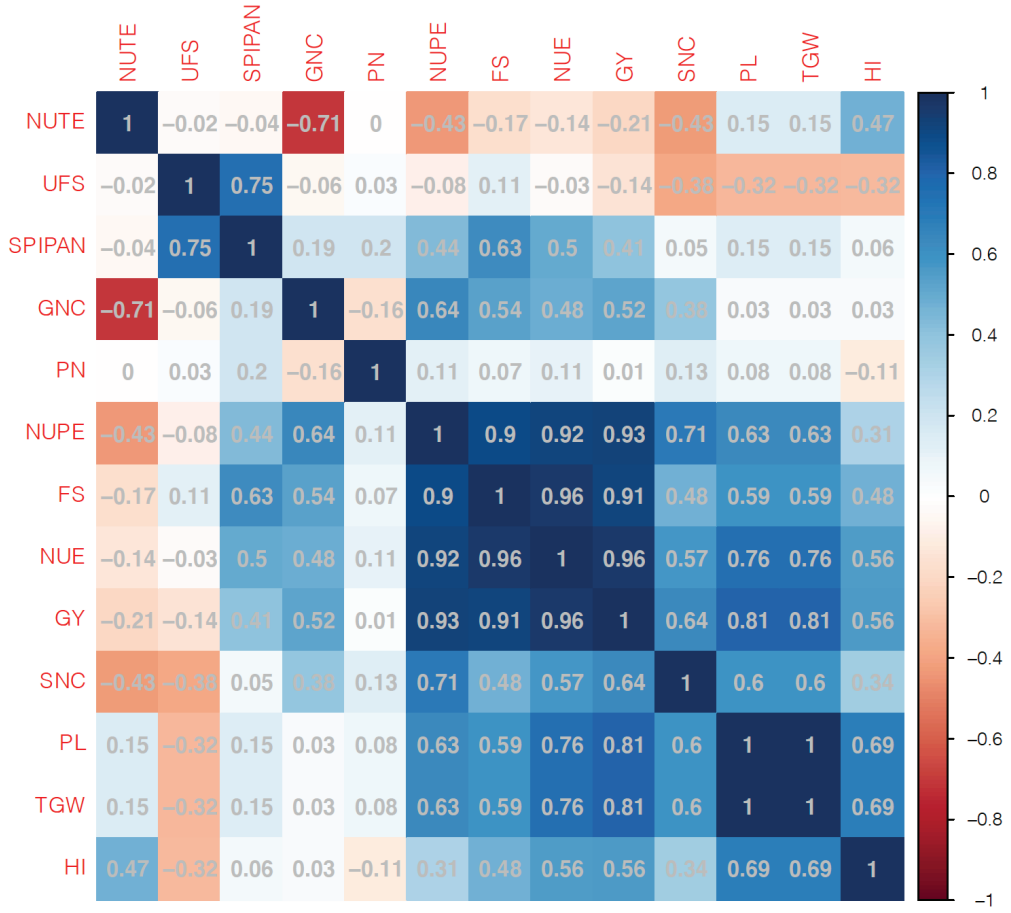

Figure 2: Correlation for yield related traits and nitrogen use efficiency in pot experiment

*, **, ns are significant at the 5 and 1% probability level and non- significant, respectively

5 Discussion

ER group are most desirable because they produce more at N0 and respond to applied N indicating their ability to strive in varied N environments. The second desirable group is E because they produce more yield under N0 level which will aid resource poor farmers. The R group may be used in breeding programs. The remaining landraces fall into the fourth group: NE, NR and are less desired in terms of NUE. Similar groupings were reported in earlier studies (*Fageria* and *Filho*, 2001; *Surekha*, et al., 2019; *He* et al., 2017).

Genetic variations showed high yielders had more FS. This indicates that number of FS promotes high grain yield due to adequate supply of N fertilizer. A study observed similar findings (*Lawal* and *Lawal*, 2002; *Rao* et al.,2018). Conversely, *Lakew* (2015) experienced reduction in FS when nitrogen was applied. UFS increased when N was applied. This could be because N

increases the SPIPAN as a result of increase in PN which may reduce production of carbohydrate from sink to support growth of all spikelet leading to a reduction in FS. Similar result was observed in a study carried out by *Yuan* et al. (2013). The reduction in PN under N0 could be due to competition for assimilates among young panicles and tillers in the course of panicle development. This leads to slow growth among many young tillers which may senesce without producing panicle (*Fageria* and *Baligar*, 2001). Analogous observations were described by other authors (*Mendhe* et al., 2002; *Uddin* et al., 2011). SPIPAN increased as nitrogen fertilizer was applied. 1000 - grain weight was relatively low between the two levels of nitrogen because it has been reported to be a genetically controlled character. Comparable results were established by other scientists and they concluded that there is little opportunity to improve grain size through agronomic management (*Maske* et al., 1997; *Ahmed* et al., 2005). High yielding genotypes had high HI indicating the importance of HI as a yield component. *Rao et al.* (2018) also reported similar results.

Although the variations between N0 and N50 was small, similar trend of NUE at N0 and N50 indicates that rice landraces in the current study are able to absorb or utilize N at N0. This may be due to the fact that they are landraces with the ability to grow mostly under low or minimal input conditions and are likely to harbor the trait of resource use efficiency such as NUE. Perhaps, higher levels of N (levels above sub-optimal level used in the present study) may have shown lower NUE as observed in previous studies (*Lakew*, 2015; *Haque* and *Haque*, 2016). The assessment of NUE in crop plants is significantly required to measure the fate of applied nitrogen and their role in improving maximum economic yield through efficient absorption or utilization by the plant. GNC and SNC increased slightly under N0 as compared to N50 indicating that GNC and SNC may not be affected by nitrogen fertilizer. This significant correlation portrays that nitrogen may boost grain nutritional quality in terms of GNC and SNC which can be used as feeds for livestock or used to improve soil nutrient. Similar results were obtained in a previous study (*Lakew*, 2015).

Broad-sense heritability estimates for traits such as FS, GY, PN, PL, TGW, SPIPAN and HI as well as NUE and components had high to very high heritability estimates. High heritability estimates can be used as a baseline for selection according to the morphological traits (*Woldeyesus* et al., 2004; *Alemayehu* et al., 2006). The difference between PCV and GCV for the yield related parameters indicates that these traits were influenced by the environment. The GCV for NUtE, GNC and SNC are same as their PCV resulting in zero environmental variance. This makes the heritability of such characters a 100%. The progeny of these lines will show semblance to their parents because there are no visible environmental effects on the expression of these characters. *Lakew*, (2015) also observed similar results in his study.

In this study, NUpE had strong association with NUE than the comparison between NUtE and NUE. Hence, NUpE seems more important in determining NUE. Earlier studies showed strong correlation between NUE and NUpE and weak correlations between NUE and NUtE (*Van Sanford* and *Mackown* 1986; *Lakew*, 2015). *Muurinen* et al. (2006) and *Woldeyesus* et al. (2004) found out that NUpE was more significant than NUtE in influencing NUE.

Variations between pot and field experiments and their correlations may be ascribed to dissimilarity in the light intensity, nutrient absorption and water availability. Pot experiment appears to be more vulnerable to no N conditions for FS, GY, PN, PL, 1000-grain weight, SPIPAN and HI, whereas, UFS seem vulnerable in field experiment at N0.

6 Conclusions

Landraces with promising yield under N0 and N50 with efficient utilization of absorbed N were identified. They include; GH2145, GH1550, GH1515, GH1535, GH1590 and GH1801. Based on these results, it can be concluded that the identified landraces can be used in breeding programs. GH 1587 was the only efficient landrace (N0) and may be beneficial in areas with resource deprived farmers whereas GH1549 was the only

responsive landrace (N50) and may be useful in breeding programs. Genotypic variations were observed among the landraces, while NUE correlated positively with FS, GY, PL, 1000-grain weight and NUpE. These traits will provide adequate variability for which selections through GWAS and QTL can be made for genetic improvement for NUE. Based on the information from this study, breeders can select rice landraces with high heritability for NUE for breeding programs.

7 Acknowledgements

The authors would like to thank *A.G. Leventis Foundation* for the partial financial support rendered. We thank *Dr. Matilda Bissah* of the Council for Scientific and Industrial Research – Plant Genetic Resources Research Institute for the seeds used for the study.

8 References

Ahmed, M., Islam, M. M., Paul, S. K., Khulna, B. (2005): Effect of nitrogen on yield and other plant characters of local Transplanted Aman rice, Var. Jatai. *Res. J. Agric. Biol. Sci.* 1, 58-161.

Alemayehu, B., Gretzmacher, R., Johann, V. (2006). Genetic variation in nitrogen-use efficiency of tef. *J. Plant Nutr. Soil Sci.* 169: 704-710.

Ali, J., Jewel, Z. A., Mahender, A., Anandan, A., Hernandez, J., Li, Z. (2018). Molecular genetics and breeding for nutrient use efficiency in rice. *Int. J. Mol. Sci. 19*(6):1–27. http://doi.org/10.3390/ijms19061762

Beatty, P.H., Anbessa, Y., Juskiw, P., Carroll, R.T., Wang, J., Good, A.G. (2010). Nitrogen use efficiencies of spring barley grown under varying nitrogen conditions in the field and growth chamber. *Ann. Bot.* 105:1171–1182.

Eze, P. N. (2008). Characterization, Classification and Pedogenesis of soils on a Legon catena in Accra plains of Ghana. (MPhil thesis), Department of Soil Science, University of Ghana, Legon.

Fageria, N. K., Baliger, V. (1993). Screening crop genotypes for mineral stresses. Proceedings of the workshop on adaptation of plants to soil stresses. Publ No. 94 -2142-159. 1-4 August 1993INTSORMIL University of Nebraska: Lincoln

Fageria, N.K., Filho, M.P.B (2001). Nitrogen Use Efficiency in lowland rice genotypes. *Commun. in Soil Sci. Plant Anal.* 32:2079 – 2089

Fageria, N.K., De Morais, O.P., Dos Santos, A.B. (2010). Nitrogen use efficiency in upland rice genotypes. *J. Plant Nutr. Soil Sci.* 33:1696–1711

Fiagbedzi, S. (1989). Soil Landscape Relationship on Legon Hills. (BSc. Dissertation). Department of Soil Science, College of Agriculture and Consumer Sciences University of Ghana Legon.

Garnett, T., Plett, D., Heuer, S., Okamoto, M. (2015). Genetic approaches to enhancing nitrogen-useefficiency (NUE) in cereals: challenges and future directions. *Funct. Plant Biol.* 42:921–941

Getachew, M., Nebiyu, A. (2018). Nitrogen Use Efficiency of Upland Rice in the Humid Tropics of Southwest Ethiopia in Response to Split Nitrogen Application. *J. Agron. 17: 68-76.* doi**:** 10.3923/ja.2018.68.76

Haefele, S. M., Jabbar, S. M. A., Siopongco, J. D. L. C., Tirol-Padre, A., Amarante, S. T., Sta Cruz, P.C., Cosico, W.C. (2008). Nitrogen use efficiency in selected rice (*Oryza sativa L.*) genotypes under different water regimes and nitrogen levels. *Field Crops Res.* 107, 137–146.

Han, M., Okamoto, M., Beatty, P.H., Rothstein, R.J., Good, A.G. (2015). The genetics of nitrogen use efficiency in crop plants. *Annu. Rev. of Genet.,* 49:269–289. https://doi.org/10.1146/annurev-genet-112414-055037

Huang, Z. A., Jiang, D. A., Yang, Y., Sun, J. W., Jin, S. H. (2004). Effects of nitrogen deficiency on gas exchange, chlorophyll fluorescence, and antioxidant enzymes in leaves of rice plants. *Photosynthetica,* 42: 357-364.

Haque, M. A., Haque, M. M. (2016). Growth, Yield and Nitrogen Use Efficiency of New Rice Variety under Variable Nitrogen Rates. *Am. J. of Plant Sci.* **7**: 612-622. http://dx.doi.org/10.4236/ajps.2016.73054

He, H., Yang, R., Li, Y., Ma, A., Cao, L., Wu, X., Chen, B., Tian, H., Gao, Y. (2017). Genotypic variation of Nitrogen Utilization Efficiency of Oilseed Rape (*Brassica napus*) under contrasting N supply in pot and field experiments. *Front. Plant Sci*. 8:1825. doi:10.3389/fpls.2017.01825

Hirel, B., Tétu, T., Lea, P. J., Dubois, F. (2011). Improving nitrogen use efficiency in crops for sustainable agriculture. *Sustainability*, *3*(9):1452–1485. http://doi.org/10.3390/su3091452

Inthapanya, P., Sihavong, P., Sihathep, V., Chanphengsay, M., Fukai, S., Basnayake, J. (2000). Genotype differences in nutrient uptake and utilization for grain yield production of rainfed lowland rice under fertilized and non-fertilized conditions. *Field Crops Res.* 65, 57–68.

Koutroubas, S., Ntanos, D. (2003). Genotypic differences for grain yield and nitrogen utilization in Indica and Japonica rice under Mediterranean conditions. *Field Crops Res.* 83, 251– 260.

Kumar, N. V. M., Uma, M. S., Lohithaswa, H. C., Hittalmani, S. (2016). Identification of Nitrogen Use Efficient Local Rice Genotypes under Low Soil Nitrogen Conditions. *Int. J. Agric. Sci.* 8(61): 3450-3455.

Lakew, T. (2015). Estimation of genetic variability and trait association in Nitrogen Use Efficiency of Upland rice varieties in North Western Ethiopia. *Int. J. Res. Rev.* E-ISSN: 2349 – 9788.

Lawal, M.I., Lawal, A.B. (2002). Influence of Nitrogen Rate and Placement Method on Growth and Yield of Rice (*Oryza sativa* L.) at Kadawa, Nigeria. C*rop Res. (Hisar)*. 23, 403-411.

Maclean, J.L., Dawe, D. C., Hardy, B., Hettel, G. P. (Eds.). (2002). Source Book for the Most Important Economic Activity on Earth. Wallington, United Kingdom: CAB International.

Maske, N.S., Borkar, S.L., Rajgire, H.J. (1997). Effects of Nitrogen Levels on Growth, Yield and Grain Quality of Rice. *J. Soils and Crops*, 7, 83-86.

Mendhe, S.N., Chaudhari, C.S., Sawaji, B.V., Farkade, B.K., Khadse, V.A. (2002) Nitrogen Requirement and Yield Performance of Promising Cultures of Transplanted Paddy. *J. Crop Soils*, 22:284-288.

Muurinen, S., J. Kleemola, J., Peltonen-Sainio, P. (2006). Accumulation and translocation of nitrogen in spring cereal cultivars differing in nitrogen use efficiency. *Agron. J.* 99, 441-449.

Olembo, N., Mmboyi, F., Oyugi, K. (2010). Success Stories in Crop Improvement in Africa (pp 1-44). African Biotechnology Stakeholders Forum, Nairobi, Kenya.

Piper, C. S. (1966). Soil and plant analysis. Hans Publishers, Bombay. 137 –153.

Rao, R. P, Neeraja, C.N., Vishnukiran, T., Srikanth, B., Vijayalakshmi, P., Subhakara, R. I., Swamy, K.N., Kondamudi, R., Sailaja, N., Subrahmanyam, D., Surekha, K., Prasadbabu, M. B. B., Subba, R. L.V., Voleti, S. R. (2014). Nitrogen Use Efficiency in Irrigated rice for climate change- A case study. Technical bulletin no. 82 / 2014,

ISBN 978-81-928249-6-3. pp 57. Directorate of Rice Research, Rajendranagar, Hyderabad 500 030, AP, India.

Rao I. S., Neeraja C. N., Srikanth B., Subrahmanyam D., Swamy K. N., Rajesh K., Vijayalakshmi P., Kiran T. V., Sailaja N., Revathi P., Rao P. R., Subba Rao L. V., Surekha K., Babu V. R., Voleti S. R. (2018). Identification of rice landraces with promising yield and the associated genomic regions under low nitrogen. *Sci. Rep.*. 8: 9200. doi:10.1038/ s41598-018-27484-0.

Rosmaina, S., Yanti, F., Juliyanti, Z. (2016). Estimation of variability, heritability and genetic advance

among local chili pepper genotypes cultivated in peat lands. *Bulg. J. Agric. Sci*, 22: 431–436

Saito, K., Futakuchi, K. (2009): Performance of diverse upland rice cultivars in low and high soil fertility conditions in West Africa. *Field Crops Res.* 111, 243–250.

Samonte, S. O. P., Wilson, L. T., Medley, J. C., Pinson, S. R. M., McClung, A. M., Lales, J. S. (2006). Nitrogen utilization efficiency: Relationships with grain yield, grain protein, and yield-related traits in rice. *Agron. J. 98*(1):168–176. http://doi.org/10.2134/agronj2005.0180

Segda, Z., Yameogo, L.P., Sie, M., Bado, V.B., Mando, A. (2014). Nitrogen use efficiency in selected NERICA varieties in Burkina Faso. *Afr. J. Agric. Res.* doi 10.5897/AJAR20. ISSN 1991-637.

Surekha, K., Nagendra, V., Sailaja, N., Neeraja, C. N. N., Subrahmanyam, D., Voleti, S. R. (2018). Genotypic variation in rice (*Oryza sativa*) for Nitrogen Use Efficiency under optimal and suboptimal Nitrogen levels. *J. Rice Res.* 11(2) pp. 54-62

Uddin, M.J., Ahmed, S., Harun-or-Rashid, M., Hasan, M.M., Asaduzzaman, M. (2011) Effect of Spacing on the Yield and Yield Attributes of Transplanted Aman Rice Varieties in Medium Lowland Ecosystem of Bangladesh. *J. Agric. Res.* 49, 465 - 476.

USDA (1999). Soil Survey Staff. A basic system of soil classification for making and interpreting soil survey. Agriculture Handbook No. 436 (2nd edition). U.S Government Printing Office, Washington, DC.

USDA (2003). Key to Soil Taxonomy. Soil Survey Staff (9th edition). U.S Government Printing office, Washington, DC.

Van Sanford, D. A., MacKown, C. T. (1986). Variation in nitrogen use efficiency among soft red winter wheat genotypes. *Theor. Appl. Genet.* 72:158-163.

Woldeyesus, S., Gretzmacher, R., Edelbauer, A. (2004). Genotypic variation for nitrogen use efficiency in Ethiopian barely. *Field Crops Res.* 85, 43-60.

Wu, L., Yuan, S., Huang, L., Sun, F., Zhu, G., Li, G., Fahad, S., Peng, S., Wang, F. (2016). Physiological mechanisms underlying the high-grain yield and high-nitrogen use efficiency of elite rice varieties under a low rate of nitrogen application in China. *Front. Plant Sci*. 7:1024.

Xu, G., Fan, X., Miller, A. J. (2012). Plant nitrogen assimilation and use efficiency. *Annu. Rev. Plant Biol. 63*:153 – 82. http://doi.org/10.1146/annurev-arplant-042811-105532

Yadav, M.R., Kumar, R., Parihar, C.M., Yadav, R.K., Jat, S.L., Ram, H., Meena, R.K., Singh, M., Birbal, A., Verma, A.P. (2017). Strategies for Improving Nitrogen Use Efficiency: A Review. *Agric. Rev. 38*, 29–40.

Optimization of Protease Enzyme Extraction from Calatropis Procera Using Aqueous Two-Phase Purification

Abdul Baak Braimah, Derrick Ackah and Philip Manu

Department of Biochemistry and Biotechnology, Kwame Nkrumah University of Science and Technology, Kumasi, Ghana

***Corresponding Author:** babdulbaak@gmail.com

ABSTRACT

Though protease enzyme extraction has mainly been from microbes, plant proteases have been sought out as a supplement to further boost production and overcome the expensive and tedious nature of microbial protease extraction. At present, efficient and easily affordable processes for the partitioning and purification of enzymes that provide ample yield and high purity of the final products have been demanded by most industries. Thus, this study seeks to optimize conditions and experimental procedures to generate a pure, folded, and dimeric enzyme in its maximum yield from Calotropis procera. The aqueous two-phase purification system (ATPS) was used for the extraction process. The factors pH, NaCl, and temperature were confirmed as having a significant impact on the ATPS and therefore were selected for further optimization to maximize yield and purity. The study found that the maximum protease recovery for the leaves was 93%, 77%, and 89% at pH 6, 20°C, and a salt concentration of 0.0 M, respectively. The maximum protease recovery for the bark was 54%, 51%, and 47% at pH 6–8, 10–20°C, and a salt concentration of 0.0 M, respectively. Additionally, it showed that the leaves had the maximum protease purity at pH 8, temperature 10, and salt concentration of 0.2 M, respectively, while the bark had the highest protease purity at pH 8, temperature 30, and salt concentration of 0.2 M, respectively. Thus, the aqueous two-phase purification method is effectively optimized for maximum yield and purity of the protease enzyme extraction from the leaves and bark of the Calotropis procera plant at or around neutral pH, a temperature range of 10–30°C, and low salt concentrations of 0.0 M–0.1 M.

Keywords: Proteases, catalysts, *Calotropis Procera*, aqueous two-phase purification system(ATPS), coagulation

1.0 Introduction

Proteases are enzymes that hydrolyze proteins into relatively smaller peptides and amino acids. They can be found in almost all organisms and they constitute a famous group of biocatalysts with a wide range of applications with respect to their biochemical qualities and substrate specificity (Pant *et al.,* 2015). Organisms produce protease to degrade improperly folded and damaged proteins to maintain homeostasis. These proteases also serve as signaling molecules, facilitate protein-protein interactions and generate novel bioactive molecules within the organisms (Lopez-Otin and Bond, 2008). These proteolytic enzymes have ultimately turned out to be extremely valuable for industrial purposes. Proteases are often employed in brewing, leather processing, meat tenderization, cheese making, detergent manufacturing, baking, and digestive aid manufacturing (Gimenes *et al.,* 2021).

For many years, fermentation processes have been used to isolate these proteases from microbial sources. Protease production from Bacteria, Fungi, and Yeasts is estimated to account for more than 40% of total global enzyme sales

due to the ease with which these microbial proteases are secreted into the fermentation broth and the ease with which the microbes can be genetically manipulated (Chiberkujwo *et al.*, 2020; Gimenes *et al.,* 2021). However, recovering the target enzyme from the fermentation broth is expensive and cumbersome, accounting for 70-90% of the protease extraction expenditure (Gimenes *et al.,* 2021). Other problems associated with microbial protease production have been the difficulty in screening microbes from the environment, the expensive medium for culturing microbes, and the difficulty in identifying suitable growth conditions (Upadhyay *et al.,* 2010). Thus, researchers have sorted to isolate protease from various sources including plants. Popular proteolytic enzymes extracted from local plants include papain from *Carica papaya*, bromelain from pineapple, and ficin from *Ficus* (Obed *et al.,* 2021). Another major plant that has lately received scientific attention due to its potential to contain a prominent proteolytic enzyme is *Calotropis procera* (Obed *et al.,* 2021). *C. procera* is a tropical and equatorial plant that is well-known for its ability to create latex (Rawdkuen *et al.,* 2011). The latex extract from *C. procera* has been employed as a curdling agent in the manufacturing of a traditional cheese variety known as Wara cheese in Southwestern Nigeria over the past decade. The ability of the extract to coagulate milk at a high temperature (over 70°C) makes it effective for the production of Wara cheese and as a replacement for rennet enzyme in cheese manufacturing (Raheem *et al.,* 2007; Oseni and Ekperigin, 2013).

Moreover, purity assessment is known to enhance enzyme activity and functional applicability. This necessitates high precision and cost-effective separation process (Porto *et al.,* 2008). At present, efficient and easily affordable processes for the partitioning and purification of enzymes that provide ample yield and high purity of the final products have thus been demanded by most industries. On this premise, the aqueous two-phase purification process (ATPS) has been employed in this study for the purification of the protease enzyme (Sripokar *et al.,* 2017). ATPS is created by combining an aqueous solution of two immiscible hydrophobic polymers or a polymer and a salt at a certain concentration. Biomolecules segregate between the two aqueous phases in accordance with their partition coefficient (Sripokar *et al.,* 2017). The ATPS has several advantages, including quick processing time, low energy consumption, a high-capacity yield, ease of scaling up, biocompatibility, and non-toxicity (Sripokar *et al.,* 2017).

Furthermore, Proteases, like all other enzymes, operate efficiently in conditions that preserve their well-defined 3-D structure. Due to the lack of appropriate operating conditions, the present proteolytic enzyme from *C. Procera* has not been able to fully meet industrial expectations. In reality, little information is known about the optimal conditions and requirements for the ample yield of protease from *C. procera* and little study has been done to characterize the enzyme. Also, conventional extraction methods often disrupt the well-defined 3D structure of the enzyme. This often results in inconsistencies between reported and observed properties and/or activities of the enzyme as well as the inability to fully explore the enzyme's uses. The problems with the enzyme stability and lack of valuable information for the utmost yield of the enzyme have thus motivated researchers to optimize conditions and experimental procedures to generate a pure, folded, and dimeric enzyme in its maximum yield.

Therefore, the goal of this work is to optimize and characterize protease enzyme extraction from *Calotropis procera* leaves and bark utilizing an aqueous two-phase purification technique. Due to the increased demand for the enzyme, it is imperative to exploit some novel sources of proteases as well as revise some existing methods to increase the production of the enzyme to satisfy its high global demand. Again, the optimization of the extraction process will result in achieving pure and active enzymes, maximum enzyme yield and maximum activity thereby boosting its product yield and catalytic efficiency. All these will increase the recognition and patronization of plant protease as the best supplement or alternative to microbial protease to satisfy the growing demand for protease. This research also serves as an encouragement for more studies to be undertaken on the prospect of

obtaining proteases from other distinct sources for commercial usage and other applications.

2. 0 Materials And Methods

2.1 Raw material collection and Study site

Calotropis procera fresh leaves and stem bark were obtained from the matured plant growing in the slightly humid zone at Kotei community in the Kumasi Metropolis of Ghana. The plant's leaves were plugged by hand whiles the bark was removed with a kitchen knife. The leaves and the bark were subsequently conveyed directly to the Department of Food Science Laboratory of the Kwame Nkrumah University of Science and Technology, Kumasi, Ghana.

2.2 Preparation of crude enzyme extract

The defect-free leaves and bark were next chosen and washed thoroughly with distilled water to eliminate surface dirt and microbes. A mass of 100 g of each plant portion (leaves and stem bark) was individually measured with an electronic balance and then blended with a laboratory blender in the presence of 100 ml of 0.05 M sodium acetate buffer adjusted to a *pH* of 5.5. Each blended mixture was then filtered through a clean cheesecloth into two separately labeled sterile beakers leaving the suspended debris behind, which was then discarded.

The filtrates from the leaves and the bark were dispensed separately into smaller volumes in 50 ml falcon tubes and clearly labeled. The filtrates were subsequently subjected to centrifugation at 4000 rpm for 15 minutes. Following that, the supernatant (crude extract) for each plant part was poured into two separate sterile glass jars (one for crude enzyme extract prepared from the leaves and the other for crude enzyme extract prepared from the bark), covered, labeled, and kept at 4°C for subsequent analysis (Obed *et al.*, 2021).

2.3 Aqueous two-phase purification of the crude extract

An aqueous two-phase extraction process was conducted by combining 2.0 ml of 50% ethanol and 2.0 ml of 50% K_2HPO_4 solutions, together with a volume of 2.0 ml crude extract in 15 ml centrifuge tubes. A glass rod was then employed to stir the mixture gently for about half an hour and then centrifuged at 4000 rpm for approximately 15 minutes before being placed in a water bath for about 30 minutes for complete phase separation to occur (Raja *et al.,* 2013). The two phases formed were separated carefully to carry out estimations in both the top phase and bottom phases and then used for further analysis (Bai *et al.,* 2013). The procedure was repeated for each crude extract obtained from the leaves and the bark of the plant.

2.4 Calotropin enzyme characterization

2.4.1 Protein Concentration Determination

Bradford method was used to estimate the protein concentrations while bovine serum albumin (BSA) served as a reference. A mass of 0.1 g BSA was dispensed in 100 ml distilled water in a conical flask and stirred gently to give the BSA solution.

Different dilutions were obtained by pipetting different volumes (10 µl, 20 µl. 40 µl, 60 µl, 80 µl, 100 µl and blank) of the prepared solution into sterile centrifuge tubes, clearly labeled and topped up with distilled water to 100 µl. The absorbance of the various BSA solutions was measured at 595 nm and their respective absorbance and concentrations were used to generate a conventional curve from which protein concentration in unknown samples was estimated (Kielkopf et *al*., 2020). A pipette was then used to transfer a volume of 100 µl of each enzyme extract (i.e., the crude enzyme prepared from the leaves and the crude enzyme prepared from the bark) into separately labeled clean tubes followed by the addition of 5 ml of Bradford reagent to each, and the absorbance of each enzyme solution measured with a spectrophotometer at 595 nm. The absorbance of a particular enzyme solution was used to trace its concentration from the standard curve (Obed *et al*., 2021).

2.4.2 Calculations of partition parameters

The partitioning of the enzyme between the two phases was further quantified by partition coefficients (K), phase volume ratio (R), and efficiency of extraction (E) defined as

$$K = \frac{C_t}{C_b} \qquad R = \frac{V_t}{V_b} \qquad E = \frac{C_t V_t}{C_t V_t + C_b V_b}$$

Where; C_t =concentration of enzyme in the top phase; C_b=concentration of enzyme in the bottom phase; V_t =volume of enzyme in the top phase; V_b =volume of enzyme in the bottom phase (Bai *et al*., 2013)

2.4.3. Analysis of calotropin activity (Gelatin hydrolysis method)

A gelatin degradation procedure was used to assess the extracts for protease activity. A volume of 1.0% gelatin solution in 0.05 M citrate phosphate buffer at a *pH* of 7.5 was heated in a water bath at 100°C for 15 minutes, chilled, and used as a substrate. A volume of 1.0 ml of each enzyme extract was then added to 1.0 ml substrate in the buffer while 1.0 ml of the substrate and citrate buffer without an enzyme extract served as a control. The reaction was terminated with 3.0 ml of cool 10% trichloroacetic acid at the end of 60 minutes of incubation at 35°C (Obed *et al*., 2021). After that, the tube was refrigerated for about an hour at 2°C to cause the precipitation of non-hydrolyzed gelatin and then centrifuged at about 3000 rpm for 15 minutes.

Next, 1.0 ml Folin Ciocalteu reagent was added to each sample to combine with liberated tyrosine to produce a blue-colored product within the supernatant. A spectrophotometer operating at 660 nm was used to measure the absorbance of the free supernatant as well as the absorbance of different standard tyrosine concentrations, while the blank served as a control. Different tyrosine concentrations (20-220 µl) were plotted against their respective absorbance to form a standard tyrosine curve from which tyrosine concentrations in the various supernatants were estimated (Upadhyay *et al.,* 2010). The quantity of the enzyme that liberates 1µmol of tyrosine per minute under the conventional assay conditions is equivalent to one unit of protease activity (Rajagopalan *et al*., 2019). This procedure was then repeated for all enzyme extracts from the bark and leave of the plant under various experimental settings.

2.4.4 Calculation of the specific activity and percentage yield of calotropin enzyme

The specific activity and the percentage recovery after the purification step of an enzyme were determined by the formulas below;

- Specific Activity = **Enzyme Activity/protein Concentration**
- Recovery / % yield = **(total activity of purified enzyme/ total activity of crude extract) *100** (Rathnasamy and Kumaresan, 2014).

2.5 Determination of the influence of different extraction process parameters on the activity and percentage yield of the calotropin enzyme.

The aqueous two-phase system was used to purify the crude enzyme extract under different *pH* values (2 to 10), different temperature conditions (0 to 40) °C, and different salt concentrations (0.0 M to 1.0 M). The concentration, activity, percentage yield, and other partitioning parameters of protease were determined for each enzyme extracted under various conditions, using the fore-mentioned procedure.

2.7 Analysis of Statistics

The research findings were calculated by averaging triplicate values and expressed as mean values while the data collected were analyzed using the SPSS software. The significant variations in average values of proteolytic activity and protein concentration of each sample were explored with one-way ANOVA, and all outcomes were displayed statistically using an MS Excel program (Obed *et al*., 2021)

3.0 Results

3.1 Purification and Characterization of Protease from Leaves and Bark Extract

Table 1: Characterization of crude extracts from leaves and bark of the plant

	Leaves	**Bark**
Absorbance by the enzyme at 595nm	0.42059 ± 0.02	0.75208 ± 0.02
Protein concentration (mg/ml)	0.805 ± 0.02	1.445 ± 0.02
Absorbance by the supernatant at 660nm	0.64191 ± 0.02	0.840 ± 0.02
Protease activity (µmol/ml/min)	0.056 ± 0.02	0.074 ± 0.02
Specific activity = Activity/Protein concentration	0.070 ± 0.02	0.051 ± 0.02
Percentage Yield = (Total activity after purification/ total activity of crude extract) *100	100%	100%
Fold purification=Specific activity of purified enzyme/Specific activity of crude extract	1	1

Table 2: Characterization of purified extracts from leaves and bark after purification

	PURIFIED ENZYME EXTRACT	
	LEAVES	**BARK**
Absorbance by the enzyme at 595nm	0.182 ± 0.02	0.091 ± 0.02
Protein concentration (mg/ml)	0.343 ± 0.02	0.167 ± 0.02
Absorbance by the supernatant at 660nm	0.864 ± 0.02	0.776 ± 0.02
Protease activity (µmol/ml/min)	0.076 ± 0.02	0.068 ± 0.02
Specific activity = Activity/Protein concentration	0.223 ± 0.02	0.410 ± 0.02
Percentage Yield = (Total activity after purification/ total activity of crude extract) *100	89%	46%
Fold purification = Specific activity of purified enzyme/Specific activity of the crude extract	3.185	8.035

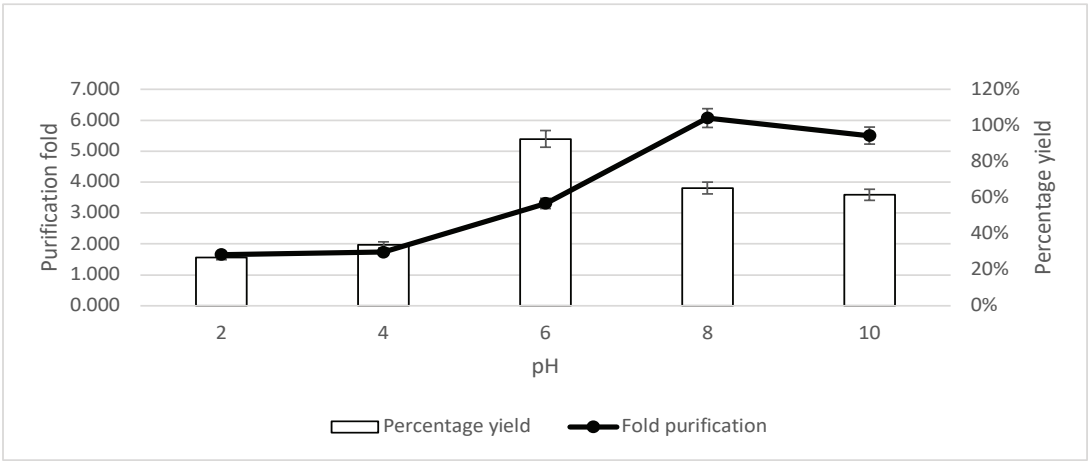

Figure 1: Effect of pH on purified extracts from leaves after the ATP system

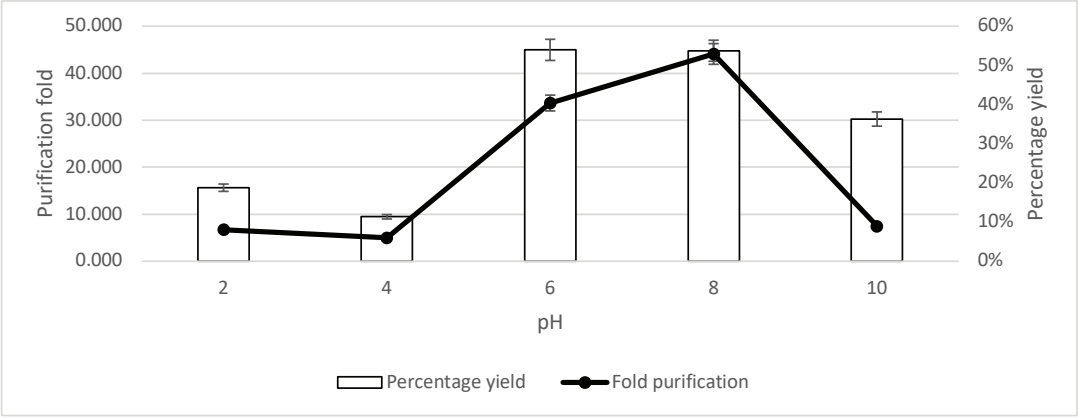

Figure 2: Effect of pH on purified extracts from the bark after the ATP system

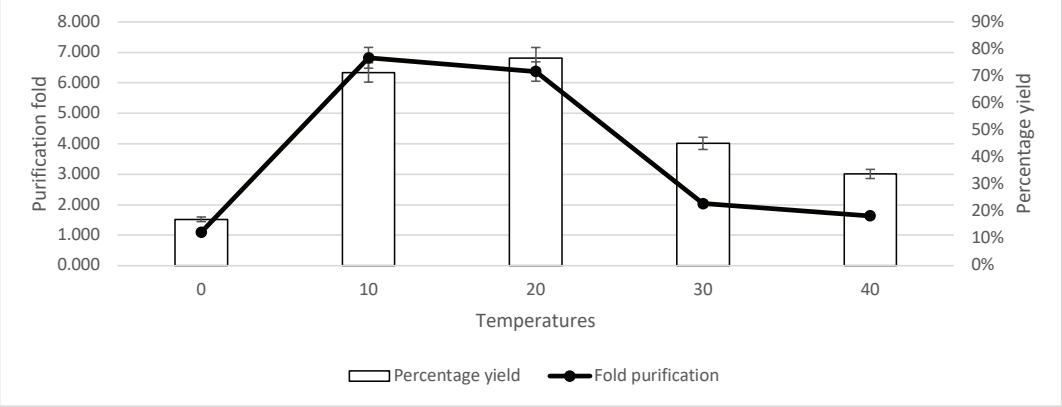

Figure 3: Effect of temperature on purified extracts from leaves after the ATP system

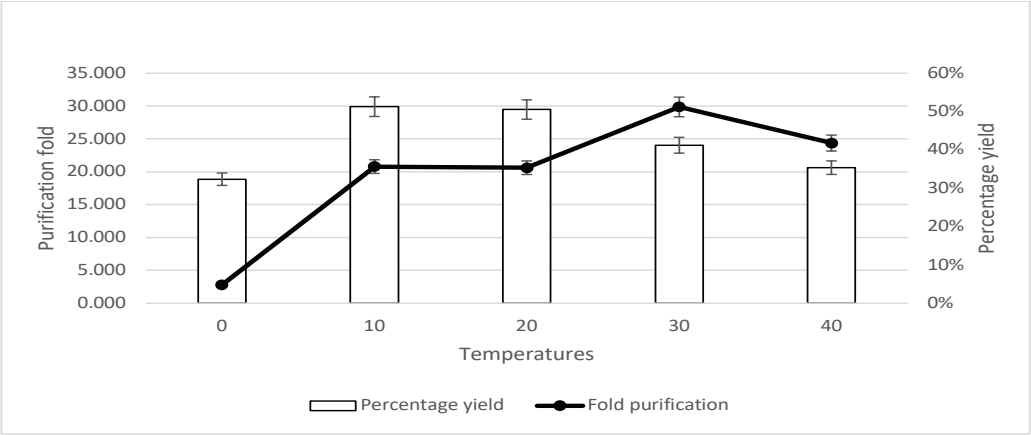

Figure 4: Effect of temperature on purified extracts from the bark after the ATP system

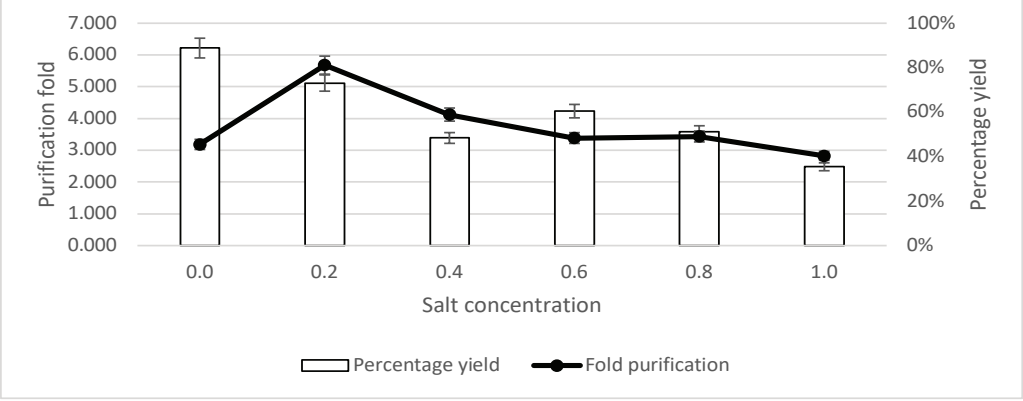

Figure 5: Effect of salt concentrations on purified extracts from leaves after the ATP system

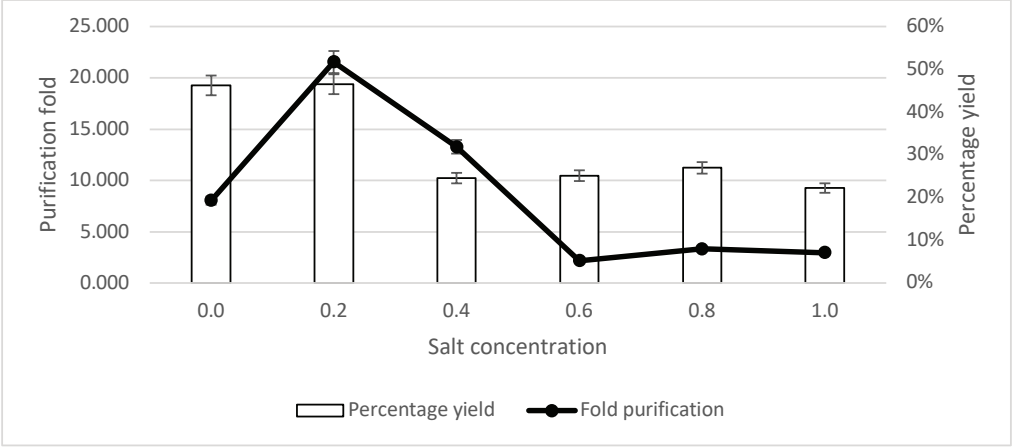

Figure 6: Effect of salt concentrations on purified extracts from leaves after the ATP system

4.0 Discussion

This work attempted to improve the extraction of protease from the crude source by developing enzyme partitioning towards one of the phases of the ATPS. The findings revealed that the ATPS tested had partition coefficient (Ke) > 1 and volume ratio (Rv) > 1 for the protease enzyme from both the leaves and bark, indicating that the enzyme was primarily distributed in the top ethanol-rich phase. The effect of various parameters on a specific activity for ATPS was studied in the search for the utmost enzyme separation. Two terms, fold Purification and percentage yield, were used to plot graphs to depict the influence of various parameters on the extraction process. Fold purification is an indication of the number of times the enzyme has been enriched following purification. Percentage yield on the other hand is an indication of the quantity of enzyme that remains after the purification step. (Saravanan *et al*., 2008).

From the results of the study, there was a significant difference ($P < 0.05$) in terms of protein concentration between the crude and purified enzyme extract in the two plant parts. In terms of the plant part, crude enzyme extract from the stem bark showed a higher protein concentration of 1.445 mg/ml, whiles 0.805 mg/ml of proteins were found in the crude enzyme extract from the leaves. Thus, stem bark has a higher protein concentration as compared to the leaves (Table 2). In both the leaves and the stern bark, the crude enzyme extracts recorded higher protein concentrations (i.e., 0.805 mg/ml and 1.445 mg/ml respectively) than the purified extracts (i.e., 0.343 mg/ml and 0.167 mg/ml respectively). This suggests that the concentration of protein is always dependent on the purification step as a significant decrease in the protein concentration was observed after crude extracts were purified. The removal of unwanted proteins from a protein solution is ensured by the purification processes, which accounts for the observed drop in protein concentrations (Obed *et al.,* 2021; Harrison *et al.,* 1997).

The proteolytic activities of the various samples for the bark and leaves (i.e., crude extracts and purified extracts by ATPS) are shown in Tables 1 and 2. Both plant portions displayed quite significant proteolytic activity. which was disclosed by the potential of the extracts to hydrolyze casein, demonstrating that calotropin enzymes are widely distributed throughout the plant's parts. There was a significant difference ($P < 0.05$) between the proteolytic activities of the crude extracts and the activities after purification by ATPS for both plant parts. Comparing proteolytic activity for stem bark and leaves, it was observed that the various samples for stem bark showed higher activity (0.074 and 0.068 μmol / min/ml) than the samples for the leaves (0.056 and 0.077 μmol / min/ml). According to Oseni & Ekperigin, (2013) who tested different *Calotropis procera* parts for protease activity, the latex of the plant exhibits the highest proteolytic activity, followed by the root, stem, leaf, and pods. The result in this study, with stem bark having a higher proteolytic activity, supports their findings.

The aqueous two-phase purification techniques, however, provided an improved value of specific activity at 0.223 U/mg with a purification fold of 3.185 and 89% yield for the leaves and an improved value of specific activity at 0.410 with a purification fold of 8.037 U/mg and 46% yield for the bark. This shows that the ATPS provided more highly purified enzymes in the bark than it did in the leaves, leading to a lower protein concentration free of impurities and an increase in proteolytic activity in the bark.

4.1: Effect of pH

Figure 1 and Figure 2 describe the influence of *pH* on the specific activity of the enzyme and hence the fold purification and percentage yield of the enzyme purified by the ATPS from the leaves and bark respectively. The results showed that the yield and purity of the enzyme in both samples increased with an increase in *pH* from 2 to 7; then it immediately declined at a *pH* above 8 (Li *et al.,* 2013). The graph in Figure 1 above shows that the highest enzyme yield of about 93% and the highest fold purification of about 6.07 were obtained for the leaves at *pH* values of 6 and 8 respectively. In Figure 2, similar observations of the highest percentage yield of

about 54% and the maximum fold purification of around 44.093 were made for the enzyme from the bark of the plant at *pH* values of 6 and 8 respectively. These findings demonstrate that the enzyme was obtained in the highest quantity and purity at *pH* values which are very close to the neutral *pH* for both samples. Raja and Murty's (2013) study indicates that the isoelectric point of the enzyme protein can be used to explain the observation regarding the percentage yield. Since plant-derived protease must be composed of soluble and globular proteins, it can have net charges above and below a *pH* of 6. Because of this, the charged protein molecules interact with both ethanol and salt, causing distribution in both the top and bottom phases. However, at/around the isoelectronic *pH*, where the enzyme protein's net charge is zero, the enzyme has no charges to interact with the salt, instead, it only interacts via hydrogen bonding with the ethanol, making it more soluble in the ethanol phase, causing partitioning of the enzyme primarily in the ethanol rich phase. This was manifested in the highest percentage yield of the enzyme in the top phase around neutral *pH* from both the leaves and the bark of the plant.

The findings regarding fold purification are explained by how *pH* affects the activity of the enzyme. Gale and Epps (1942) asserted that the number of electrostatic charges in an enzyme's active site determines its catalytic activity. The structure and hence the function of the enzyme might be impacted by *pH* changes since alterations in *pH* can change crucial ionization states and potentially break crucial bonds. The *pH* range of 6 to 8 may contain the protease enzyme's *pl* since it has the most specific enzyme activity and, hence, the highest fold purification (around *pH* ~7.0). The small increase in *pH* values above 7 improves the specific activity and hence fold purification value. The fold purification showed maximum values from *pH* of 6 to 8 for both samples, indicating that the protease present in *C. Procera* is most likely a neutral protease. The strength of the acidic or alkaline solution that influences the enzyme property is illustrated by a dramatic decline in the fold purification and thus in specific enzyme activity values (Pereira and Coutinho, 2020). Thus, the enzyme's optimal *pH* for activity and partitioning in an aqueous two-phase system is in the range of 6 to 8 (roughly the neutral *pH*) in both the plant's leaves and bark (Goja *et al.*, 2013).

4.2 Effect of temperature

The impact of temperature on the enzyme activity in the ATP system is depicted in Figure 3 and Figure 4. The endothermic nature of the process, in which greater values of temperature influence the protease partition, was disclosed as the enzyme activity and, consequently, recovery, rose as the temperature of the ATP system increased. The protease exhibits the greatest enzyme extraction for the leaves at 20°C and for the bark at 10–20°C, with the highest enzyme recovery values of 77% and 51%, respectively. Increasing temperature, according to Li *et al.* (2013), causes a reduction in fluid viscosity and an increase in the kinetic energy of biomolecules that are partitioning towards a particular phase, which causes an increase in the number of enzyme molecules moving to the top phase. As a result, the protease enzyme's extraction efficiency should have improved from 15°C to 55°C. But the extraction efficiency started to drop at temperatures exceeding 30°C. This was attributed to denaturation, which made the protease enzyme unstable at relatively high temperatures. At 40°C, more enzyme molecules were broken down, and the extraction efficiency for the leaves and bark, respectively, fell to 35% and 34%. Thus, a further increase in temperature over the optimal value impacts the enzyme activity due to denaturation (Li *et al.*, 2013).

The temperature also indicated a significant positive effect on the purification fold. The increase in temperature not only alters the structure of biomolecules but also changes the specific activity. From Figure 3, upon extracting protease from the leaves under different temperature conditions ranging from 0°C to 40°C, the highest specific activity of 0.478, and subsequently the highest fold purification value of 6.822 was observed at a temperature of 10°C. From Figure 4, the highest specific activity was 1.524, and a fold purification value of 29.877 for protease extracted from the bark was observed at 30°. Thus, at a temperature range of 10-30, the process yields more purified enzymes than at any other temperature.

5.3 Effect of salt

The addition of NaCl in the ATPS had a considerable impact. For the NaCl concentrations studied in this research (from 0.0 M to 1.0 M), it is observed from both samples that the addition of salt decreased the partitioning towards the top ethanol-rich phase. The extraction yield decreased from 89% to 35% for enzyme extraction from the leaves and decreased from 46% to 22% for the enzyme extraction from the bark (Figure 5 and Figure 6). This is because changes in the electrostatic potential difference of the enzyme result in an increase in the interaction of biomolecules with the salt-rich bottom phase. The affinity charge of the protease enzyme improves as the NaCl concentration increases which positively directs the partition coefficient of the system toward the bottom salt-rich phase. Further addition of salt concentration above the optimized value increases the anion content and resists the protease separation towards the bottom phase which manifested itself with a gradual rise in enzyme partitioning towards the ethanol-rich top phase at the 0.6-0.8 M salt concentration for both samples (Li *et al.,* 2013). However, a high concentration of neutral salts may cause denaturation of proteins existing in the system, thus low concentration range from 0.0 to 1.0 M is preferred but it favors partition towards the salt-rich phase rather than the ethanol-rich phase. (Goja *et al*., 2013).

Different salt concentrations (from 0.0 to 1.0 M) raised the enzyme's fold purification to a peak at 0.2 M, after which the enzyme activity again declined, indicating that salt enhanced the enzyme purity at low doses. However, the addition of higher concentrations of neutral salts (above 0.2 M) may denature proteins present in the system, resulting in a reduction in the specific enzyme activity and, consequently, the fold purification values for the enzymes extracted from both the plant's leaves and bark (Li *et al*., 2013).

5.0 Conclusion

This current study conducted revealed high protein concentration and proteolytic activity of calotropin enzyme from the leaves and stem bark of *the Calotropis procera* plant. Thus, protease assays can be used with various *Calotropis procera* components. Moreover, the aqueous two-phase purification process has proven to be very quick and efficient in the purification of the enzyme as compared to standard purification methods. The factors *pH*, NaCl, and temperature were confirmed as having a significant impact on the ATPS. The studies revealed that the aqueous two-phase purification process is efficiently optimized for maximum yield and purity of the protease enzyme extraction from the leaves and the bark of *Calotropis procera* plant at/around neutral *pH*, temperature range of 10-30°C and at low salt concentrations of 0.0 M-0.1 M.

Recommendation

In this work, the extraction process was optimized using a one-factor-at-a-time technique, in which the influence of one variable is studied at a time, leaving all other parameters constant and ignoring the interactions between two or more variables. Iqbal *et al.,* (2016) stated that optimization without considering the interactions between the variables could result in poor and false optimal conditions. Therefore, it is hereby advised that a multivariate statistical technique known as "Design of Experiments (DoE)" be utilized for the optimization of ATPS in subsequent similar research to remove uncertainty and assure flawless optimization and characterization. In DoE experiments are run at different combinations of the variables. Without a doubt, such a factorial design may provide very accurate results by accounting for potential variables interactions, but the number of experiments will increase.

Acknowledgement

Our sincere thanks and deep appreciation go to Professor H. D. Zakpaa, for his invaluable guidance, essential support, and uplifting inspiration throughout this research work. Our special thanks and deep appreciation also go to the entire team of Laboratory Technicians at both the Biochemistry and Food Science Departments

at the Kwame Nkrumah University of Science and Technology.

References

Bai, Z., Chao, Y., Zhang, M., Han, C., Zhu, W., Chang, Y. and Sun, Y. (2013). Partitioning behavior of papain in ionic liquids-based aqueous two-phase systems. *Journal of chemistry*.

Chimbekujwo, K. I., Ja'afaru, M. I. and Adeyemo, O. M. (2020). Purification, characterization and optimization conditions of protease produced by *Aspergillus brasiliensis* strain BCW2. *Scientific African*, 8, e00398.

Gale, E.F. and Epps, H.M. (1942). The effect of the *pH* of the medium during growth on the enzymic activities of bacteria (*Escherichia coli* and *Micrococcus lysodeikticus*) and the biological significance of the changes produced. Biochemical Journal, 36(7-9), p.600.

Gimenes, N. C., Silveira, E. and Tambourgi, E. B. (2021). An overview of proteases: production, downstream processes, and industrial applications. *Separation & Purification Reviews*, 50(3) pp. 223-243.

Goja, A.M., Yang, H., Cui, M. and Li, C. (2013). Aqueous two-phase extraction advances for bioseparation. *J. Bioprocess. Biotechnol, 4(1), pp.1-8.*

Harrison, M. J., Neil, A. B. and Ian, H. H. (1997). Catalytic mechanism of the enzyme papain: predictions with a hybrid quantum mechanical/ molecular mechanical potential. *Journal of the American Chemical Society* 119, no. 50 (1997): 12285-12291.

Iqbal, M., Tao, Y., Xie, S., Zhu, Y., Chen, D., Wang, X., and Yuan, Z. (2016). Aqueous two-phase system (ATPS): an overview and advances in its applications. *Biological procedures online*, 18(1), pp. 1-18.

Kielkopf, C. L., Bauer, W. and Urbatsch, I. L. (2020). Bradford assay for determining protein concentration. *Cold Spring Harbor Protocols*, 2020(4), pp. 102269.

Li, Y.F., Han, J., Wang, Y., Ma, J.J. and Yan, Y.S. (2013). Partitioning of Cephalexin in Ionic Liquid Aqueous Two-Phase System Composed of 1-Butyl-3-Methylimidazolium Tetrafluoroborate and' Journal of Chemistry, 2013.

Lopez-Otin, C. and Bond, J. S. (2008). Proteases: Multifunctional Enzymes in Life and Disease. *The Journal of Biological Chemistry* 283, pp. 30433-30437

Murti, Y., Yogi, B. and Pathak, D. (2010). Pharmacognostic standardization of leaves of *Calotropis procera* (Ait.) R. Br. (*Asclepiadaceae*). *International journal of Ayurveda research*, 1(1) pp. 14.

Obed, A. O., Zakpaa, H. D., Theophilus, A., Yeboah, S. I. I. K. and Prince, E. (2021). Extraction, Purification and Characterization of Plant Enzyme (Calotropain) from the Unripe Pods and Bark of Sodom Apple (*Calotropis procera* (AIT). *Asian Journal of Biochemistry, Genetics, and Molecular Biology*, pp. 30-36.

Oseni, O. A. and Ekperigin, M. M. (2013). Partial characterization of proteolytic and milk clotting enzymes in Sodom apple *Calotropis procera* (Ait.) R. Br. (*Asclepiadaceae*) plant. *American Journal of Biochemistry and Molecular Biology*, 3(2) pp. 256-263.

Pant, G., Prakash, A., Pavani, J. V. P., Bera, S., Deviram, G. V. N. S., Kumar, A. and Prasuna, R. G. (2015). Production, optimization and partial purification of protease from *Bacillus subtilize*. *Journal of Taibah University for Science*, 9(1) pp. 50-55.

Pereira, J.F. and Coutinho, J.A., (2020). Aqueous two-phase systems. *In Liquid-phase extraction* (pp. 157-182). Elsevier.

Porto, T. S., Silva, G. M., Porto, C. S., Cavalcanti, M. T. H., Neto, B. B., Lima-Filho, J. L. and Pessoa Jr, A. (2008). Liquid–liquid extraction of proteases from the fermented broth by PEG/citrate aqueous two-phase system. *Chemical Engineering and Processing: Process Intensification*, 47(4), pp. 716-721.

Raja, S. and Murty, V.R. (2013). Optimization of aqueous two-phase systems for the recovery of soluble proteins from tannery wastewater using response surface methodology. *Journal of Engineering.*

Raja, S., Murty, V.R., Thivaharan V., Rajasekar V. and Ramesh, V. (2011). Aqueous two-phase systems for the recovery of biomolecules-a review. *Sci Technol*, 1 pp.7–16.

Rajagopalan, A., Soundararajan, M. and Sukumaran, B. O. (2019). Proteases from *Calotropis gigantea* stem, leaf and calli as milk coagulant source. *Turkish Journal of Biochemistry*, 44(3) pp. 240-247.

Rathnasamy, S. and Kumaresan, R. (2014). Partition coefficient studies of calotropain from its crude latex using ionic liquid based aqueous two-phase extraction system.

Rawdkuen, S., Pintathong, P., Chaiwut, P. and Benjakul, S. (2013). The partitioning of protease from *Calotropis procera* latex by aqueous two-phase systems and its hydrolytic pattern on muscle proteins. *Food and Bioproducts Processing*, 89(1), pp. 73-80.

Saravanan, S., Rao, J. R., Nair, B. U. and Ramasami, T. (2008). Aqueous two-phase poly (ethylene glycol)-poly (acrylic acid) system for protein partitioning: influence of molecular weight, pH and temperature. *Process Biochem*. 43, pp. 905–911.

Sripokar, P., Chaijan, M., Benjakul, S., Yoshida, A. and Klomklao, S. (2017). Aqueous two-phase partitioning of liver proteinase from albacore tuna (*Thunnus alalunga*): application to starry triggerfish (*Abalistes stellaris*) muscle hydrolysis. *International journal of food properties*, 20(2), pp. 1600-1612.

Upadhyay, M. K., Kumar, R., Kumar, A., Gupta, S., Kumari, M., Singh, A. and Verma, H. N. (2010). Optimization and characterization of an extracellular protease from *Aspergillus flavus* MTCC 277. *African Journal of Agricultural Research*, 5(14), pp. 1845-1850.